Cost evaluation of different medium solids for Air Dense Medium Fluidized Bed coal separation

Kundayi Marshall Chagwedera
(1484014)

A Masters dissertation submitted to Faculty of Engineering and the Built Environment, University of the Witwatersrand, Johannesburg, South Africa, in fulfilment of the requirements for the degree of Master of Science in Engineering

Supervisors:
Dr Samson Bada and Prof Rosemary Falcon

December 2017

DECLARATION

I declare that this dissertation is my own unaided work. It is being submitted for the degree of Master of Science in Engineering to the University of the Witwatersrand, Johannesburg, South Africa. It has not been submitted before for any degree or examination to any other University.

…………………………

(Signature of Candidate)

……..… day of ………………………….…… 2017

(Day) (Month) (Year)

ABSTRACT

Dense medium processing of high-ash coals with liquid dense media (water and magnetite) is currently the conventional means of beneficiating coal in South Africa (SA)). Hence, large volumes of waste water are produced along with a high cost of treating this effluent, both factors of which constitute a major disadvantage to this technique. This study presents an experimental account of Air Dense Medium Fluidized Bed (ADMFB) as an alternative dry processing approach for beneficiating SA coals. Magnetite is the conventional medium in ADMFB application this medium material is costly and limited in quantity. Pyrrhotite, granulated blast-furnace slag, silica sand and coal discards were investigated as alternative air dense medium materials to either replace or augment magnetite. Each of the materials utilized was prepared for a specific size range (-425+106 µm) and characterised according to their physical properties. The materials were then tested individually, first as sole fluidized media followed by further tests where the materials were blended in various proportions. The purpose was to establish their fluidization characteristics and suitability for coal separation. Uniformity and stability of the bed density were considered the key performance parameters for facilitating coal quality separations and therefore these were used as the main criteria for selecting the potential best medium material. Initial beneficiation tests with density tracers in lieu of coal were used for the purpose of optimizing operating parameters and separation efficiency for each of the media utilized. Based on the results obtained from the trial tests, coal was then tested in the ADMFB fluidized bed separator.

Magnetite and pyrrhotite, individually, provided the most uniform and stable bed densities with bed density variation less than 0.7% and standard deviation less than 0.0025 g/cm^3. A 100% magnetite bed produced a clean coal product with an ash content of 20.30% and calorific value of 25.24 MJ/kg from a feed coal (-13+6 mm size fraction) of 39.27% ash and CV of 18.76 MJ/kg. The bed's cut-point/separation density (ρ_{50}) was 1.82 g/cm^3 while coal product yield and Ep of 60.26 – 60.89% and 0.070 – 0.075, respectively were obtained. A cleaner coal product with 14.50% ash and a calorific value of 27.30 MJ/kg was obtained from a blend of pyrrhotite and magnetite at a weight ratio (%) of 40:60. The same blend reduced the total sulphur content in the feed coal from 2.49% to 0.41% sulphur at a cut density of 1.63 g/cm^3, with a yield and Ep of 52.67% and 0.083, respectively.

Pyrrhotite appears to be the most superior dense medium material amongst the materials tested as an alternative media to magnetite. More uniform and stable bed densities were achieved using the pyrrhotite-magnetite (40:60) blend, compared to these materials as individual media alone. A cleaner coal product with less ash and sulphur content was obtained from this blend compared to using magnetite as the sole medium. From an economic perspective, the partial replacement of magnetite by blending with pyrrhotite ore, which is considered a reject “no cost rejects material”, is likely to reduce the cost of operating a coal ADMFB process to a considerable extent and may well prove this process to be more sustainable in future.

ACKNOWLEDGEMENTS

Glory is to God!

My sincere gratitude goes to my supervisors Dr Samson Bada and Prof Rosemary Falcon for their unwavering guidance and support throughout the completion of this research. Special mention goes to Mr. Paul Den Hoed for provision of critical equipment and constant guidance.

I am grateful for the financial support of Coaltech Research Association (Project No: 4.8.5 c) and the Clean Coal and Sustainable Energy Group of the University of the Witwatersrand. I also acknowledge the School of Chemical and Metallurgical Engineering for access to research facilities.

The warmest appreciation goes to my parents, siblings, relatives and friends for their encouragement and prayers. Taona, Ruvimbo, Tawonga and Audrey you are the best!

PRESENTATIONS

The conference papers from this research are listed below:

1. **Kundayi Chagwedera**, Samson Bada, Rosemary Falcon. Evaluation of alternative medium solids for Air Dense Medium Fluidized Bed coal beneficiation. **Oral Presentation**. South African Coal Processing Society Conference, Secunda, South Africa. 21 – 24 August 2017.

2. **Kundayi Chagwedera**, Samson Bada, Rosemary Falcon, Paul Den Hoed. Air dense medium fluidized beds in dry coal beneficiation: Correlating dense medium with performance. **Oral Presentation**. Industrial Fluidization South Africa (IFSA 6) Conference, Johannesburg, South Africa. 3 – 5 October 2017.

3. **Kundayi Chagwedera**, Samson Bada, Rosemary Falcon. Evaluation of alternative medium solids for Air Dense Medium Fluidized Bed coal beneficiation. **Extended Abstract - Oral Presentation**. Fossil Fuel Foundation Conference in Sustainable Development of Southern Africa's Energy Resources, Glenhove Conference Centre, South Africa. 29 – 30 November 2017.

CONTENTS

LIST OF FIGURES

LIST OF TABLES

Chapter 1 : Introduction

1.1 BACKGROUND AND MOTIVATION

South Africa (SA) has vast coal reserves and its economy is heavily dependent on this abundant resource for its primary energy needs. From the estimated 333.6 Mt of ROM (Run of mine) produced in 2014, in which approximately 74.8 Mt was discarded, about 128.2 Mt was used in the generation of electricity (Prevost, 2015). Therefore, the demand for coal in South Africa as the primary energy source will not change in the near future.

The Witbank coalfield in Mpumalanga region is known to possess SA's largest coal reserves and continues to supply approximately 50% of SA's saleable export as well as domestic coal (Hancox and Götz, 2014). This has undoubtedly drastically reduced the reserves of best quality coals which are now near exhaustion leaving behind coals of considerably lower quality. The increase in the depletion of high-grade coal in this region, has led to the development of the Waterberg coalfield by one large and several smaller mining companies. The Waterberg coalfield was estimated to contain about 40 to 50% of South Africa's remaining mineable reserves, rendering it one of the last major coal deposits in South Africa (Hancox and Götz, 2014).

The most critical issue facing the Waterberg coalfield is the lack of water, which presents a major challenge in implementing the conventional wet beneficiation techniques when upgrading the high ash coals (i.e. when separating the inorganic minerals from the organic materials in coal) in that region. Large quantities of water are currently used or lost during the coal preparation and the cost of managing and treating large quantities of aqueous slurries generated during the wet process has become considerable. These challenges associated with wet beneficiation have given rise to the idea of beneficiation of coal through dry beneficiation techniques. Dwari and Rao (2007) have also shown that the dry beneficiation products "coal" retain higher thermal heating value, thereby motivating this investigation.

The dry beneficiation technique is based on the differences in the characteristics of the coal constituents such as specific gravity, grindability, friability, shape, size, magnetic susceptibility, electrical resistivity and frictional coefficient (Bada *et al.*, 2010; Dwari and Rao, 2007). These differences have been used as a basis for the beneficiation of coal and other minerals, using equipment such as the tribo-electric separator, air dense medium fluidized bed separator, pneumatic jig, pneumatic table, FGX dry separator and the coal X-ray sorting machine (Bada *et al.*, 2012; Honaker *et al.*, 2008; Choung *et al.*, 2006; Chen and Yang, 2003). However, most of the methods are characterised by limitations ranging from specific narrow feed particle size range, low product yield, specific coal hardness and narrow cut-point densities coupled with generally high Ecart Probable Moyen (EPM) values (Dwari and Rao, 2007). In order to utilize the proposed approach in this study for beneficiating high ash South Africa Coal (SAC), a thorough understanding of the principles of coal beneficiation using Air Dense Medium Fluidized Bed (ADMFB), along with the complete knowledge of the ROM coal, in terms of its chemical and mineralogical composition is very important.

The ADMFB process has been under investigation for a number of decades and some of the earlier investigations were patented as early as 1926 (Fraser and Yancey, 1926). The foundation for the industrial application of ADMFB coal separation was based on studies conducted by different authors over the past decades. The investigation conducted by Zhao *et al.* (2016) presents the most recent work on the industrial application of an ADMFB using a large scale (40 – 60 ton/hr) plant. The results indicated that the solid medium material used in the ADMFB separator is one of the key factors for efficient coal separation. The choice of media was shown to influence the stability and uniformity of the bed density, thereby dictating the separation efficiency of the system. Magnetite has been widely used as the medium by many investigators in their dry beneficiation studies. However, the demand for magnetite has increased because of its use in other industries such as steel making, catalysis and in conventional wet coal beneficiation thus rendering it low in availability and difficult to obtain. Future cost and security of supplying magnetite to the coal industry are a concern (Honaker and Bimpong, 2009).

Studies conducted by numerous researchers have shown that minerals such as silica sand, silica-zircon mixture, magnetic pearls and paigeite can be used as an alternative medium or as a blend with magnetite for ADMFB coal separation (Azimi *et al.*, 2013; Firdaus *et al.*, 2012; Zhao *et al.*, 2011; Fan *et al.*, 2001). Against this background, the current study set out to focus on utilizing locally available alternative solid medium materials solely or as a blend at different weight ratios for effective separation of South African coal qualities, namely, separating organic high value coal material from its inorganic (ash) content. The solid medium materials tested in this investigation include magnetite as the control medium, pyrrhotite, granulated blast furnace slag, silica sand and coal rejects. Pyrrhotite, along with coal rejects and granulated blast furnace slags are known to be "rejects" dumped to tailings during the concentration of nickel (Ni) and the processing of Platinum Group Metals (PGM), coal processing and iron making. The use of Pyrrhotite as a solid medium in a fluidized bed was considered to be a new and significant material for testing since no publications have been found in open literature in which this material has been used for dry coal processing. The magnetic property exhibited by pyrrhotite (in order to aid in recovery) and its density ($3g/cm^3$) rendered it a potential material suitable for dense medium application both alone and as a blend component (magnetite/pyrrhotite). These attributes were tested in order to establish whether pyrrhotite would make a suitable dense medium for coal beneficiation in an ADMFB separator along with other solid materials as listed above.

Against the background summarised above, this research study has sought to characterise the physical and chemical properties of each of the proposed alternative solid medium materials followed by determining the fluidization properties of the fluidized bed created by each of the materials. These properties which include the average bed density, stability and uniformity of the bed, were used to determine the optimum operating conditions and to select the most effective dense medium material. The solid medium material with the most effective fluidization characteristics based on varying air superficial velocity, static bed height and blend ratios was used to carry out the preliminary beneficiation tests utilizing density tracers. The optimum set parameter achieved from the beneficiation of the density tracers was applied to the beneficiation of coal at -13+6 mm size range. The analysis of the results lead to a recommendation at the conclusion of this research.

1.2 PROBLEM STATEMENT

Magnetite is an expensive and potentially difficult to obtain medium for use in the dry fluidized bed beneficiation process in future, so an alternative medium needs to be found to replace it or to extend its use through blending. Key operating conditions using such media are then required to create an equally effective means to beneficiate coal.

Efficient coal beneficiation using the ADMFB process is heavily dependent on creating and maintaining a stable and uniform bed density throughout the fluidized bed. However, there are several problems faced that inhibits the accomplishment of these conditions. One of the problems is the back mixing of the medium solids caused by air bubbles passing through the bed. The extent of the disturbance is mainly influenced by the particle size of the fluidizing medium solids and bed depth (Mohanta *et al.*, 2012). Therefore, to improve separation efficiency, correct particle sizing and different static bed height will be investigated. In addition the superficial velocity for each media will also be investigated.

Another limitation of ADMFB is that the bed density (ρ_b) depends on the particle density of the medium solids (ρ_s) and the void fraction (ε). Equation 1-1 below shows the relationship between these parameters.

$$\boldsymbol{\rho_b = (1 - \varepsilon)\rho_s} \qquad \textit{Equation 1-1}$$

Fluidized bed density is dependent on the void fraction and the density of the solid medium, and this can be adjusted by varying these two parameters. The bed density can be manipulated by varying the solid medium material to expand the density range of the bed (Zhao *et al.*, 2011). For a given product or cut, an appropriate solid medium at appropriate size ranges can be selected to increase the range of separating density of the fluidized bed. Typically, magnetite has been used in ADMFB to perform low-density separation. However, cheaper and locally available alternatives are required. Therefore, in addressing the limitations associated with ADMFB discussed above, the stability and uniformity of the bed will be determined using coefficient of variation and standard deviation of density distribution model.

1.3 AIM AND OBJECTIVES OF THE STUDY

The prime aim of this research is to evaluate proposed solid media materials both individually or in a blend in order to expand the choice of solid media materials suitable for ADMFB coal separation. The specific objectives of the project are as follows:

I. To characterise all the proposed solid medium materials, along with coal for use in ADMFB separation
II. To investigate the separation efficiency of ADMFB for cleaning coal as against a standard sink/float technique

III. To determine the density of various positions in the bed using the static pressure difference method and the impact of these variations on the separation efficiency of coal
IV. To ascertain the effect of a solid medium alone and in a blend with magnetite on the performance of the ADMFB in terms of product grade and yield
V. To establish the cost benefit of blending magnetite with the best alternative medium for ADMFB application.

1.4 RESEARCH QUESTIONS

The research questions were formulated based on the challenges as reported in the literature. Therefore, this investigation seeks to provide solutions to the questions below since all materials have different properties:

I. Will the proposed solid medium materials achieve normal fluidization in the ADMFB?
II. Will the density of various positions in the ADMFB be the same?
III. What is the impact of the density distribution on the separation efficiency?
IV. Which sole medium or blend will yield the most effective separation?
V. How will the blend ratio of an individual medium to magnetite affect the performance of an ADMFB?
VI. Once a medium has been selected, will it be cost effective to recommend for use in future?

1.5 LAYOUT OF THE DISSERTATION

The dissertation has five chapters comprising of:

I. Chapter One which introduces the subject with a background and motivation for the study. The research aim and objectives of the study are also included in this chapter.
II. Chapter Two gives a review of most of the important literature related to dry beneficiation and especially ADMFB processes. Some basic principles of fluidization are also presented along with some information on the characteristics of the solid medium materials to be tested.

III. Chapter Three outlines a detailed experimental approach used in this investigation. This includes detailed experimental procedures and information on the standards utilized.

IV. Chapter Four presents the outcomes of the experiments carried out accompanied by discussions of these results to establish their significance. The results include material characterization, fluidization characteristics and beneficiation test results. Also included is the cost evaluation of the proposed potential dense medium material as a blend for use in dry coal beneficiation. This cost only provides a rough indication or estimated cost of magnetite and the selected medium of choice and does not address cost to construction, transportation and related matters.

V. Chapter Five provides conclusions of the study along with the recommendations for future studies and/or implementation of potential alternative dense medium materials.

Chapter 2 : Literature Review

2.1 DRY COAL BENEFICIATION

The beneficiation of coal using dry techniques is based on the differences in the physical properties of the coal and of its gangue mineral matter. These properties include density, size, shape, magnetic susceptibilities, electrical conductivity just to mention a few (Dwari and Rao, 2007). In recent years the dry process has gained renewed interest because of some of its advantages which include:

I. Suitability to arid areas because no water is required for the beneficiation process.
II. Retention of high thermal value of the coal produced due to less moisture content.
III. Lower capital cost for dry plants which are estimated to be as low as one third of the conventional wet plant while operating costs could be at one third to half (Korte, 2014).
IV. Significantly less environmental pollution because of the absence of large volumes of wastewater.
V. Availability of semi mobile plants, allowing easy relocation, suitable for small scale miners.

The different beneficiation techniques that have been used in past decades include sorting, air table and jigs, magnetic separation, electrostatic separation and fluidized bed separators which are described below.

2.1.1 Sorting

The sorting process utilizes the appearance and colour of the minerals within the ore for separation. Optical sorting is one of such techniques, which uses reflectance of the material to identify coal and gangue material. However, optical sorting is only effective for separation where the coal has very little carbonaceous shale and there is a clear distinction between clean coal and the rock. A similar limitation exists in the microwave process (Dwari and Rao, 2007). The microwave technique, a radioactive process, monitors the ash content of the coal and gangue material in order to identify and separate coal from its mineral constituents such as clay, pyrite, quartz and carbonate minerals. Another technique is Nuclear Magnetic Resonance (NMR) which uses the hydrogen content in organic particles of coal to distinguish them from mineral rich particles and their associated gangue minerals. The latter, however, is limited in its use because hydrogen is also found in the moisture content in coal (Dwari and Rao, 2007).

2.1.2 Air Tables and Jigs

Air tables and jigs use the density characteristics of coal for the separation of clean organic rich coal particles from their inorganic mineral rich ones. Settling rates are used to separate coal from the gangue material as the material passes over a porous vibrated bed in which the heavy gangue falls to the bottom while clean coal floats. Both the table and the jig work on the same principle but the difference is in the direction of movement of the two products, i.e. the clean coal and its gangue particle (Dwari and Rao, 2007). In an air jig process, both clean coal and its gangue particles move in the same direction and separation is achieved by a splitter. The air jig has a vibrating feedbox and a pulsating air current, which passes through an air distributor at the bottom of the jigging box. The combination of vibration and air results in the stratification of the bed. An air jig was used by Sampaio *et al.* (2008) to separate pyrite nodules and clays from a Brazilian coal with an ash content of 51% and sulphur content of 1.8%. The resulting cleaned coal product had an ash content of 47%, 0.7% sulphur and a yield of about 71%. A feed coal (-13+4 mm) with an ash content of 43% was also beneficiated using an Allair stratification jig (Boylu *et al.*, 2015). A clean coal product of 17.4% ash and a yield of 48.8% was achieved.

In an air table, material moves in different directions due to the fluidization of the bed and separation is achieved through the vertical stratification of the coal. The fractions of clean coal and middlings are removed along the length of the table through skimmers (Kretzschmar, 2010). Some work has been done to determine the effects of operating parameters such as table frequency, longitudinal angle and transverse angle on air tables product yields using statistical design experiments (Patil and Parekh, 2011). The conclusion drawn by the author was that product yield increases with increasing transverse inclination and longitudinal angle but decreases with increasing table frequency. The results obtained by the author showed that a feed coal with an ash content of 27% was reduced to about 10 – 12% with a yield of 75 – 80%. Çicek (2008) studied the technical and economic feasibility of dry beneficiation using industrial modified air table. The author beneficiated two different feed coals at three different size fractions (-3+1) mm, (-5+3) mm, and (-8+5) mm. A satisfactory result was obtained with the (-3+1) mm size fraction; its ash content was reduced from 42.36 to 21.82% and 29.73 to 17.94% with an Ep value of 0.09 and 0.20 respectively for the two coal samples tested. This study shows the influence of particle size range and its limitation for separating coal with particle size greater than 3 mm.

2.1.3 Magnetic separation

This process utilizes the difference in the magnetic susceptibility of coal and its mineral constituents for separation. Coal is known to be diamagnetic; however, the gangue mineral may contain iron (Fe) allowing separation under a high magnetic field (Zhao *et al.*, 2014). Amongst the techniques employed for separating coal from its ash forming minerals under magnetic process are High-Gradient Magnetic Separation (HGMS) and Open-Gradient Separation (OGMS) (Dwari and Rao, 2007). HGMS involves generation of high magnetic field gradients using an electromagnet that produces a uniform magnetic field. Within the magnetic field generated, a ferromagnetic material with sharp edges or small dimensions is positioned to generate high field gradients, which enable the separation of magnetic particles from weakly magnetic particles (Hise *et al.*, 1981). The magnetic material (Fe containing gaunge minerals) is attracted to the matrix and retained by the ferromagnetic material while clean coal passes through.

In an OGMS, the magnetic field and field gradients are generated from special solenoids. The forces generated are used for the deflection (rather than attraction and retention) of particles depending on their magnetic susceptibility (Hise *et al.*, 1981). The major difference between the two techniques is the amount of magnetic force applied and the magnetic field distance over which it is applied. HGMS applies a large magnetic force on short magnetic field distance while OGMS applies a smaller force on longer magnetic field distance (Hise *et al.*, 1981). Jiao *et al.* (2009) investigated the relationship between magnetic susceptibility and magnetic field density. The author found that there is a linear correlation between magnetic susceptibility and magnetic density, and the study further provided information on the separation efficiency of the magnetic process. The ash reduction and desulphurization rates of fine coal were 64.41% and 55.52%, respectively. One of the limitations of magnetic separation is that the feed coal has to be highly dissociated to allow removal of gangue from coal, and the degree of particle dissociation depends on their magnetic susceptibility (Zhao *et al.*, 2014).

2.1.4 Electrostatic separation

The process makes use of the difference in electrical resistivity and conductivity of coal and its gangue minerals. The three main mechanisms used are conductive induction, contact or tribo-electrification, and ion or corona bombardment (Dwari and Rao, 2007).

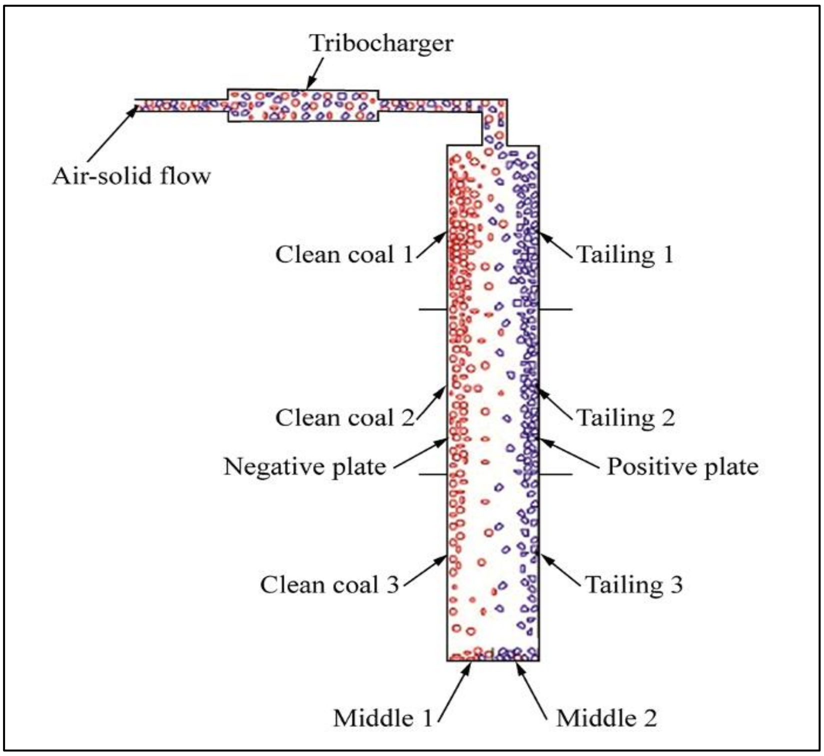

Figure 2-1: Principle of electrostatic separator and sampling rule (Xin-xi et al., 2009)

The principle of triboelectrostatic was illustrated by Xin-xi *et al.* (2009) as shown in Figure 2-1 above. The feed coal is passed through the tribocharger where the material is electrified with either positive or negative charge. The charged particles under free fall pass through a separation chamber with an electrostatic field. The coal and its mineral are attracted to opposite plates producing products and tailings streams. Bada *et al*. (2010) reviewed some of the studies conducted on electrostatic separation and one of the limitations cited was the inability of corona technique to separate particles or minerals/ash in coal with similar closeness in work functions. Zhao *et al.* (2014) also noted that triboelectrostatic separation requires a feed that has a certain degree of dissociation meaning that each particle has to be independent to allow for deflection as it passes through the electrostatic field. Despite the fact that to date the yield from this technique is relatively low, the product coals obtained are of a very high quality, namely, low ash and very high heat content.

2.1.5 Fluidized bed separators

In this research, the choice of separator was the fluidized bed separator, which works on the principle of creating a gas-solid pseudo-fluid with the correct bed density to separate coal by density. The clean product "coal" will float and the ash forming minerals "rock" (containing high ash and sulphur) will sink. The different types of dry fluidized bed processes that have been investigated over the past two decades, which include Magnetically Stabilized Fluidized Beds (MSFB), Vibrated Fluidized Beds (VFB), Dual Density Fluidized Beds (DDFB) and Air Dense Medium Fluidized Beds (ADMFB), are discussed below.

2.1.5.1 Magnetically Stabilized Fluidized Bed (MSFB)

In a MSFB separator, air and the magnetic field are used for fine coal separation. The magnetic field generated is uniformly applied to suppress bubble formation as the gas velocity is increased (Fan *et al.*, 2001). This has the effect of creating a bed that expands instead of bubbling and as a result; magnetized fluidized beds are able to prevent back mixing of gas or solids. Fan *et al.* (2001) investigated the MSFB using magnetic pearls from coal-fired power plant ash with the main particle size ranges less than 98 µm. In this study fine coal (-6+1 mm) was beneficiated and the efficiency of separation achieved as measured by probable error (Ep) was 0.066 at an effective cut density of 1 516 kg/m^3. Fan *et al.* (2003) also studied the effect of magnetic field intensity on the rheological properties of medium used in MSFB separator. The rheological properties include yield stress, solids settling velocity and solids discharge rate. Results from this investigation showed that the yield stress increases, while solids settling velocity decreases with increasing magnetic field intensity. The solids settling velocity determines the capacity of the separator and their relationship is directly proportional. The solids discharge rate remains unchanged at low magnetic field intensity and decreases sharply as the magnetic field continues to increase. Song *et al.* (2012) confirmed the relationships above while investigating the settling mechanism of particles in a MSFB separator by carrying out free settling and quasi-zero settling tests on tracing particles.
MSFBs have visible limitations of requiring ancillary equipment such as magnetic coils and media with specific magnetization susceptibility. This potentially makes it more expensive than other fluidized bed techniques.

2.1.5.2 Vibrated Fluidized Beds (VFB)

Vibrated Fluidized Beds are a type of gas and solid fluidized bed system where an external vibrating force is introduced for the purpose of beneficiating fine coal, less than 6 mm. The vibration force is used to strengthen and maintain the contact between gas and solid phases, thereby improving the fluidization characteristics of the bed. A study conducted by Mohanta *et al.* (2013a) has shown that the quality of fluidization in a vibrated fluidized bed depends on parameters such as vibration frequency, gas flow rate and formation time of the bubble in the system.

Different investigations have been conducted on the mechanisms of energy transfer in a VFB, with respect to the use of an autogenous medium and the effect of agitation on characteristics of the bed (Wang *et al.*, 2016; Yang *et al.*, 2013; Wang *et al.*, 2000). Wang *et al.* (2000) investigated vibration energy transfer in a VFB, that is, from the vibrating base to the particle bed. The energy transfer in the VFB was found to be through pressure wave propagation and the dissipation of wave energy was mainly by the wave oscillation caused by wave reflection at the medium boundary (top and bottom). The same author also studied the effect of agitation on the fluidization characteristics of the bed, including bed density and average bubble rise velocity. The result obtained indicated that the bed pressure drop decreases while minimum fluidization velocity increases with an increased agitation speed. The fluidization performance measured by the standard deviation of the bed density fluctuation (δ) was as low as 0.0286 g/cm^3 at an agitation speed of N = 75 r/min. The study also showed a decreased bubble rise velocity at higher agitation speed proving that agitation enhances fluidization quality.

Yang *et al.* (2013) beneficiated fine coal (-6 mm) in a VFB using autogenous medium. The autogenous medium bed material was consisted of high ash coal mainly -1+0.5 mm and a small fraction of -0.5 mm. Separation efficiency with an Ep of 0.14 was achieved. Luo *et al.* (2008) investigated vibrational energy transmission and the interaction between vibration and gas flow. The results indicated that for a fine coal (-6 mm), a separation efficiency with an Ep value of 0.07 and uniform bed with a maximum relative error of 1.68% was achievable. The process limitations cited by Luo *et al.* (2008) include non-uniform transmission of vibration force due to interfering factors associated with large adhesive friction between the bed wall and the particles. It was also shown that back mixing increased with increasing vibration intensity which is a drawback in forming a stable bed. To limit the effects of the challenges described above, the VFB has to be operated with a shallow bed to ensure good fluidization. This has the definite effect of a reduced throughput capacity when compared to the ADMFB.

2.1.5.3 Dual Density Fluidized Beds (DDFB)

The Dual Density Fluidized Bed is a fluidized bed with a specifically designed bed structure. This structure consists of a pyramidal middle part and a smaller and larger rectangular prism in the lower and upper parts respectively. Two medium solids, magnetic pearls and magnetite was investigated by Luo *et al.* (2003) in beneficiation of coal range between -50+6 mm. The bed was designed to enable the segregation of the two medium materials by creating an upper low density layer of magnetic pearls and a lower high density layer of magnetite. The DDFB scheme had two separate areas, each with a different density formed in a fluidized cascade. For each separation area the density obtained was uniform and the magnitude was set to be able to achieve the three-product coal stream. In this case, for a feed coal (-50+6 mm), two clean coal products and one stream of gangue material were produced at a separating density of 1.49 g/cm^3 with a probable error (Ep) of 0.06 and separating density of 1.85 g/cm^3 with an Ep of 0.07, respectively (Luo *et al.*, 2003).

Wei *et al.* (2003) likewise investigated the DDFB using density tracers (substitute for coal), with magnetite and magnetic pearls as medium solids. The probable error in the upper and low density area was 0.06 for the 13 mm density tracers and 0.13 for the 6 mm tracers, respectively. One very clear limitation of the DDFB process is the need for a specifically designed fluidized bed which potentially makes the equipment and the process more expensive compared to an ordinary ADMFB.

2.2 AIR DENSE MEDIUM FLUIDIZED BEDS

In this study, an Air Dense Medium Fluidized Bed was investigated. ADMFB involves creating a medium by suspending solid particles in an upward airflow and the pseudo fluid created used as a beneficiation medium, whereby, the light (clean coal) and the heavy particle (shale) are stratified according to their densities in this medium (Mohanta *et al.*, 2012). The process has been investigated for a number of decades and some of the earliest work was patented as early as 1926 (Fraser and Yancey, 1926).

2.2.1 History of ADMFBS

In the last decade, a lot of significant research has been carried out with the aim of providing more information on the mechanism of ADMFB separation and how to improve the technique. Zhenfu and Qingru (2001) described the basic principle of separation in ADMFBs while analyzing coal. The author conducted a test on -50+6 mm coal using a 50 ton/hr ADMFB separator and magnetite powder was used as the solid medium to create a stable fluidized bed that achieved separation efficiency with an Ep value of 0.06. A feed coal (-50+6 mm) of about 21.48% ash was beneficiated in a magnetite bed, and a clean coal product of 11.80% ash and organic efficiency of 99.92% was obtained by Zhenfu *et al.* (2002).

Chen and Yang (2003) discussed the characteristics of different dry coal beneficiation techniques with emphasis on the uniqueness of ADMFB and its advantages. The advantages highlighted are: high precision; low investment; no water pollution; lower freight cost per gigajoule because of less moisture in coal and wide ranges of beneficiation densities.

Choung *et al.* (2006) conducted a study on the effect of coal feed size and bed height on separation efficiency. The author observed that particle sizes less than 1 mm are not effectively separated and separation efficiency only increases as bed height decreases. Good separation efficiency with an Ep of 0.03 for -5.6+3.35 mm size coal and Ep of 0.10 for -1+0.42 mm size coal was achieved by the author. It was also noted that the medium size fraction has to be distinct (in this case -106+45 µm) to enable ideal superficial gas velocity to be achieved and hence uniform bed density. The influence of low density cut was studied by Luo *et al.* (2007) on a feed coal of (-50+6 mm) using a magnetic pearls as the solid medium. The fluidizing characteristics of the magnetic pearls were determined for a specific size distribution and microbubble formation was also studied. A clean coal product with an ash content of 13.95%, tailing ash content of 56.82% and yield of 90.80% were achieved.

Zhao *et al.* (2010) using the Syamlal-O'Brien drag model simulated and studied the hydrodynamics of an ADMFB with a -0.3+0.15 mm Geldart B magnetite powder. Both experimental and numerical methods were used for the optimization of the solid medium in the fluidized bed. The magnetite was found to have good fluidization characteristics with a uniform and stable bed density, and there was a correlation between the experimental and the simulated results. The pilot bed utilized by the author demonstrated that a clean coal of 11.79% ash, Ep of 0.07 and a yield of 98.26% is obtainable from a feed coal (-50+6 mm) of 23.74% ash.

In the past five years, significant milestones have been reached towards the commercialization of ADMFB. Zhao *et al.* (2011) investigated a new modularized 40 – 60 ton/hr system which has lower construction and running costs compared to previous designs. A novel method for maintaining stability, uniformity and height of the fluidized bed was developed using a magnetite powder at -0.3+0.06 mm size fraction and fine coal of -1 mm. The experimental results were found to correlate with the data obtained from the numerical studies of the hydrodynamics. The separation results for -50+6 mm coal indicated separating densities of 1.33 g/cm^3 and 1.61 g/cm^3 with an Ep value of 0.05 and 0.06, respectively. The stability of the bed is one of the key requirements for efficient separation. Sahu *et al.* (2011) investigated the stability of an ADMFB separator by characterizing it using different expressions like pressure drop ratio, fluidization index, particulate expansion function, Froude number and Reynolds number. The pressure drop ratio was observed to be the best indicator to verify the stability of the bed. The author also scaled up the process from laboratory to pilot scale (600 kg/hr) while beneficiating an Indian coal with a high near gravity material (NGM) in the density range of 1.4 – 1.7 g/cm^3. The feed coal (-25+6 mm) ash content was reduced from 40% to (32 – 35.5%) with a yield of (60 – 72%).

A study aimed at expanding the choice of medium solids for ADMFB coal separation at low density with good physical properties and at low cost was conducted by Zhao *et al*. (2011). The author investigated the physical properties of a medium solid called paigeite powder and its gas-solid characteristic in a fluidized bed. In addition, the effect of the medium size ranges for effective separation and for developing a blend that could result into the most efficient separation was conducted. Paigeite powder of -0.3+0.074 mm size range was used to separate -13+6 mm coal at a separation efficiency (Ep) of 0.075. The coal ash was reduced from 22.37% to 9.88% with a clean coal recovery of 60.64%.

The effect of feed coal size on separation efficiency has been investigated by several authors (Chikerema and Moys, 2012; Firdaus *et al.*, 2012; Mohanta *et al.*, 2011). Mohanta *et al.* (2011) conducted a study in which they developed a model which predicts the relationship between sharpness of separation and feed size. Three feed coal sizes were used, i.e., -50+25 mm, -25+13 mm and -13+4.75 mm. The results revealed that the separation of both coal at -50+25 mm and -25+13 mm size fraction has lower Ep values. This finding was supported by the model developed by the author showing that Ep decreases with an increasing feed size until it becomes fairly constant and shows no size effect above 25 mm. Firdaus *et al.* (2012)

investigated the effect of particle size and bed height on the separation efficiency of ADMFB as measured by cut-point and probable error. A silica/zircon mixture of 75:25 wt.% ratios was used as the solid medium material while bed heights of 10 cm and 15 cm were investigated. The feed coal size fractions were -10+5 mm, -14+10 mm, -20+14 mm, -25+20 mm and -31.5+25 mm. The results obtained showed that the deeper bed (15 cm) and the smallest particle size (-10+5 mm) had the highest probable error of 0.19 compared to 0.06 for the shallower (10 cm) bed. This demonstrated that particle size and bed height have a strong influence on separation efficiency.

Zhao *et al.* (2015) also investigated the effect of solid medium particle size on the stability of the fluidized bed density. Magnetite at different size ranges of (-0.4+0.3 mm, -0.3+0.225 mm, -0.225+0.15 mm and -0.15+0.074 mm) were tested in order to establish the size that gives the most effective fluidization characteristics for fine coal separation. The optimum magnetite size range with a low minimum fluidization velocity for fine coal (-6+3 mm) separation was found to be that of -0.15+0.74mm fraction. Coal products with ash contents of 19.55% and 60.01% were achieved at the top and bottom layers of the bed, respectively. A similar study was likewise conducted by Fu *et al.* (2016) using magnetite in the same four size ranges (-0.4+0.3 mm, -0.3+0.225 mm, -0.225+0.15 mm and -0.15+0.074 mm). The result obtained shows that the magnetite with the smallest particle size range (-0.15+0.074 mm), produces the most effective separation. The ash content and total sulphur was reduced from 45.92% to 31.29% and 3.02% to 2.57%, respectively, with a clean coal yield of 27.33%.

An investigation into the effects of feed coal particle size, particle density and particle shape on performance of an ADMFB was conducted by Chikerema and Moys (2012). The results of this study showed that the coarser particles (-53+37 mm and -31.5+22 mm) separated more efficiently than finer particles (-22+16 mm and -16+9.5 mm). Probable error (Ep) of 0.05 was obtained for the -53+37 mm and -31.5+22 mm size fraction, and at a stable cut density. The -22+16 mm and -16+9.5 mm fraction was found with a fluctuating cut density and higher Ep of 0.07 and 0.11 respectively. The author also demonstrated the effect of particle shape on the ADMFB separation. They found the separation of particles with blockish shape to be faster and with low and constant Ep value of approximately 0.10 compared to the flat and sharp-pointed prism shaped particles. A model was also developed by Mohanta *et al.* (2012) to predict the relationship between the minimum fluidization velocity and the size of the solid magnetite powder without running the experiments. Based on this model, the author found that a strong correlation does exist between the minimum fluidization velocity and the particle size of the medium (magnetite powders) utilized.

With vast research having been performed to look into the feasibility of dry beneficiation of coal using the ADMFB process, optimization of the procedure has become significant. Mohanta, *et al.* (2013b) conducted an optimization test on three key operating parameters (i.e. superficial gas velocity, bed height and coal to magnetite ratio) of an ADMFB separator to determine the response of product ash and combustible recovery. The aim of the study was to determine the correlation between various operating parameters and their combined effect on ADMFB performance, without using the traditional "one variable at a time approach". The results obtained from this investigation showed that the optimum conditions achieved were: 18.94 – 20.42 cm/s superficial velocity, 25.94 – 29.36 cm bed height and 0.02 coal to magnetite ratio. An Ep value of 0.115, ash content reduction from 39.14% to 32% and combustible recovery values ranging between 31.1% and 77.42% was obtained under the set conditions.

Azimi *et al.* (2013) studied the factors affecting the beneficiation of a low ash lignite coal using ADMFB. An investigation on the effect of superficial velocity (V), residence time (T), and bed height (H) on the performance of the separator was carried out. The results revealed that all the three variables had a negative effect on the organic material recovery to clean coal product, i.e. each variable inversely affected the organic material recovery. The order of influence of these operating variables on recovery was H > V > T. Maximum recovery was achieved at optimum conditions of 15 cm/sec, 90 sec and 15 cm for V, T, H, respectively. A clean coal of approximately 10.6% ash and yield of 86% was obtained from a feed coal of 14.4%. The effect of the different cross sectional shape of the fluidized bed (circular, square and rectangular) on the stability characteristics of the bed was investigated by Sahu *et al.* (2013). The degree of the bed stability was measured using the fluidization index, particulate expansion, pressure drop of bed and distributor, minimum fluidizing and bubbling velocity. The author found that the stability of the bed increases with an equivalent aspect ratio and the rectangular shaped bed had the best stability.

The influence of blending ratio on solid medium (paigeite and magnetite) for ADMFB separation was investigated by He *et al.* (2013). The study revealed that if two individual solid medium cannot provide an effective fluidization characteristic, a blend of the two can be obtained through a mathematical model to achieve the desired ratio with a stable bed. A bed with a blend of magnetite/paigeite (70/30 by weight) was used to reduce a feed coal ash (33.43%) at a particle size of (-13+6 mm) to 11.63%, with an Ep of 0.07 and a recovery efficiency of 98.59%.

Research work by different authors over the past decades has developed the foundation for the ADMFB coal separation with the ultimate goal being the industrial application of this technology. The recent investigation by Zhao *et al.* (2016) presents the current finding on the suitability of ADMFB for industrial application using a large scale (40 – 60 ton) plant. The solid medium utilized by the separator was a blend of magnetite powder (-0.3+0.06 mm) and fine coal (-1 mm). A clean coal product of 3.46% ash, a yield of 67.88% and an Ep value of 0.05 was attained from a feed coal of about 23.98% ash. According to the author, the cost of operating this plant was $2 per ton of raw coal and the solid medium loss during operation was 0.42 kg per ton of coal processed. A photograph of the plant is depicted in Figure 2-2 and its operational flowsheet in Figure 2-3 below.

Figure 2-2: World's first modularized dry coal beneficiation plant (Source: Zhao et al., 2016)

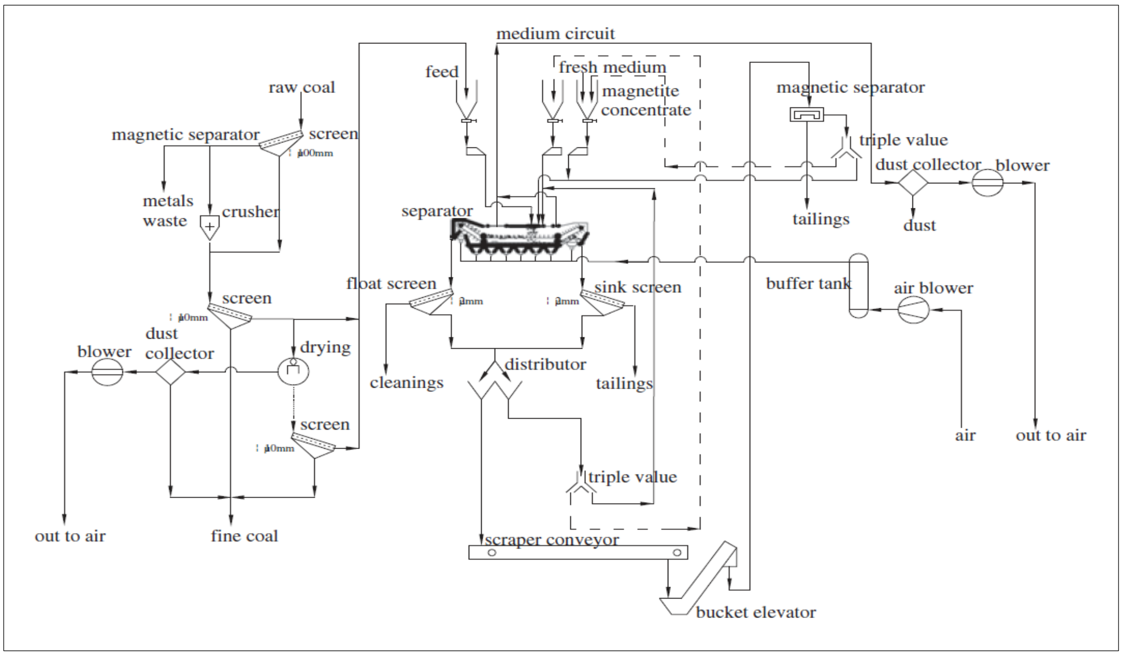

Figure 2-3: Engineering flowsheet of the modularized system (Source: Zhao et al., 2016)

2.3 THE THEORY OF FLUIDIZATION

2.3.1 Geldart classification of powders

Geldart (1973) classified the behavior of solids fluidized by gases into four clearly recognizable groups characterised by the density difference between the particles and the fluidizing medium ($\rho_p - \rho_f$), and by the mean particle size(d_p). The density of the particles and the density of the fluidizing medium is represented by (ρ_p) and (ρ_f), respectively. The particles, which are in powder form are grouped into A, B, C and D.

Group A: This group represents powders that are aeratable and fluidize well. The fluidized beds formed from materials in these groups experience significant bed expansion before bubbling commences and when the gas supply is cut off, the collapsing of the bed is slow. These beds have circulation that also results in rapid mixing (Geldart, 1973). The powders in this category have a small mean particle size (30 – 100 µm) and/or low particle density (less than about 1.40 g/cm^3).

Group B: Most powders within this category have a mean particle size of 40 – 500 µm and density in the range of 1.4 – 4.0 g/cm^3. Unlike Group A powders, these powders have smaller bed expansion and bubbling occurs slightly above minimum fluidization velocity. Slugging may occur under this group as a result of very large bubbles formed in the system. In addition, coalescence is predominant with bubbles rising faster than the interstitial gas velocity. The most typical powder in this group is sand, and when used, the bed is seen to collapse rapidly when the gas supply is shut off (Geldart, 1973).

Group C: The powders are cohesive and difficult to fluidize, and do rise as a plug in small diameter tubes or channeling. The effect may be minimized by stirring and agitation of the medium. With these powders there is no bubble formation. The inter particle forces are greater than those a fluid can exert on the particle resulting in this phenomenon. The mean particle size is very small typically less than 30 µm (Geldart, 1973).

Group D: Powders in this group have the largest mean particle size (1000 µm) and highest density (> 4.0 g/cm^3). The minimum fluidization velocity is high and huge bubbles are formed during fluidization. The gas velocity in the dense phase is high, solids mixing relatively poor; consequently back-mixing of the dense phase is small. The Geldart's classification of the powders is summarised in Figure 2-4 below.

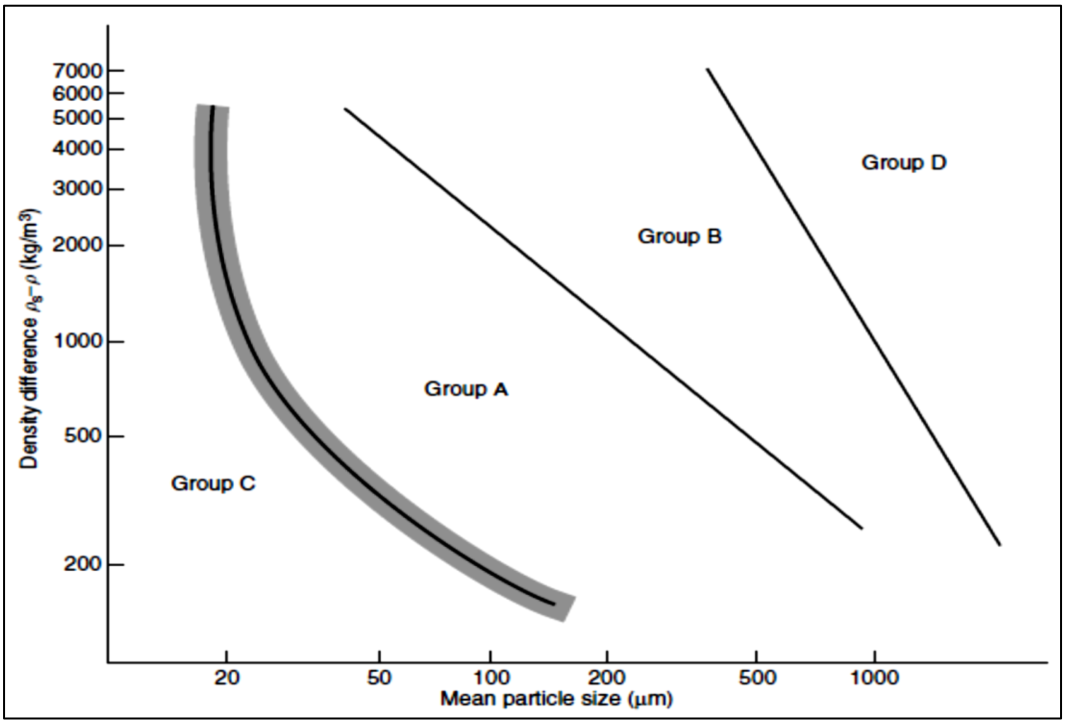

Figure 2-4: Powder fluidization classification diagram (Richardson et al., 2008)

2.3.2 Fluidization regimes

The fluidization regimes that occur in fluidized beds are classified as either particulate (smooth) or aggregative (bubbling). Liquid fluidized beds exhibit particulate fluidization where the solid particles disperse relatively uniformly in the fluidizing medium. Air Dense Medium Fluidized Beds which are gas fluidized beds exhibit heterogeneous or bubbling fluidization and voids/bubbles containing no solids are observed in the bed. The gas fluidized beds like the ADMFB have a number of distinguishable regimes of fluidization such as fixed bed, particulate fluidization, bubbling fluidization, slugging fluidization and turbulent fluidization (Yang, 2003). These regimes are associated with the increase in gas superficial velocity in the fluidized bed, as described below by Richardson *et al.* (2008).

Fixed bed: This occurs at the lowest superficial gas velocities where particles in the bed remain in contact with each other and the bed structure is stable. The stable phase continues until the velocity is increased to the point where the pressure drop is equal to the weight per unit area of the particles.

Particulate fluidization: Under this regime, a uniform bed expansion at high velocity does take place, but this type of fluidization may not be clearly visible due to the bed transition to the bubbling phase.

Bubbling regime: This is characterised by bubbles passing through the bed as high gas velocities are achieved and it results in rapid mixing of the dense particulate phase.

Turbulent regime: Occurs in the bed where there is a coalescence of the gas bubbles and the bed becomes chaotic.

Fast fluidization: This represents the level of highest superficial gas velocity, where the bed begins to transport particles in a vertically upward position. All the regimes described above can be seen as depicted in Figure 2-5 below.

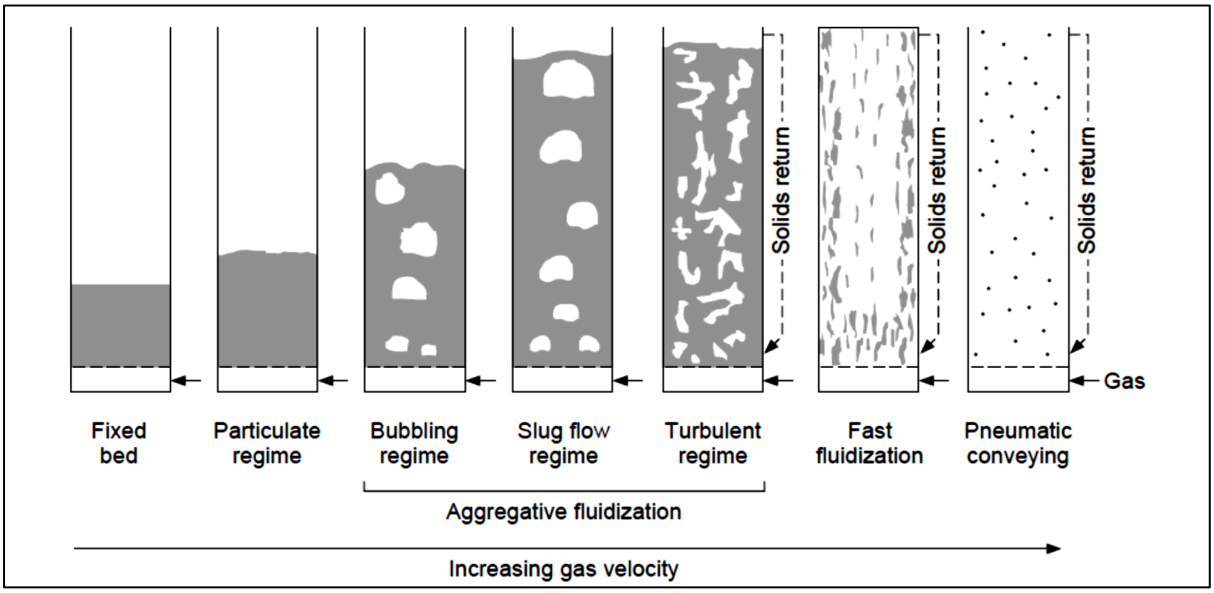

Figure 2-5: Fluidization regimes (Source: Perry et al., 1997)

2.3.3 Effect of gas velocity on fluidization regimes

The type of fluidization regime that occurs in a system is a function of the relationship between the gas velocity, medium particle size and medium density. Therefore, the transition can be explained using Geldart's classification of powders. For Group B and Group D powders, bed transition from fixed fluidized bed to bubbling fluidized bed occurs when the gas velocity exceeds the minimum fluidization velocity of the system. Group A powders however, behave differently, the bed will expand homogeneously and no bubbles will be observed until the minimum bubbling velocity is exceeded. Homogeneous expansion only occurs in Group A powders. In summary, the transition point from fixed bed to bubbling regime for Group B and Group D powders occurs at minimum fluidization velocity, while for Group A powders it is at the minimum bubbling velocity (Yang, 2003). Figure 2-6 below shows the transition of regimes with increasing gas velocity.

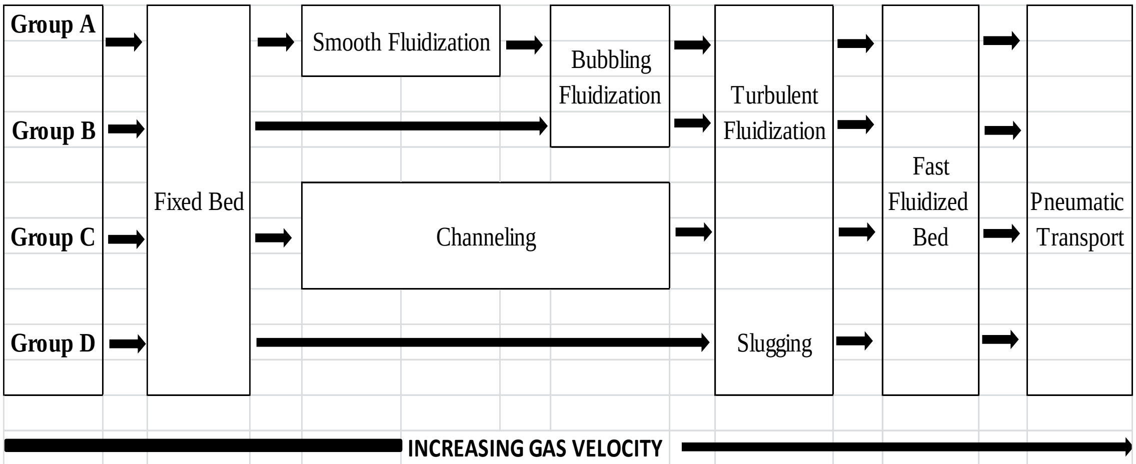

Figure 2-6: Flow regime map of powders (De Vasconcelo et al., 2011)

2.3.4 Minimum fluidization velocity

The minimum fluidization (U_{mf}) velocity is defined in terms of fluidization regimes as the transition point from fixed bed to the bubbling regime for Group B and Group D powders. At this point in ADMFB separation all the solid medium particles are essentially supported by the gas stream. Mohanta *et al.* (2012) consider the minimum fluidization velocity of a medium particle to be one of the most important hydrodynamic parameters that strongly influence the design of a separator, making its accurate prediction important. The author attempts to develop a suitable correlation for accurate prediction of the minimum fluidization velocity of magnetite powder. The minimum fluidization velocity required for an efficient separation in the bed can be determined by either a theoretical method or by experimentation. The experimental route involves fluidizing particles in a fluidized bed and taking pressure drop measurements as the superficial velocity increases. The data collected is used to plot a pressure drop versus velocity graph and the minimum fluidization velocity can be determined from the plot as shown in Figure 2-7 below.

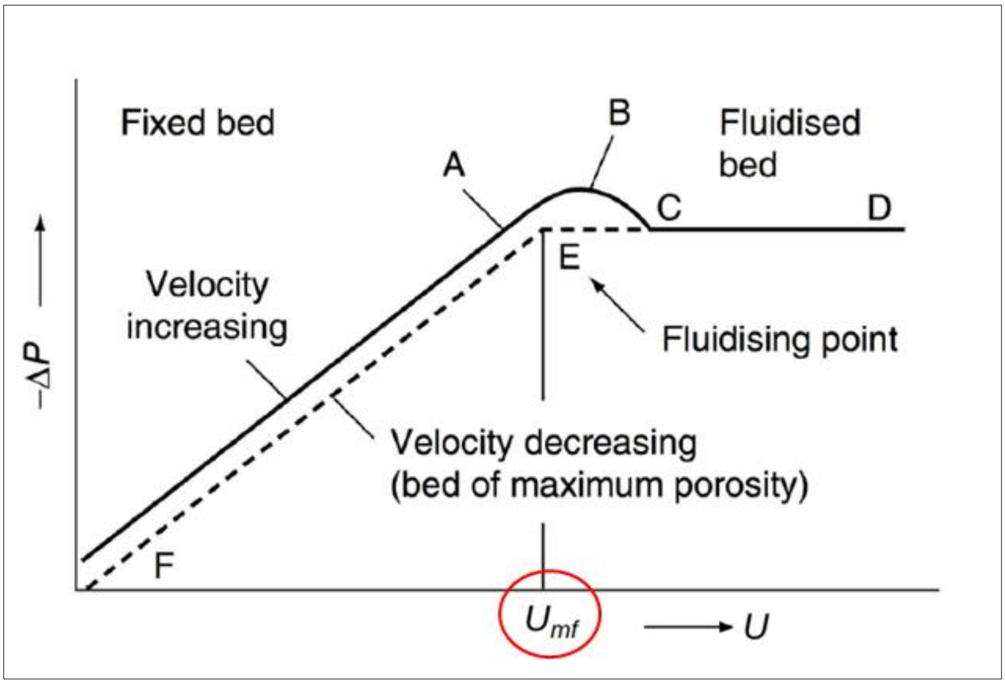

Figure 2-7: Pressure drop vs superficial velocity diagram (adapted from Richardson *et al*. (2008))

2.3.5 Bed density

One of the factors influencing the efficiency of separation performance of an ADMFB is the distribution of the density stratification. The pseudo fluid characteristics in an ADMFB separator form a gas-solid suspension with a certain bulk density and average density of the bed (ρ_b) given by Sahu *et al.* (2009):

$$\boldsymbol{\rho_b = (1-\varepsilon)\rho_s + \varepsilon\rho_a = W/(LAg)} \qquad \textit{Equation 2-1}$$

Where:

ε is the bed porosity, fraction;

ρ_s and ρ_a are the density (kg/m^3) of the medium and air, respectively.

L (m) is the depth of the bed

A is cross sectional area (m^2) of the fluidized system

g is acceleration due to gravity (m/s^2)

W is the total weight (kg) of the medium.

Equation 2-1 may be used in calculating the average bed density of a bed, and there are other experimental methods that can be applied in determining the density of an ADMFB separator. He *et al.* (2003) studied the density of an ADMFB separator using the differential pressure method. A density device designed by the author was used to measure the pressure in the air fluidized bed utilized and this was correlated with the bed density. A mathematical method was also developed to study the correlation between the bed density and the fine coal used in the bed. In the same study, the author also conducted a horizontal and vertical density distribution test, using their findings to explain the principle of the density stratification phenomenon. Investigation conducted by Chikerema (2011) showed how the density distribution in the bed from the bed pressure drop can be determined. The method involved plotting the pressure drop data against the corresponding bed levels, and the gradient obtained from the graph was used to calculate the bed density distribution.

2.3.6 Bed stability

For effective separation to take place a stable bed is required. The stability can be measured using different expressions such as the pressure drop ratio, Reynolds number of particle, Froude number of particle, particulate expansion and fluidization index (Sahu *et al.*, 2011). The stability of a system is considered stable when the system is operating between minimum fluidization velocity and minimum bubbling velocity. One of the stability characterization parameters is the fluidization index which is the ratio of minimum bubbling velocity to minimum fluidization velocity. The minimum fluidization velocity is always less than the minimum bubbling velocity, and the ratio is in the range of 1 – 2. For a greater stability region, the fluidization index has to be as high as possible.

Sahu *et al.* (2013) conducted a study on series of methods to characterise the stability of a fluidized bed through expressions like particle expansion function, Froude number, fluidization index, Reynolds number and pressure drop ratio. A ratio of the expanded bed height to the initial static bed height obtained by the author provided the information on characterizing the fluidized bed and scaling up of the equipment. Another stability characteristic is a pressure drop ratio, which is a ratio of distributor pressure drop and bed pressure drop(P_d/P_b).

2.3.7 Solid medium materials

The solid medium material used in an ADMFB separator contributes to the characteristics and effective separation of the particles in the bed. Some of the medium's most critical physical properties are its density and its particle size distribution, which determines the average bed density of the fluidized bed. Other characteristics include hardness and magnetism which affect the recoverability and consumption of the media.

From Equation 2-1 above, since ρ_a is much smaller than ρ_s, it can be seen that bed density:

$$\boldsymbol{\rho_b = (1 - \varepsilon)\rho_s} \qquad \textit{Equation 2-2}$$

Therefore, fluidized bed density is dependent on the void fraction (ε) and the density of the solid medium (ρ_s), and this can be adjusted by varying these two parameters. The bed density can be manipulated by varying the solid medium materials (materials of different density) and the particle size range to expand the density range of the bed (Zhao *et al.*, 2011). Blending of solid medium materials has also been used to create fluidized beds with the desired average bed density. He *et al.* (2013) showed the effectiveness of utilizing mixed medium solids (paigeite and magnetite blend) in a fluidized bed. The blend of paigeite-magnetite medium achieved superior fluidization characteristics and higher separation efficiencies compared to each separate sole medium material.

2.4 AIR DENSE MEDIUM MATERIAL

As highlighted in section 2.3.7 above, the material used as a dense medium in a fluidized bed contributes to the characteristics of the fluidized bed. In this study alternative materials to magnetite were studied to determine which material could give the most effective separation of coal and consequently be used as a substitute to magnetite. These materials, including magnetite are reviewed below.

2.4.1 Magnetite for air dense medium separation

Magnetite has been used for many years in the conventional wet beneficiation of coal and this is mainly due to its physical and chemical properties. The attributes which make it suitable for wet beneficiation and now consequently dry dense medium separation are:

I. Excellent chemical inertness
II. High specific gravity (at least 4 700 kg/m^3) to give the required average bed density
III. Wear resistance
IV. Easy recoverability and regeneration by magnetic separation due to its high magnetic content.

The magnetite used in wet dense medium coal separation process is however finer (> 70% passing 45 µm) compared to that typically used in the dry dense medium process. De Korte (2014) showed that the magnetite that is currently in use at a commercial dry dense medium separation plant (50 ton/hr) in Shenhua China is coarser than that which is used in wet beneficiation plants in South Africa. Table 2-1 below shows the size distribution of the Shenhua magnetite.

Table 2-1: Size analysis of magnetite used at Shenhua (De Korte, 2014)

Screen Size (µm)	**Circulating medium**	
	Fractional %	**Cumulative %**
+1000	4.7	4.7
- 1000 + 500	3.7	8.4
- 500 + 250	17.5	25.9
- 250 + 125	29.2	55.1
- 125 + 75	34.3	89.4
- 75 + 45	9.0	98.4
- 45 + 0	1.6	100.0

The magnetite particle size suitable for ADMFB application can be derived from the Geldart fluidization classification as seen in Figure 2-4 above. Mohanta *et al.* (2012) states that for an effective separation to take place, the magnetite particles should be able to fluidize easily, and should be in a different Geldart group to coal. Calculated particle size ranges for coal and magnetite of different Geldart groups are shown in Table 2-2 below.

Group C and A are unsuitable as they are difficult to fluidize and are prone to back-mixing of coal particles, respectively. The suitable size range is that of Geldart B group (-425+45 µm) (Mohanta *et al.*, 2012). Other authors who have studied ADMFB have used magnetite in different size ranges with the majority falling within the same -425+45 µm category. However, the demand for magnetite has increased because of its use in other industries such as steel making and catalysis, as well as in conventional wet coal beneficiation processes. For these reasons, the cost and supply of magnetite may well become of concern for those installing ADMFB in future (Honaker and Bimpong, 2009).

Table 2-2: Magnetite and coal size ranges per Geldart group (Mohanta et al., 2012)

	Particle size range (µm)			
Geldart Group	**C**	**A**	**B**	**D**
Magnetite (ρ_s = 5.2 g/cm^3)	< 20	20 – 43	43 – 438	> 438
Coal (ρ_s = 1.2 g/cm^3)	< 23	23 – 187	187 – 913	> 913
Coal (ρ_s = 1.7 g/cm^3)	< 21	21 – 132	132 – 767	> 767

* Density of air (ρ_s) = 0.0012 g/cm^3

2.5 ALTERNATIVE AIR DENSE MEDIUM MATERIAL

The alternative materials discussed in this study were pyrrhotite, silica sand, granulated blast furnace slag and coal rejects.

2.5.1 Pyrrhotite ore

Pyrrhotite ($Fe_{(1-X)}S$) is one of the most commonly occurring metal sulfide minerals and is recognized in a variety of ore deposits including nickel-copper, lead-zinc and platinum group elements. The pyrrhotite is rejected to the tailings in many nickel processing plants and this is done to control circuit throughput and concentrate grade, consequently reducing sulfur dioxide emission (Becker, 2009). Pyrrhotite is known to naturally occur in different forms with varying physical and chemical attributes. There are two forms of pyrrhotite; magnetic (Fe_7S_8) and non-magnetic pyrrhotite (Fe_9S_{10}, $Fe_{10}S_{11}$ and $Fe_{11}S_{12}$). The principal nickel ore mineral, i.e. pentlandite, almost ubiquitously occurs with pyrrhotite (Becker, 2009).

2.5.1.1 Magnetic pyrrhotite

The magnetic form of pyrrhotite is referred to as the 4C monoclinic pyrrhotite which has unit cell parameters of *c* equal to four times the dimension of *c* in the NiAs unit cell, with unit cell parameters of $a = 2\sqrt{3}\mathbf{A}$, $b = 2\mathbf{A}$, $c = 4\mathbf{C}$ where **A** and **C** represent the NiAs sub cell dimensions. This is based on the hexagonal structure of the mineral nickeline/niccolite (NiAs) and the nomenclature of the various pyrrhotite superstructures is based on the unit cell parameters of the NiAs structure (Wyckoff, 1963). The ideal composition of magnetic 4C pyrrhotite is Fe_7S_8 which is a compositional range between 46.6 and 46.9 atomic % iron (Carpenter and Desborough, 1964). The formula Fe_7S_8 can also be described as $Fe_2^{3+}Fe_3^{2+}S_8$ to account for the non-stoichiometry in the pyrrhotite structure (Bertaut, 1953). Becker (2009) states that 4C magnetic pyrrhotite is one of the most commonly documented pyrrhotite forms in natural terrestrial occurrences. However, a study by Arnold (1967) shows that naturally occurring mixtures of 4C and non-magnetic NC pyrrhotite are far more common (73% of samples analyzed from different geographical locations around the world). Non-magnetic NC pyrrhotite structure is a mixture of ferric and ferrous iron and the NC are similar to the magnetic 4C as follows: $Fe_7^{2+}Fe_2^{3+}$, $Fe_8^{2+}Fe_2^{3+}S_{11}^{2-}$, $Fe_9^{2+}Fe_2^{3+}S_{12}^{2-}$ (Becker, 2009).

2.5.1.2 Nkomati Mine Pyrrhotite

The pyrrhotite sample used in this study was collected from the Main Mineralized Zone (MMZ) of the Nkomati Nickel Mine (Uitkomst Complex) situated in the Mpumalanga province, near Badplaas. Becker (2009) investigated the mineralogy and crystallography of the pyrrhotite from selected nickel ore deposits including Nkomati Mine. Four samples were collected and analyzed by the author from the Nkomati mine, two each from the Massive Sulfide Body (MSB) and the Main Mineralized Zone (MMZ). Results from this investigation revealed that after treatment with a magnetic colloid, one sample (MMZ-1) was entirely magnetic while another (MMZ-4) had inter-grown magnetic and non-magnetic pyrrhotite. It was also observed that there was variability in the relative proportion of magnetic to non-magnetic pyrrhotite in the MMZ-4 sample.

Furthermore, the iron and sulphur content determined from the magnetic pyrrhotite sample MMZ-4 is similar in composition to that of magnetic pyrrhotite from MSB, and both were found to coexist with magnetic pyrrhotite. The MMZ-1 sample (magnetic pyrrhotite) was found to exist solely, with less iron content (58.4 – 59.3 wt.% Fe) compared to other Nkomati magnetic pyrrhotite (59.1 – 60.2 wt.% Fe). The sulfur content on the other hand was the same in MMZ-1 and MMZ-4 samples (39.0 – 39.9 wt.% S). The nickel content showed that the

MMZ-4 sample generally had less nickel (0.26 – 0.67 wt.% Ni) compared to magnetic pyrrhotite, MMZ-1 sample (0.66 – 1.20 wt.% Ni). The metal/sulfur ratios (Figure 2-8) distribution based on the mineral chemistry was also developed by the same author. The results showed that all the magnetic pyrrhotite from Nkomati were similar in composition in terms of their atomic metal composition. The magnetic pyrrhotite from Nkomati had an ideal composition close to Fe_7S_8 based on the metal/sulfur ratio of 7.00 – 7.05 per 8 sulfur units for the MSB, and 6.90 – 6.95 per 10 sulfur units. The non-magnetic metal/sulfur ratio was found with 8.90 – 8.95 per 10 sulfur units. Therefore, magnetic Fe_7S_8 and non-magnetic Fe_9S_{10} were identified for the Nkomati pyrrhotite.

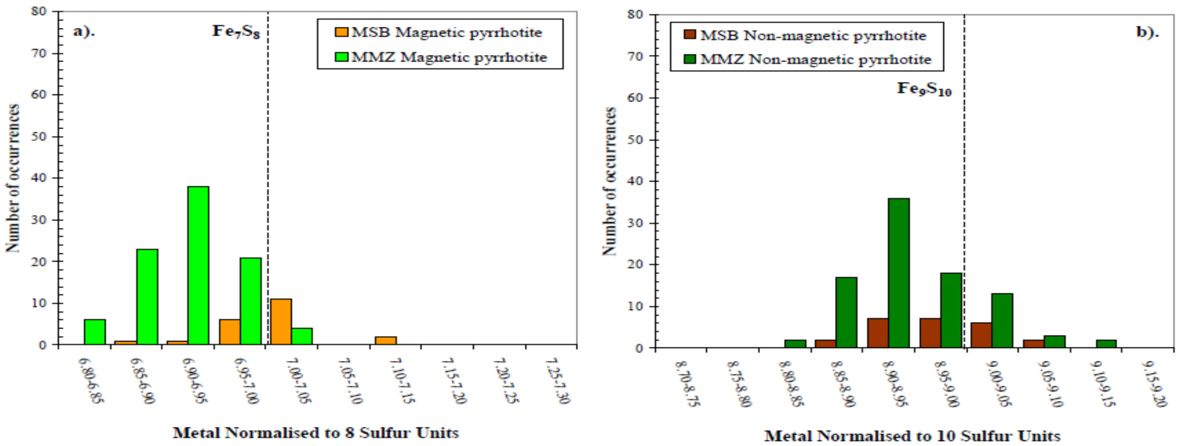

Figure 2-8: Metal/sulfur ratios normalized to differing sulfur contents for (a) Nkomati magnetic and (b) non-magnetic pyrrhotite (Becker, 2009)

Therefore, the proven existence of magnetic pyrrhotite at Nkomati mine made it attractive and potentially suitable for use as an air dense medium material. This was coupled with the fact that pyrrhotite is considered a reject in the processing of nickel making it an available and cheap alternative.

2.5.2 Granulated Blast Furnace Slag

2.5.2.1 Blast Furnace slag

Blast furnace slag is a byproduct in the production of molten pig iron. The form of the slag produced is dependent on the method used to cool the molten slag. The slags produced are classified as granulated blast furnace slag (GBFS), air-cooled blast furnace slag (ACBFS), pelletized slag and expanded or foamed slag.

- **ACBFS**: This is a hard lump crystalline structure formed as a result of the slow cooling of slag under ambient conditions.
- **Expanded/Formed Slag**: This is a slag that is of high porosity and low bulk density compared to ACBFS. It is formed by cooling in water, air or steam under a controlled cooling agent, which allow accelerated cooling and solidification.
- **Pelletized slag**: It is in the form of pellets which are produced through water and air cooling in a spinning drum. The process can be controlled to produce either more vitrified (glassy) or more crystalline pellets, both of which have different uses.

2.5.2.2 Granulated Blast Furnace Slag Production and Properties

GBFS is formed when the molten slag is rapidly cooled with high pressure water or in a pond of water. This forms a granular and almost fully non-crystalline granulated slag. The slag composition changes depending on ores, fluxing agents and coke feed impurities (Özbay *et al.*, 2016). Usually more than 95% of the blast furnace slag's composition consists of silica, calcium, magnesium and oxygen. Özbay *et al.* (2016) showed that the typical GBFS chemical composition differs with the countries it was produced. Table 2-3 below shows the typical chemical composition of GBFS .

Table 2-3: Typical chemical composition of GBFS (Özbay et al., 2016)

Chemical composition (%)	**USA**	**South Africa**	**Turkey**
CaO	29 – 50	30 – 40	34 – 41
SiO_2	30 – 40	30 – 36	34 – 36
Al_2O_3	7 – 18	9 – 16	13 – 19
Fe_2O_3	0.1 – 1.5	-	0.3 – 2.5
MgO	0 – 19	8 – 21	3.5 – 7
MnO	0.2 – 1.5	-	1 – 2.5
S	0 – 2	1 – 1.6	1.2
SO_3	-	0	-

The GBFS used in this study was obtained from ArcelorMittal Newcastle Works, South Africa. The flowsheet in Figure 2-9 shows the iron and GBFS production process at this facility.

The fluid slag is granulated at the blast furnace by tapping the hot slag onto a high-pressure water stream. The product (which has a sandy appearance) is pumped into a settling dam. It is then reclaimed from the slag bay, and left to stand for drying. A sample of the molten slag is collected before granulation and the typical chemical composition of this slag is shown in Table 2-4 below.

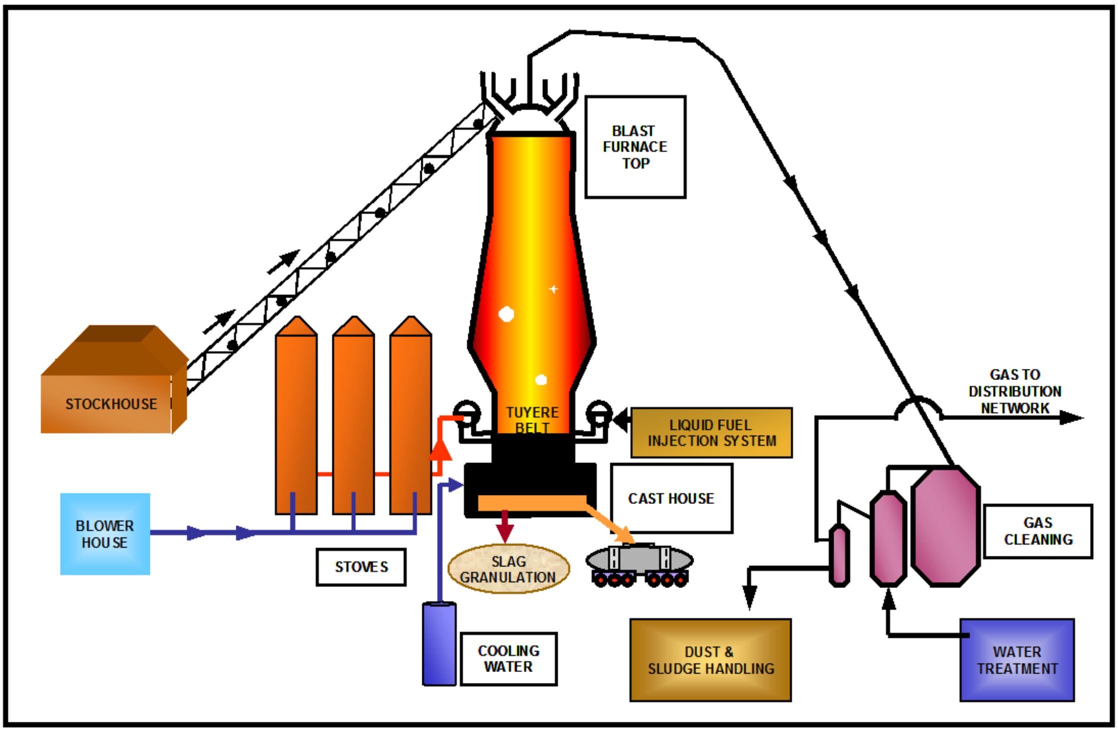

Figure 2-9: Blast Furnace N5 Process Flow (Source: ArcelorMittal Newcastle Works)

Table 2-4: Typical chemical composition of blast furnace N5 (Source: ArcelorMittal Newcastle Works)

Element	CaO	SiO_2	Al_2O_3	FeO	K_2O	MnO	MgO	Na_2O	S	TiO_2	Zn
Composition (%)	34.4	37.5	13.6	0.4	0.9	0.6	10.3	0.4	0.9	1.0	0.3

Granulated blast furnace slag is generally inert with a basicity of 0.92, and is a by-product of iron making process at ArcelorMittal Newcastle Works. The GBFS is sold at ZAR 56.00 per tonne making it an affordable alternative to magnetite; therefore, it was worth considering GBFS in this study.

2.5.3 Coal rejects

Coal rejects/discards are the gaunge product produced as a result of the coal (Run-of-Mine) beneficiation process. The coal discard used in this study was sourced from Greenside Colliery, Mpumalanga and the typical characterization test results of these rejects are shown in Table 2-5 below.

Table 2-5: Physico-chemical properties of coal discard

Proximate analysis (wt%, Ar)	
Fixed Carbon	7.97
Volatile Matter	12.64
Ash Content	78.31
Moisture	1.08
Ultimate analysis (wt%, Db)	
Hydrogen	1.69
Nitrogen	0.28
Carbon	11.26
Sulphur	0.32
Oxygen	86.77
Calorific value (MJ/kg)	1.84

* Ar: As received; Db: Dry basis; Oxygen: 100-(H+C+N)

2.5.3.1 Coal Rejects in South Africa

The Department of Mineral Resources (DMR) estimated the total volume of discard coal at more than a billion tonnes a decade ago (DME, 2001). The annual production was said to almost equal the volume of exported coal. Figure 2-10 below shows that the amount of coal rejects generated can be assumed to be 90% of the export volume per annum on average.

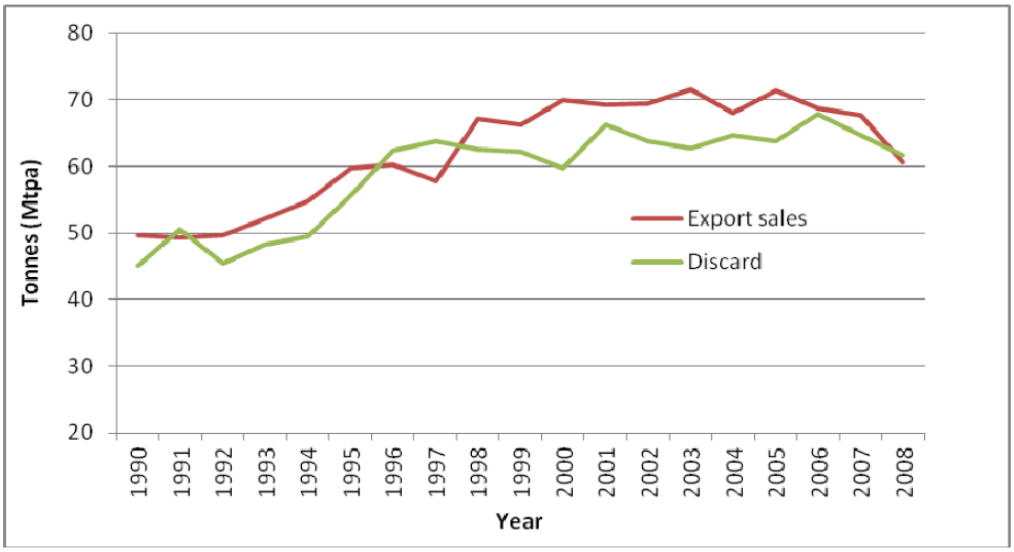

Figure 2-10: Comparison of discard coal and export volumes (Source: Le Roux, 2014)

Le Roux (2014) estimated the quantities of discard coal in South Africa using export coal volumes. The volume of coal rejects in the country was extracted from existing databases, and this information was based on the yield percentages of export coal after beneficiation and updated in terms of current and future production. That is, the information from the database was based on the assumption that, for a typical coal washing plant, 70 – 80% of the Run-of-Mine product is the total average yield of saleable coal product (export quality coal and middling combined) with 20 – 30% representing coal discards as generated in the process. Le Roux (2014) collated various company annual reports (2011/2012) to provide details on coal export volumes and the probable discard production from the various collieries belonging to those companies. Table 2-6 below provides the figures on the estimated volume of usable discard produced within the Witbank coalfields.

Table 2-6: Estimated usable discard production – Witbank coalfield (Le Roux, 2014)

<table>
<tr><th>Mine</th><th>Owner</th><th>Export volume (Mtpa)</th><th>Est. yield² (%)</th><th>Est. discard (Mtpa)</th></tr>
<tr><td>Arthur Taylor Colliery (ATC)</td><td>X-strata</td><td rowspan="2">3.60</td><td>58%</td><td rowspan="2">2.70</td></tr>
<tr><td>Arthur Taylor Opencast Mine - (ATCOM)</td><td>X-strata</td><td>58%</td></tr>
<tr><td>Goedgevonden Colliery</td><td>X-strata</td><td rowspan="2">8.70</td><td>55%</td><td rowspan="2">6.53</td></tr>
<tr><td>Tweefontein Complex</td><td>X-strata</td><td>55%</td></tr>
<tr><td>Goedehoop Colliery</td><td>Anglo</td><td>5.20</td><td>53%</td><td>3.90</td></tr>
<tr><td>Greenside Colliery</td><td>Anglo</td><td>2.90</td><td>58%</td><td>2.18</td></tr>
<tr><td>Kleinkopje Colliery</td><td>Anglo</td><td>1.70</td><td>70%</td><td>1.28</td></tr>
<tr><td>Landau Colliery</td><td>Anglo</td><td>3.80</td><td>58%</td><td>2.85</td></tr>
<tr><td>Mafube Colliery</td><td>Anglo</td><td>1.40</td><td>74%</td><td>1.05</td></tr>
<tr><td>Inyanda Coal Mine</td><td>Exxaro</td><td>1.50</td><td>70%</td><td>1.13</td></tr>
<tr><td>Klipspruit Colliery</td><td>BHP Billiton</td><td>3.00</td><td>90%</td><td></td></tr>
<tr><td>Middelburg/Wolvekrans</td><td>BHP Billiton</td><td>11.00</td><td>71%</td><td>8.25</td></tr>
<tr><td>Optimum Colliery</td><td>Optimum Holdings</td><td>5.00</td><td>71%</td><td>3.75</td></tr>
<tr><td>TOTAL</td><td></td><td>47.80</td><td></td><td>33.60</td></tr>
</table>

It can be seen from the 2011/2012 figures (Table 2.6) that the estimated Greenside Colliery coal discard of 2.18 million tonnes per annum would have been a potential and abundant low cost source of dense medium material provided the discard coal possessed a suitable fluidizing characteristic. However, the discard coal did not exhibit adequate fluidization characteristics.

2.6 SUMMARY

Dry coal beneficiation has the distinct advantage of non-reliance on water for upgrading Coal. Literature has also shown that ADMFB technique provides a relatively better separation efficiency characterised by low Ep values compared to other dry techniques. The medium material used in air dry fluidized bed has been shown to influence uniformity and stability of the bed density. It is, therefore, of paramount importance to study the future of dry coal beneficiation in South Africa. This forms the prime objective of this study, namely to establish the characteristics of a range of alternative medium materials for dry fluidized bed beneficiation.

Chapter 3 : Materials and Experimental Procedures

This chapter outlines in detail the experimental approach used in this investigation. This includes the source and characterization of the materials utilized, the equipment and detailed experimental procedures for the experiments carried out and information on the standards used.

3.1 INTRODUCTION

In this study, five potential dense medium materials were tested to determine their ability to create a medium in which solid particles are suspended in an upward air flow for effective separation in an Air Dense Medium Fluidized Bed (ADMFB). Each of the materials utilized was prepared to a specific size range and characterised according to their physical properties. The materials were then fluidized solely and as a blend to establish their fluidization characteristics and suitability as a medium for coal separation. The initial beneficiation test was carried out using density tracers to determine the optimum operating condition for the separator and the most suitable dense medium material out of the five tested. Based on the results obtained from the trial test, coal was then tested in the ADMFB fluidized bed separator.

3.2 MATERIALS

The materials selected for the study were magnetite, pyrrhotite, silica sand, granulated blast furnace slag and coal discards. The solid medium materials were obtained from different sources within South Africa and prepared in accordance to ISO 3082:2009 into the required size range (-425+106 µm). The density tracers used were cube shaped particles of 6 × 13 mm, and within the density range of 1.2 – 2.0 kg/m^3. Another set of density tracers used in the study was dome shaped particles of a single size 16 × 8 mm. The coal used was a Run-Of-Mine (ROM) from Kleinkopje Colliery, Witbank No.2 seam. The coal was prepared according to ISO 13909:2016 and screened to -13+6 mm fraction.

3.3 EQUIPMENT

3.3.1 Fluidized bed

The fluidized bed used in this study was constructed from a Perspex material that was reinforced with a steel frame, with a square cross section of 40 cm × 40 cm and height of 60 cm. The overall equipment setup showing the bed and the auxiliary control equipment which includes air supply system and bed pressure measurement is shown in the process flow diagram in Figure 3-1. The bed air distributor was made of a canvas material compacted between two pieces of wire mesh. The inlet air pressure to the system was maintained at 450 kPa through the use of a pressure regulator. An air filter was also connected to the regulator to clean and dry the compressed air utilized. The air flow into the system was measured using a rotameter with the gas flow rate being controlled by a valve located on top of the rotameter. The rotameter used was a "TROGOMID" Plastic Tube VA Flowmeter with a flow range (10 – 100%) 321 – 3212 Sl/min Air metered at 6.35 bar (abs) and 20º C.

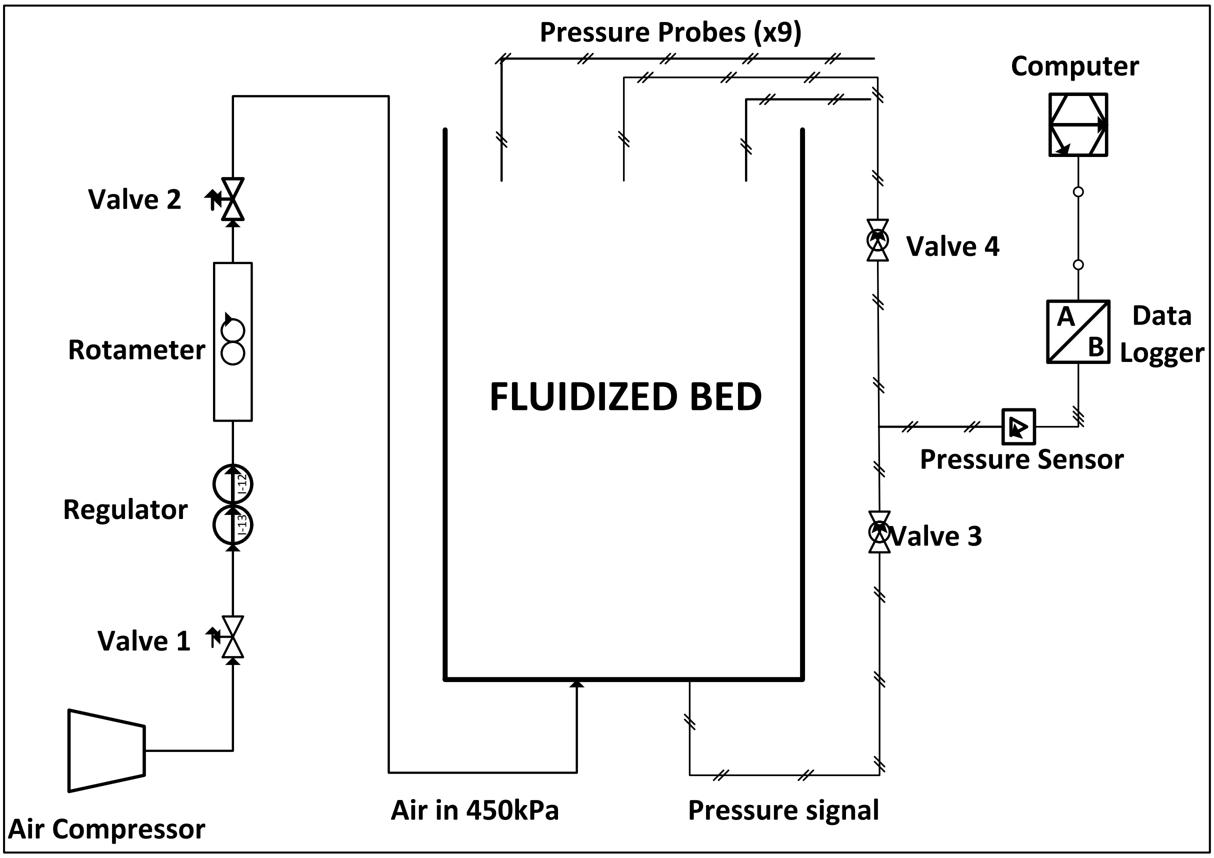

Figure 3-1: Process flow diagram showing equipment setup

3.3.2 Bed pressure measurement

The pressure in the fluidized bed (FB) was measured from nine (9) different points across the bed's cross-sectional area. The measurements were taken using pressure probes (6 mm copper tubing and flexible plastic hose) at each point, and were connected to pressure transducers. The data from the pressure readings were recorded on an Agilent 34970A data logger which was connected to the pressure transducers. A probe rig was used to maintain the positions of the probes across the bed and along bed depth during pressure measurements. The assembly is shown below in Figure 3-2.

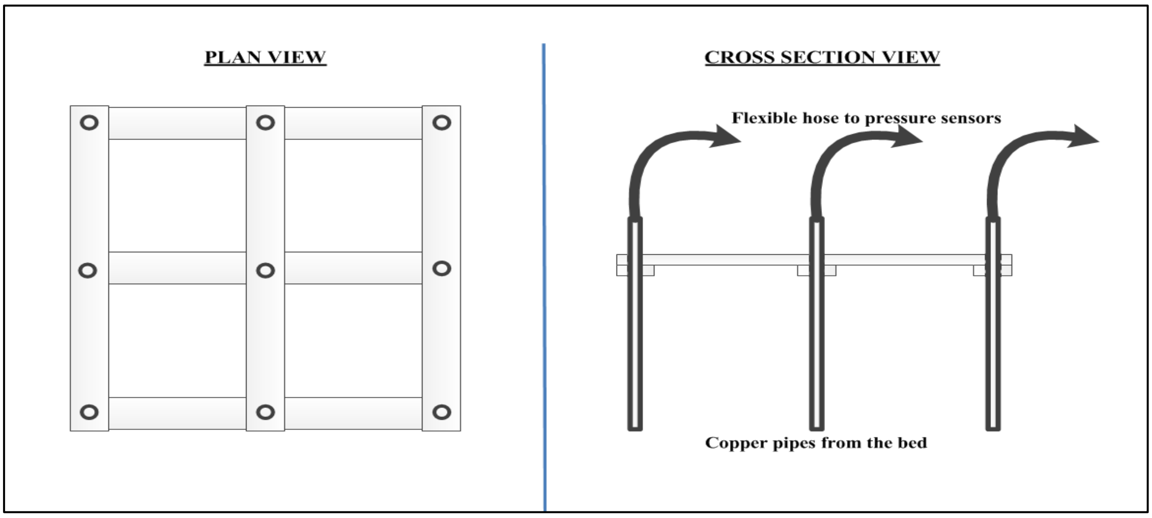

Figure 3-2: Probe rig system for measuring pressure across the bed

The bed pressure drop was determined from the readings taken using the assembly described above, which was the difference in pressure between two points in the bed. In addition, all the pressure sensors were calibrated using a Pennwalt Wallace & Tiernan precision pneumatic Calibrator. The calibration graphs are shown in Appendix B.

3.4 EXPERIMENTAL PROCEDURE

The test experimental procedure involved three main phases, material characterization, fluidization characterization and beneficiation test work. Figure 3-3 below shows the process flow diagram of how the experiments were conducted.

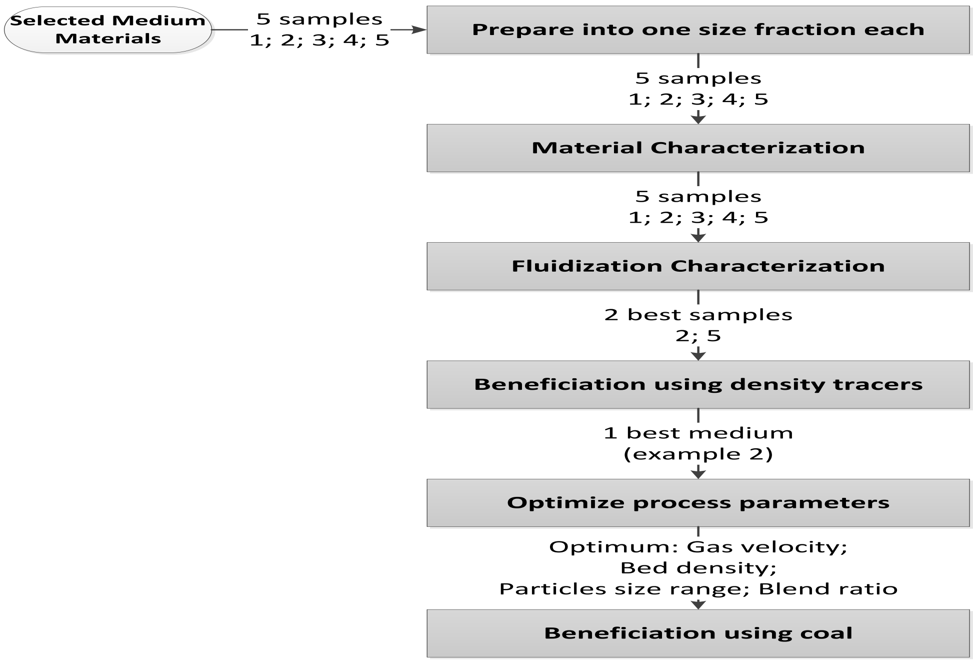

Figure 3-3: Experimental procedure process flow

3.4.1 Solid medium and coal sample preparation

Each of the 'as received' solid medium material was prepared by crushing, milling and screening in accordance to ISO 3082:2009. The resulting sample for each of the solid medium material was reduced to a size fraction of -425+106 µm which was used for the experiments. The feed coal received (-100+12 mm) was prepared according to ISO 13909:2016, and was first screened on a vibrating shaker using a 13 mm × 6 mm screen. The -13+6 mm fraction was kept, while the -6 mm fraction was discarded. The +13 mm fraction was fed into a jaw crusher and the product was screened again. The cycle was repeated with the objective of obtaining the required -13+6 mm particle size for testing. All the -13+6 mm fractions were then combined, blended and sub sampled. The sub samples were used for further coal characterization tests and beneficiation tests (sink/float and ADMFB).

3.4.2 Material characterization

The material used for the laboratory experiments which includes the proposed solid medium materials and the coal were characterised before and after the experiments. The characterization tests conducted on both the solid medium materials and the coal utilized in this study are described in the subsequent sections.

3.4.2.1 Solid Medium characterization

A Malvern Mastersizer 2000 was used to measure the particle size distribution of each of the solid medium materials in accordance to ISO 13320: 2009. The sub samples collected during sample preparation were analyzed using a laser diffraction technique which measures particles of size ranging from 0.01 to 1000 µm. The system uses a series of lenses and scattered light detection units which are connected to a computer with the instrument's software. The computer generates the initial size distribution from scattering patterns and uses Mie theory to report the final size distribution.

The true density of each solid medium material was determined using a gas pycnometer in accordance with ISO 12154:2014 standard. The system uses volumetric gas displacement to determine the skeleton density of a solid material whose form may be powdered or not and including irregular in shape.

The Davis Tube test in accordance with ISO 8833:1989 was used to determine the magnetic content of the medium materials

An SPECTRO XEPOS spectrometer was used to measure the elemental composition of the elements in all the solid medium materials in accordance with ISO TR 18336:2016. This energy dispersive spectrometer uses a 50 W/60 kV X-ray tube and TurboQuant II software to analyze and record the data.

3.4.2.2 Coal Analysis

The coal used for both the sink/float and the ADMFB beneficiation, along with the product stream (clean coal and discard) were tested for their physicochemical properties. The proximate analyses for all samples were conducted in accordance with the ASTM D5142, using approximately 1 g in determining the inherent moisture, ash content and volatile matter present. The fixed carbon is expressed as the 100% − (ash content + volatile matter + moisture content). The ultimate and sulphur analyses of all samples were performed according to ASTM D5373-02 and ASTM D4239-05 for CHN and sulphur content, respectively using LECO CHN 628 with add on 628 S module. The calorific value was determined with an approximately 1 g sample using a Leco AC 500 bomb calorimeter in accordance with ASTM D5865-04. In this system, an electronic thermometer with an accuracy of 0.0001 ºC is used to measure the temperature at six seconds intervals and the results are obtained in 5.0 to 7.5 minutes.

3.4.3 Fluidization characterization

The fluidized bed was loaded with one dense medium material at a time, with three static bed heights (20, 25 and 30 cm) used for each test material. The approximate mass of each material in the fluidized bed is shown in Table 3-1 below.

Table 3-1: Approximate bed weight (kg) at different static bed heights

Bed Material	Static bed height		
	20 cm	**25 cm**	**30 cm**
Magnetite	94	117	141
Pyrrhotite	57	72	86
GBFS	52	65	78
Silica Sand	46	58	69
Coal Rejects	41	51	61

The initial tests during fluidization characterization involved a process of determining the minimum fluidizing velocity and consequently the operating superficial velocity. Once the operating velocity was determined the pressure drop measurements were taken at different points in the bed. A total of nine (9) pressure points (A, B, C, D, E, F, G, H, I) readings were collected at each bed height (0, 5, 10, 15, 20, 25, 30 cm) at specific intervals (1 reading per 500 milliseconds). The positions of the pressure sampling points on the cross section of the fluidized bed from a plan view are shown in Figure 3-4 below.

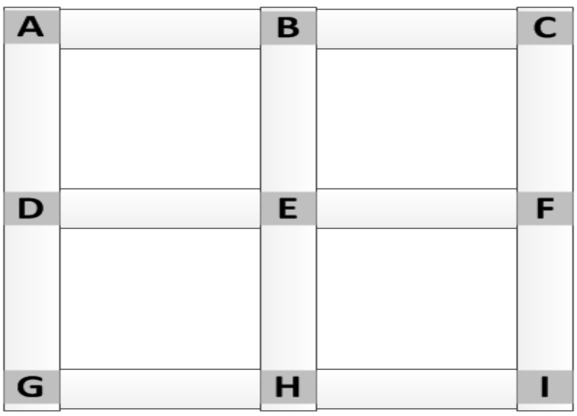

Figure 3-4: Plan view of positions of pressure sampling points on the fluidized bed

The data from each pressure sampling point was used to plot the pressure drop profiles for the respective point in the bed. The pressure drop profile was used to determine the bed density at each measured point in the bed and consequently the bed density distribution. Information on the bed density distribution profile was used to establish the most suitable medium material and the static bed height at which it could potentially give the best air dense medium separation characteristics. Therefore, the data obtained from the bed density distribution for all the materials were compared and the medium materials with the best fluidization characteristics were selected to be used for the beneficiation tests.

3.4.3.1 Determination of minimum fluidization velocity

The minimum fluidization velocity (U_{mf}) of each solid medium was determined using a plot of pressure drop versus air velocity graphs. This was achieved by taking the air velocity reading at the point where the pressure drop remains constant even with an increase in air velocity. This U_{mf} is illustrated as the velocity at point C in Figure 3-5.

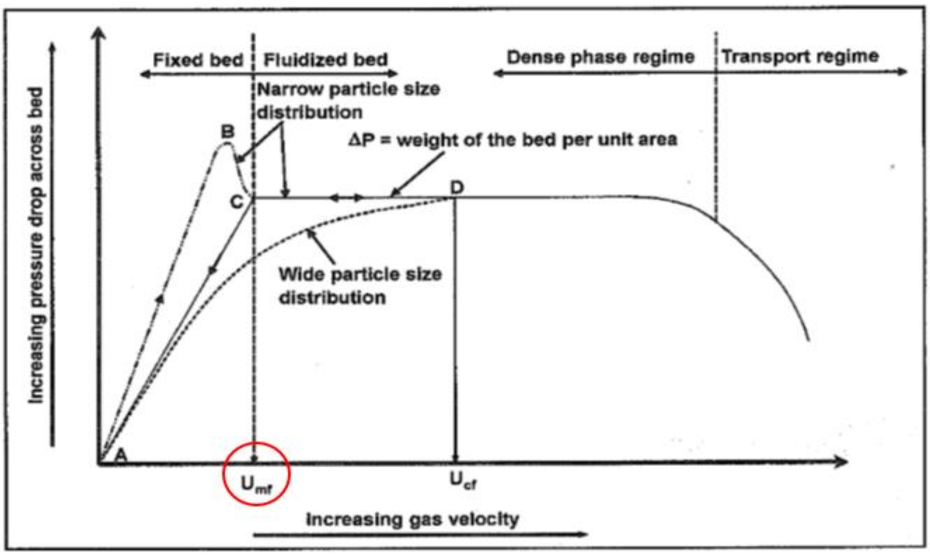

Figure 3-5: Illustration of minimum fluidization velocity

3.4.3.2 Evaluation of segregation

Depending on the particle size distribution of the feed solid medium material, segregation of particles may occur in the bed. Particle segregation has the negative effect of reducing the stability and uniformity of the fluidized bed. To determine if there was any particle segregation, after fluidizing the bed for a given period of time, air supply was shut off and random samples were collected from three (3) levels (top, middle, and bottom) in the bed. A particle size distribution analysis was conducted on each of the samples and compared to the original feed particle size distribution results. The result obtained shows similar particle size distribution, indicating there was no particle segregation.

3.4.3.3 Determination of bed density

The density at different points in the bed was obtained by using the static pressure difference method from the bed pressure measurements. The bed density was determined by plotting the bed pressure drop against the bed height graph and using the gradient of the graph in the Equations 3-1 to 3-3.

$$\boldsymbol{P = -\rho_{bed} g(h_{top} - h)}$$ *Equation 3-1*

$$\boldsymbol{dP = -\rho_{bed} g . dh}$$ *Equation 3-2*

Where; $\boldsymbol{P}$ is the pressure drop (Pa)

$\boldsymbol{\rho_{bed}}$ is the bed density (kg/m^3)

$\mathbf{g}$ = 9.81m/s^2

The gradient of the pressure drop against bed height plot gives the bed density:

$$\boldsymbol{\rho_{bed} = \frac{-(gradient)}{9.81} \times 10000}$$ *Equation 3-3*

Where, 10000 is a conversion factor.

3.4.3.4 Determination of bed density distribution profile

Upon determination of the bed density at various points in the bed as described in section 3.4.3.3 above, the density distribution was obtained. This was done by plotting a graph of bed density versus bed level, and analysing the distribution vertically per each sampling point and horizontally per multiple sampling points. The average bed density was calculated from the various measured densities.

3.4.3.5 Determination of bed stability

The stability and uniformity of the fluidized bed was determined by establishing the standard deviation of density distribution (S_P) for each point. The (S_P) was determined from Equation 3-4;

$$\boldsymbol{S_P = \sqrt{\frac{1}{N}\sum_{I=1}^{N}(\rho_i - \bar{\rho})^2}} \qquad \textit{Equation 3-4}$$

Where, **N** is the total number of the density measuring points

$\boldsymbol{\rho_i}$ is the density of point i, kg/cm^3

$\boldsymbol{\bar{\rho}}$ is the average density of all points, kg/cm^3

On the other hand the coefficient of variation (CoV) was also used in this study to further determine the extent of variation of the bed density from its mean at each horizontal bed level. The CoV was calculated using Equation 3-5;

$$\boldsymbol{CoV = \left(\frac{Standard\ Deviation\ of\ density\ for\ a\ bed\ level}{Average\ density\ for\ that\ level}\right) \times 100} \qquad \textit{Equation 3-5}$$

3.4.4 Beneficiation studies

3.4.4.1 Davis tube test work on the proposed solid medium

The Davis tube test was conducted in accordance to ISO 8833:1989, to separate the magnetic and non-magnetic fraction within the proposed medium materials at different amps, ranging between 0.5 to 2.0 amps. A Davis Tube uses an electromagnet that generates a magnetic field, which separates the feed (25 g) in a glass tube that rotates and moves forward and backwards at the same time. The glass tube was placed between two magnetic poles at an angle in which the sample in a slurry form is run through and flushed with water. This process allows the magnetic fraction to be collected within the high magnetic intensity zone and the non-magnetic fraction to be washed off and collected separately. The test provided an insight on the magnetic composition of each solid medium material, and gives an indication of the recovery potential of each of the medium material when used as a solid medium in an ADMFB process.

3.4.4.2 Heavy Liquid Separation Test work on feed coal

Prior to the ADMFB beneficiation, float and sink tests were performed on 2 kg batches of the raw coal (-13+6 mm) in accordance with ISO 7936:1992 to determine its washability characteristics. Zinc chloride solution was used to perform the tests at relative density (RD) of 1.3, 1.4 up to 1.86. The washability data from the sink/float process was used to establish a baseline performance for the ADMFB technique. The separation efficiency of the process was determined from the partition curve of the sink/float (products and discards).

3.4.4.3 Beneficiation using density tracers

In the beneficiation process, the Air Dense Medium Fluidized Bed (20 cm static bed height) was allowed to reach a stable fluidization state first before the density tracers were introduced from the top of the bed. When the tracers were introduced the bed was operated for specific time intervals (15, 30, 60, 120, 240, 600 s) and then air supply was shut off. A brush and flat scraper (40 cm length) was used to gently scrap off the medium material at intervals of 1cm. All the density tracers collected from the top of the bed to 10 cm depth were consolidated and recorded as ‘floats’. While tracers collected from 10 – 20 cm depth were considered ‘sinks’. Each test run was repeated at least three times in order to improve on the precision and accuracy of the results. Data from beneficiation tests with density tracers was collected and used to plot partition curves. The separation efficiency represented as probable error (Ep) was calculated for each solid medium, and formed the basis for selecting the medium material with the best potential for separating coal in the fluidized bed utilized in this study.

The separation efficiency of the process was determined by calculating the probable error (Ep) using Equation 3-6;

$$\boldsymbol{Ep} = \frac{\boldsymbol{\rho_{75}} - \boldsymbol{\rho_{25}}}{\mathbf{2}} \qquad \textit{Equation 3-6}$$

Where $\boldsymbol{\rho_{75}}$ is the relative density at which 75% of the particles report to the sinks

$\boldsymbol{\rho_{25}}$ is the relative density at which 25% of the particles report to the sinks

After establishing the bed optimum operating condition using the density tracers and the potential solid medium, the ADMFB was then evaluated for coal beneficiation.

3.4.4.4 Beneficiation using coal

This process involved feeding 1 kg of coal into the fluidized bed and performing the separation at the established optimum conditions. The same procedure used for collecting density tracers was performed to collect coal 'products' and 'tailings' from the bed. All the coal particles collected from the top of the bed to 10 cm depth were consolidated and recorded as 'floats'. While coal particles collected from 10 – 20 cm depth were considered 'sinks'. Each test run was repeated at least three times in order to improve on the precision and accuracy of the results. The percentage total mass of feed at discrete cut density was determined; the total mass and cumulative to sinks; the total mass and cumulative floats; cumulative yields; % reconstituted feed; % sinks and nominal specific density were all calculated. This data were used to develop the partition curves and at the same time determine the separation efficiency of the process, using equations 3-7 to 3-15 adapted from Wills (2011).

$$\boldsymbol{Floats\ analysis}\ (\boldsymbol{wt.}\%) = \left(\frac{masss\ of\ floats\ recovered\ within\ a\ specific\ density\ fraction}{total\ mass\ of\ the\ float\ particles}\right) \times 100 \qquad \textit{Equation 3-7}$$

$$\boldsymbol{Sinks\ analysis}\ (\boldsymbol{wt.}\%) = \left(\frac{masss\ of\ sinks\ recovered\ within\ a\ specific\ density\ fraction}{total\ mass\ of\ the\ sink\ particles}\right) \times 100 \qquad \textit{Equation 3-8}$$

$$\boldsymbol{Floats}\ \%\ \boldsymbol{of\ feed} = \left(\frac{masss\ of\ floats\ recovered\ within\ a\ specific\ density\ fraction}{total\ mass\ of\ the\ feed\ particles}\right) \times 100 \qquad \textit{Equation 3-9}$$

$$\boldsymbol{Sinks}\ \%\ \boldsymbol{of\ feed} = \left(\frac{masss\ of\ sinks\ recovered\ within\ a\ specific\ density\ fraction}{total\ mass\ of\ the\ feed\ particles}\right) \times 100 \qquad \textit{Equation 3-10}$$

$$\boldsymbol{Reconsituted\ feed}\ \% = Floats\ \%\ of\ feed + Sinks\ \%\ of\ feed \qquad \textit{Equation 3-11}$$

$$\boldsymbol{Nominal\ specific\ gravity}\ (\boldsymbol{S.G}) = Average\ S.G\ per\ density\ fraction \qquad \textit{Equation 3-12}$$

$$\boldsymbol{Partition\ coefficient} = \left(\frac{Sinks\ \%\ of\ feed}{Reconstituted\ feed}\right) \times 100 \qquad \textit{Equation 3-13}$$

$$\boldsymbol{Yield}\ (\%) = \left(\frac{Total\ mass\ of\ the\ floats}{Total\ mass\ of\ the\ feed}\right) \times 100 \qquad \textit{Equation 3-14}$$

$$\boldsymbol{Organic\ efficiency}\ (\%) = \left(\frac{Actual\ yield\ at\ specific\ ash\ content}{Theoretical\ yield\ at\ specific\ ash\ content}\right) \times 100 \qquad \textit{Equation 3-15}$$

3.5 SUMMARY

Five solid medium materials were prepared to a specific size range (-425+106 µm) and tested. Each material was characterised according to its physicochemical properties and fluidization potential in the ADMFB. The operating parameters were optimized using density tracer separation tests results. Based on the results obtained from the trial test, coal (-13+6 mm) was then tested in the ADMFB fluidized bed separator. Proximate, ultimate and sulphur analyses on the feed and clean coal product was used to determine the effectiveness of the ADMFB and the respective medium material used. The results and discussions of the experiments carried out are presented in the next chapter (Chapter 4).

Chapter 4 : Results and Discussion

4.1 INTRODUCTION

The results obtained from the material characterization, fluidization and beneficiation tests are presented in this chapter. The solid medium materials were characterised to determine their physico-chemical properties as a medium for ADMFB application. The fluidization behaviour, including minimum fluidization velocity, segregation, bed pressure drop, bed density distribution and bed stability were evaluated. The effect of operating parameters such as static bed height, blend ratio (for mixed medium) and feed particle size was also evaluated with a view to determining the most effective parameters for coal beneficiation.

4.2 MATERIAL CHARACTERIZATION

4.2.1 Physical and chemical properties of solid medium materials

The physical properties of the solid medium materials used in the fluidized bed application are presented in the sections below. Such factors are known to have an influence on the stability of the bed. The material density influences bed overall bed density as shown in Equation 1-1. In addition, the particle size distribution, especially the average particle size of the medium, influences the Geldart fluidization classification (described in section 2.3.1) of the material and consequently the behaviour of the solids when fluidized in the air.

4.2.1.1 Particle Size Distribution Analysis

Table 4-1 below shows the particle size distribution of the five medium materials tested in this study.

Table 4-1: Particle size distribution of the solid medium materials

Material	**Particle Size (μm)**		
	D_{90}	**D_{50}**	**D_{10}**
Magnetite	338	113	51
Pyrrhotite	390	200	83
GBFS	409	229	98
Silica Sand	402	232	102
Coal Rejects	410	218	92

The particle size for all the media utilized in this study was -425+106 µm, and from Table 4-1 above, it can be seen that the median particle size (D_{50}) for the materials was within 113 to 232 µm which could be classified under Geldart Classification of powders as group B powder.

4.2.1.2 Material Density Analysis

The density of each solid medium material used in this study is depicted in Table 4-2 below.

A study conducted by Mohanta *et al*. (2012) has shown that the most suitable solid medium particle size for an ADMFB application can be established from the Geldart fluidization classification. The author concluded that the most effective material for fluidization is that of the Geldart group B.

The results of the particle size distribution and material density analysis conducted in this study (Table 4-1 and 4-2) show that each of the materials can be classified as Geldart group B (mean particle size 40 – 500 µm). This group is known to have a smaller bed expansion and with bubbling occurring slightly above the minimum fluidization velocity (U_{mf}), as described by Geldart (1973). More so, bubbles formed from group B powders are found to coalesce as they rise through the bed and collapse rapidly once air supply is cut off. This means that the size of the bubbles formed is influenced by the static bed height and this in turn affects bed stability. It is for this reason that bed height was investigated in this study.

Table 4-2: Particle density and Geldart classification of solid medium materials

Sample name	Particle Density (kg/m^3)	Geldart Group
Coal reject	2 112	B
Silica sand	2 410	B
GBFS	2 699	B
Pyrrhotite	2 983	B
Magnetite	4 880	B

4.2.1.3 Davis Tube Test

The Davis tube test was conducted in order to determine the magnetic content of the entire solid medium utilized in this study. The magnetic and non-magnetic fraction within the proposed medium materials (25g feed sample) was separated at different amps, ranging between 0.5 to 2.0 amps as seen in Table 4-3 below. According to the results, pyrrhotite was the only medium out of the four proposed media that has a magnetic and non-magnetic material of about 30% and 70%, respectively. This result confirmed that the pyrrhotite utilized in this study is a ferromagnetic material.

Table 4-3: Davis tube test results for solid medium materials

Sample	**Magnetite**	**Pyrrhotite**	**GBFS**	**Silica S**	**Coal Rej**
Magnetic %	100	30	0	0	0
Non-magnetic %	0	70	100	100	100

Pyrrhotite				
Current (amps)	**0.5**	**1.0**	**1.5**	**2.0**
Magnetic (g)	1.37	5.56	6.32	7.19
Non-magnetic (g)	22.46	17.87	17.14	16.37

4.2.1.4 X-ray Fluorescence Analysis

The XRF analysis was conducted on the feed pyrrhotite, magnetic and non-magnetic fractions from the Davis tube test. Table 4-4 below shows that the magnetic fraction (pyrrhotite) has a higher concentration of iron (Fe) compared to that of the non-magnetic fraction. This test further supports the utilization of pyrrhotite as a medium that can be used with magnetite for dense medium coal separation.

Table 4-4: XRF analysis results of pyrrhotite, magnetite and GBFS

Element	**Fe (%)**	**S (%)**	**Ni (%)**	**Si (%)**	**Al (%)**	**Mg (%)**	**Ca (%)**	**Na (%)**	**K (%)**	**Ti (%)**
Magnetite	54.96	0.09	0.02	1.11	0.58	5.36	1.52	2.02	0.07	0.97
Pyrr. feed	10.66	1.03	0.16	23.93	4.41	19.55	7.05	2.32	0.45	0.41
Pyrr. mag	21.77	6.97	0.34	17.80	2.64	23.30	4.01	2.09	0.22	0.33
Pyrr. non mag	8.35	0.67	0.35	24.62	5.61	18.11	7.77	3.52	0.63	0.41
GBFS	0.32	0.78	0.00	21.97	9.90	11.94	23.06	3.37	1.16	0.36

* Pyrr: Pyrrhotite; mag: magnetic; non mag: non-magnetic and GBFS: Granulated blast furnace slag

4.2.2 Characterization of the feed coal

4.2.2.1 Properties and the washability of the feed coal

The physicochemical properties of the feed coal are shown in Table 4-5 below. Based on the result obtained from the empirical investigation conducted, the ROM coal sample was classified as a high ash coal, low in fixed carbon, Grade D3 in terms of Calorific Value (CV) and is low in volatiles (Code 3) according to the South African Standard Classification for Coals. It possesses notably high sulphur content.

Table 4-5: Physicochemical properties of the feed Coal

	FC %	**VM %**	**Ash %**		**TM %**
Proximate (As-received)	38.77	19.80	39.32		2.11
(Dry basis)	39.61	20.23	40.17		-
Calorific value	18.76 MJ/kg				
Ultimate analysis	**C%**	**H%**	**N%**	**S%**	**O%**
(Dry basis)	49.40	2.57	1.20	2.49	2.06

C: Carbon; H: Hydrogen; N: Nitrogen; S: Sulphur; O: Oxygen by difference [100-(H+C+N+Ash+$H_2$0+S)];
FC: Fixed Carbon; VM: Volatile Matter; TM: Total Moisture

The float and sink tests were performed on the feed coal in order to evaluate the potential of the ADMFB for coal beneficiation. The washability curves provides information on the yield (recovery) that can be achieved and at what cut-point for a desired product with specific ash content. The proximate and CV analysis was also carried out on the fractions collected from the float and sink tests. Figure 4-1 below shows that a clean coal product with an ash content of 14% can be achieved at a separation density of approximately 1.64 g/cm^3 and with a yield of approximately 53%. From the same washability test, a clean coal product of about 5.54 % ash with a yield of 1.18 % was also obtained at 1.3 RD. Table 4-6 below also shows that as the cut-density increases, the ash content of the particles increases. It can be envisaged that during the beneficiation of this coal, a higher ash and lower calorific value coal product will be produced as the bed density (ADMFB) is increased.

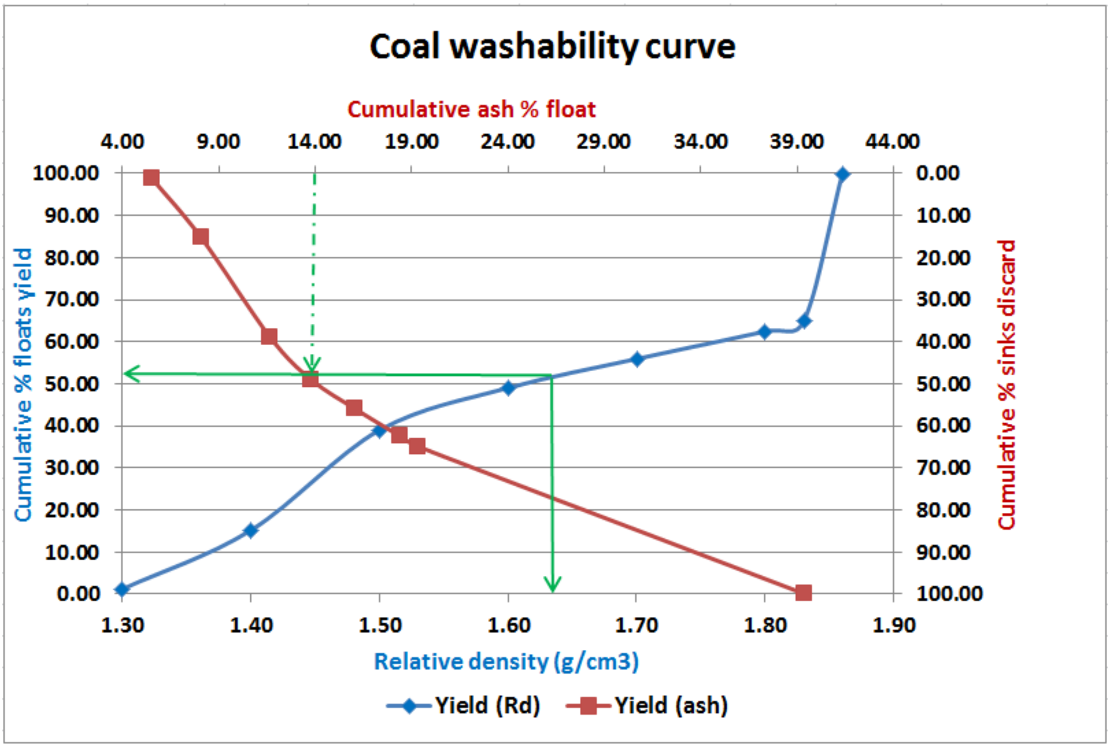

Figure 4-1: Washability curves illustrating cut density and yield

Table 4-6: Proximate and CV analysis results of feed and float-sink fractions

Sample	**FC %**	**VM (%)**	**TM (%)**	**Ash (%)**	**CV (MJ/kg)**	**Yield (%)**
Feed	38.77	19.80	2.11	39.32	18.76	100
F @ 1.30	63.22	28.31	2.93	5.54	31.47	1.18
F @ 1.40	62.32	26.72	2.67	8.29	30.47	13.99
F @ 1.50	60.35	23.06	2.62	13.96	27.70	23.81
F @ 1.60	53.30	22.00	2.66	22.05	24.10	10.04
F @ 1.70	46.79	18.60	2.54	32.06	19.83	6.90
F @ 1.80	40.13	18.84	2.47	38.56	17.73	6.55
F @ 1.86	38.47	16.14	2.61	42.79	15.81	2.45
S @ 1.86	11.20	10.70	1.57	76.53	4.08	35.08

		C%	**H%**	**N%**	**S%**	**O%**
Ultimate analysis (Dry basis)	F @ 1.30	80.6	4.36	2.18	0.71	3.51
	F @ 1.50	75.9	3.79	1.77	0.37	1.21
Sulphur	F @ 1.30	0.71				
	F @ 1.50	0.37				

* FC: Fixed Carbon; CV: Calorific Value; VM: Volatile Matter; TM: Total Moisture; S: Sulphur; C: Carbon; H: Hydrogen; N: Nitrogen; O: Oxygen by difference [100-(H+C+N+Ash+H_20+S)]

4.3 FLUIDIZED BED CHARACTERISTICS

4.3.1 Repeatability of measurements

As described in section 3.4.3, pressure drop measurements were performed and the data used to plot pressure drop profiles for each of the sampling points in the bed. Eventually, the bed density at each of the points was calculated and the bed density distribution determined. This information was used in determining the uniformity and stability of the bed. The measurement taken at each of the sampling point was tested for repeatability and minimum fluctuation by taking up to 120 readings at 500 milliseconds interval and the process repeated 3 times to give a total of 720 readings over a 2 minute range. The readings were averaged and the results taken as the pressure drop for that particular sampling point.

The coefficient of variation was used in determining the extent of variation of the readings from the mean at each point. The coefficient of variation of each of the readings was 0.0000017 – 0.0000018% indicating the negligible variation in the results and therefore, good certainty of results. The average pressure readings plotted against time for a given sampling point can be seen under Appendix B, which shows minimum fluctuation of the readings.

4.3.2 Minimum fluidization velocity

Figure 4-2 below depicts the graphical representation of the minimum fluidization velocity of the pyrrhotite ore used in this study. The minimum fluidization velocity, U_{mf} of each medium material used in this study was obtained by plotting the pressure drop versus velocity profile of the fluidized bed. The U_{mf} was determined as described in section 2.3.4 and Appendix B shows the U_{mf} graphs for the other dense medium materials. The results of the U_{mf} for each of the solid medium are shown in Figure 4-3. From the results, the U_{mf} decreases from magnetite to coal rejects. The results show that the minimum fluidization velocity is a function of the material's density. The higher the density of the material, the higher the minimum fluidization velocity. After the U_{mf} was established for all the solid medium, a series of pressure drop measurements were taken to establish the optimum operating fluidization velocity (U_{of}) at which the tests were conducted.

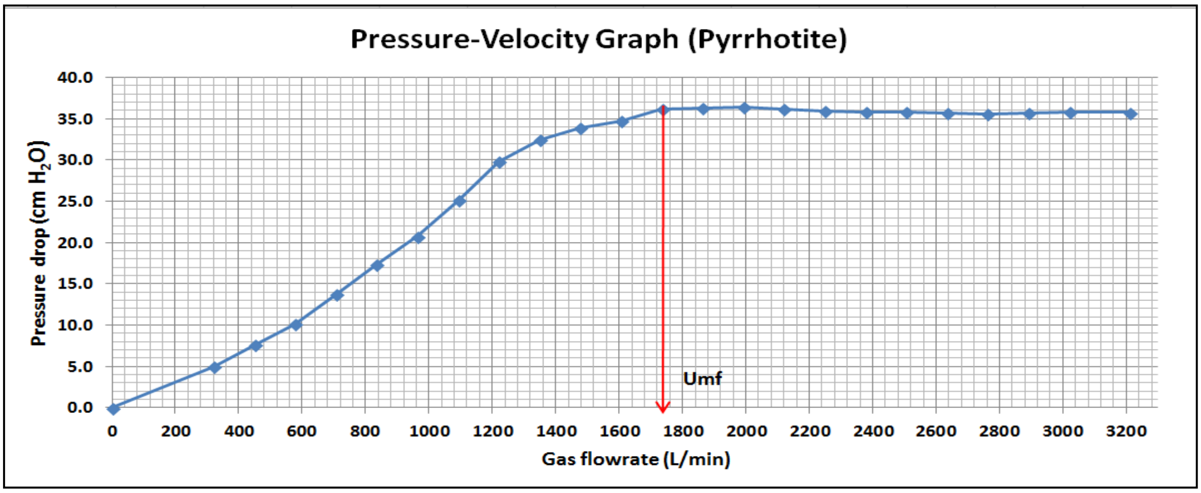

Figure 4-2: Illustration of minimum fluidization velocity

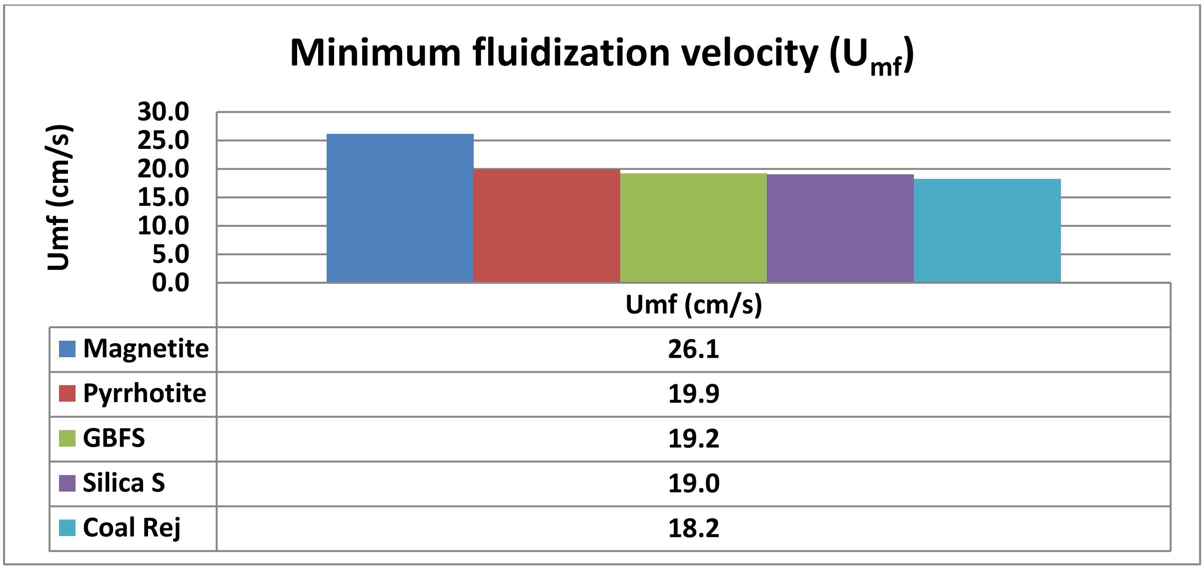

Figure 4-3: Minimum fluidization velocities of the solid medium materials.

4.3.3 Segregation evaluation

In order to ensure that the particle size range chosen for each material would achieve a uniform fluidization, a segregation evaluation was conducted. A PSD analysis of samples collected from different levels (top, middle and bottom) of the fluidized bed was used to determine the particle uniformity throughout the bed. Figure 4-4 below shows the PSD analysis of magnetite and pyrrhotite; the plots show that there was no segregation of particles as all the curves are seen overlapping each other. The same graphs were plotted for other solid materials, and all the dense medium materials exhibited uniform fluidization (Appendix B).

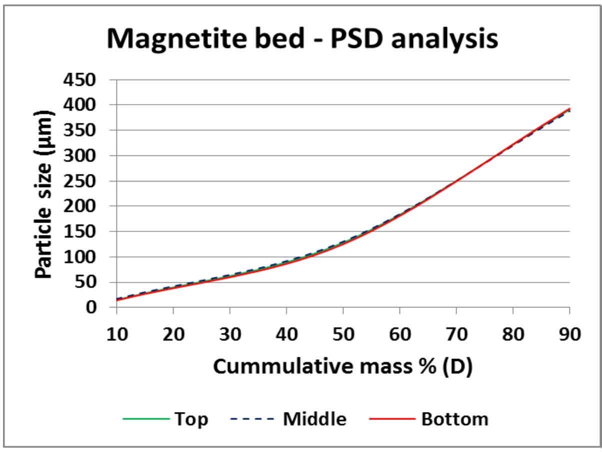

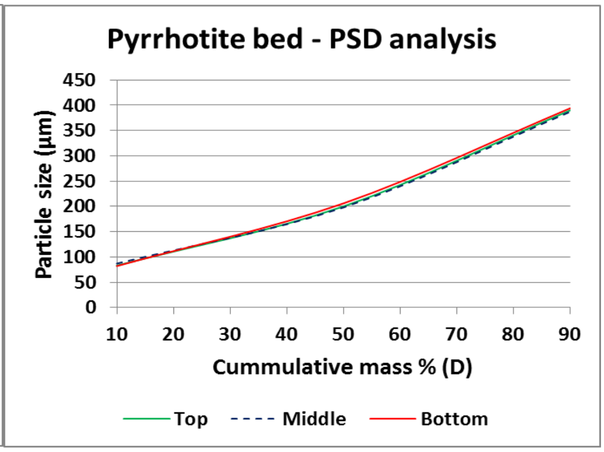

Figure 4-4: PSD analysis showing segregation evaluation of magnetite and pyrrhotite

4.3.4 Pressure drop profiles

The probe rig and pressure measurement system described in Section 3.3.3 was used to provide the data needed in plotting the pressure drop profiles for each of the sampling points (A to I). Figure 4-5 depicts the pressure drop profile of magnetite at 20 cm static bed height. The profile shows that, for each sampling point, the pressure drop generally increased uniformly from the top to the bottom of the bed. The behaviour of the bed on a vertical plane for each sampling point was uniform as shown by the quadratic fit which had a strong coefficient of determination ($R^2 > 0.9969$). The same procedure was carried out for all the solid medium materials used in this study at three static bed heights (20 cm, 25 cm and 30 cm), and the rest of the results are presented in Appendix B**.** The pressure drop profiles were used to calculate the bed density at each sampling point using Equation 3-3, and to establish the bed density distribution. The bed density distribution and hence uniformity and stability was then used as the criteria for selection of the medium material with the best fluidization characteristics.

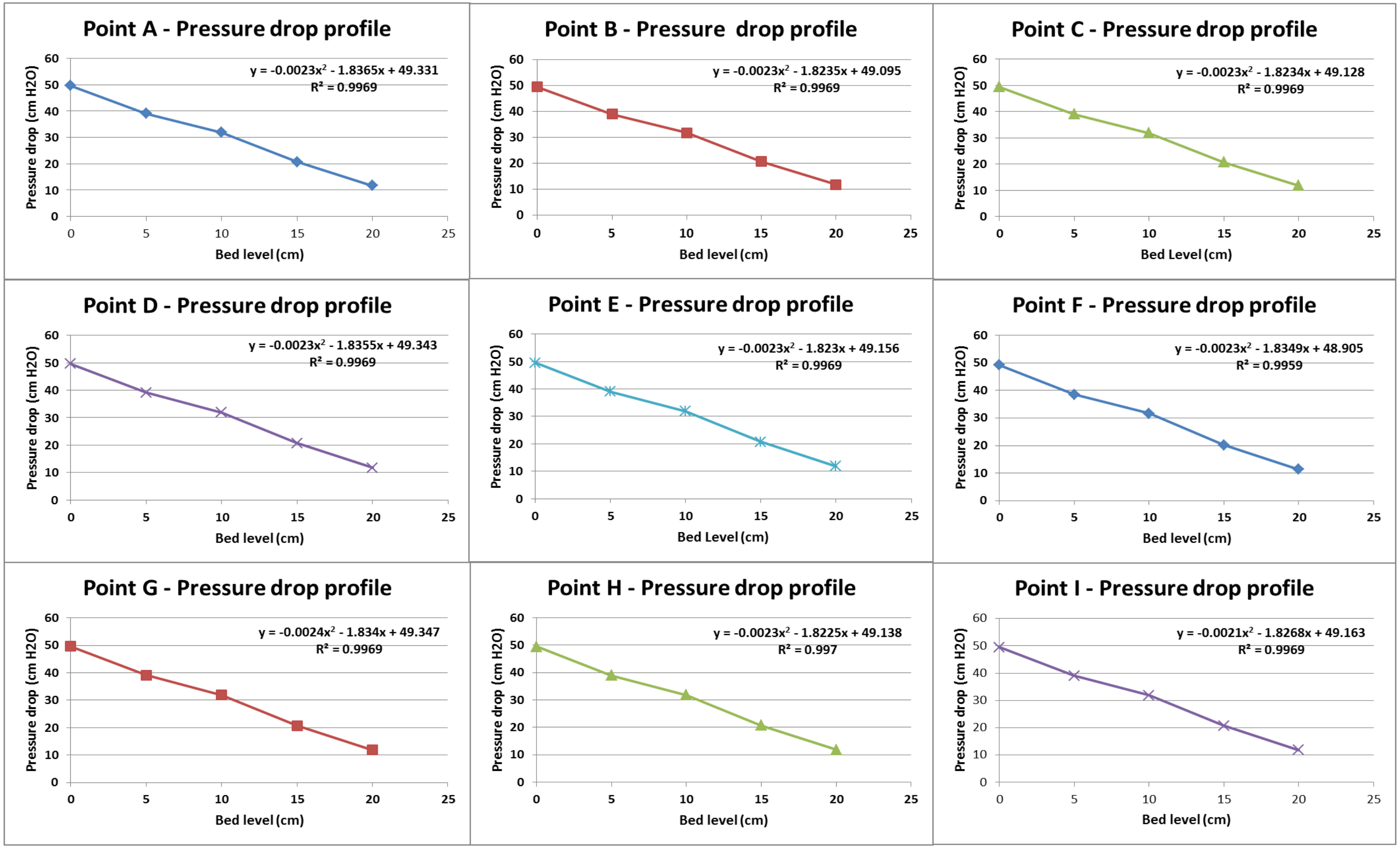

Figure 4-5: Pressure drop profile for Magnetite 20 cm bed height

4.3.5 Bed density distribution and profiles

Table 4-7 shows the corresponding bed densities at each sampling point for the magnetite 20 cm bed illustrated above (Figure 4-5). The corresponding density profile in Figure 4-6 shows how the density at each sampling point (A to I) changes with the depth of the bed. The coefficient of determination (R^2 ~ 1) also shows a strong uniform change in the density profile of single sampling point on a vertical plane.

Table 4-7: Results of bed density distribution for magnetite 20 cm bed

	Density (kg/m^3)								
Level (cm)	**A**	**B**	**C**	**D**	**E**	**F**	**G**	**H**	**I**
0	1871	1859	1859	1871	1858	1870	1870	1858	1862
5	1895	1882	1882	1894	1882	1894	1894	1881	1884
10	1918	1906	1906	1918	1905	1917	1918	1905	1905
15	1941	1929	1929	1941	1929	1941	1943	1928	1926
20	1965	1953	1952	1965	1952	1964	1967	1952	1948

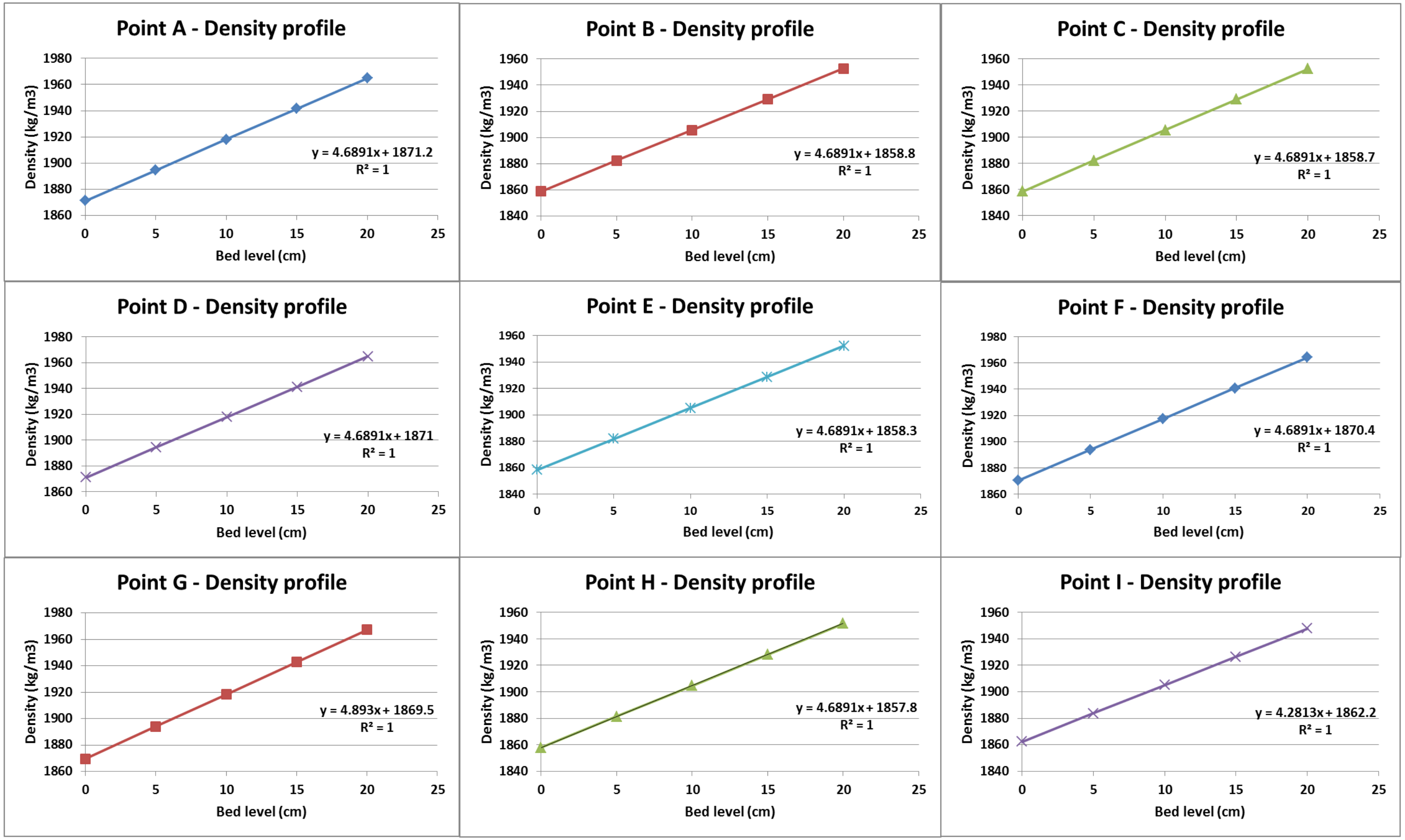

Figure 4-6: Density profile for Magnetite 20 cm bed height

4.3.6 Bed stability

The stability and uniformity of the bed density are essential for an efficient separation in an ADMFB separator. These two parameters were determined by calculating the coefficient of variation of bed density (CoV) and the standard deviation of bed density (S_P) using equation 3-4 and 3-5. Both (CoV and S_P) were calculated for each horizontal plane at 0 cm, 5cm, 10 cm up to 30 cm depending on the static bed depth. This data was used to determine how the bed's density varies at a specific bed level. Table 4-6 depicts the bed uniformity and stability of the magnetite 20 cm bed.

From Table 4-8 below**,** it can be seen that the CoV ranges between 0.33 – 0.37% while the S_P ranges between 2.05 and 2.41 kg/m^3. This indicates a very stable and uniform bed was achieved under these operating conditions. These results illustrated the potential of the magnetite as an efficient solid medium material for air dense medium separation.

Table 4-8: Bed uniformity and stability of magnetite 20 cm bed

	Density (kg/m^3)				
Sampling Point	**0 cm**	**5 cm**	**10 cm**	**15 cm**	**20 cm**
A	1871	1895	1918	1941	1965
B	1859	1882	1906	1929	1953
C	1859	1882	1906	1929	1952
D	1871	1894	1918	1941	1952
E	1858	1882	1905	1929	1952
F	1870	1894	1917	1941	1964
G	1870	1894	1918	1943	1967
H	1858	1881	1905	1928	1952
I	1862	1884	1905	1926	1948
CoV (%)	**0.33**	**0.34**	**0.35**	**0.37**	**0.37**
Sp (kg/m^3)	**2.05**	**2.13**	**2.24**	**2.37**	**2.41**

The same procedure for determining the uniformity and stability of the bed density was repeated for all the solid medium and the results are shown in Appendix B.

After performing calculations for CoV and S_P for all the materials at the different static bed heights, the data was presented in a chart to summarise the properties of each bed after fluidization. Two important parameters (CoV and average bed density) were used to describe each bed.

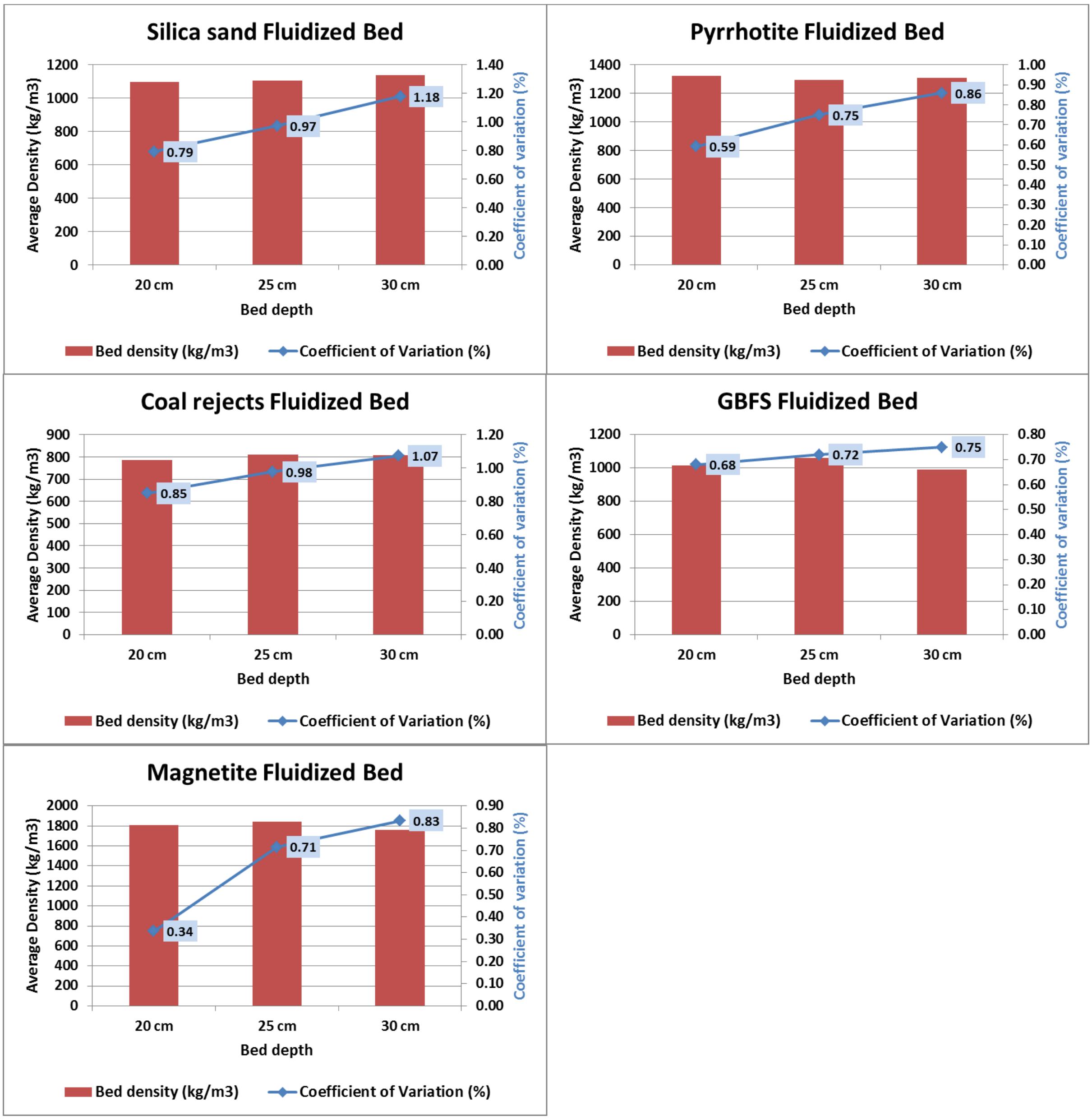

Figure 4-7: Summary of fluidized bed properties of the different solid medium materials

The chart above (Figure 4-7) was used to select the solid medium material and the static bed height at which the bed density is stable and uniform. The magnetite, pyrrhotite and GBFS at 20 cm bed height, all had a coefficient of variation less than 0.7 %. Figure 4-7 shows that the magnetite, pyrrhotite and GBFS bed indicate more uniform and stable beds compared to the other solid medium materials.

However, the GBFS bed had an average density of about 1 000 kg/m^3 coupled with its lack of magnetism, making it unsuitable for coal separation as a sole medium but with some possibility as a blend with magnetite. Silica sand on the other hand, had a slightly higher average bed density of about least 1 100 kg/m^3 and coefficient of variation 0.79 % for the 20 cm bed indicating potential for a blend with magnetite. Nevertheless, its lack of magnetism affects media recovery and can be a potential drawback for its application.

It was also important to note the apparent effect of the bed height on the fluctuation of bed density and consequently the stability of the bed. Therefore, the bed height was further investigated in beneficiation tests and the results are presented the in the next section 4.4.1.

4.4 BENEFICIATION RESULTS (DENSITY TRACERS)

Based on the information on bed stability and average bed densities obtained from Figure 4-7 above, the magnetite and pyrrhotite ore were chosen as a solid medium for the initial ADMFB test, using density tracers (6 × 13 mm cube shaped). Magnetite was used as a benchmark, and based on its separation efficiency; the static bed height which provided the best results was established for comparison with the other potential solid medium materials. Pyrrhotite was selected over other solid medium materials based on its slightly higher calculated average bed density, and its magnetic property. However, even though pyrrhotite had a higher calculated average bed density (approximately 1 300 kg/m^3), this density was not adequate to achieve a cut density high enough to beneficiate the tracers (1.2 – 2.0 kg/m^3) and SA coal. Therefore, a blend of magnetite and pyrrhotite was utilized in the investigation.

4.4.1 Effect of bed height

According to the results presented in section 4.3.6, the most stable and uniform bed was achieved at 20 cm static bed height for magnetite. Beneficiation tests at varying static bed heights (20, 25 and 30 cm) using density tracers were conducted to confirm the result obtained from the fluidized bed characteristics tests (section 4.3.6).

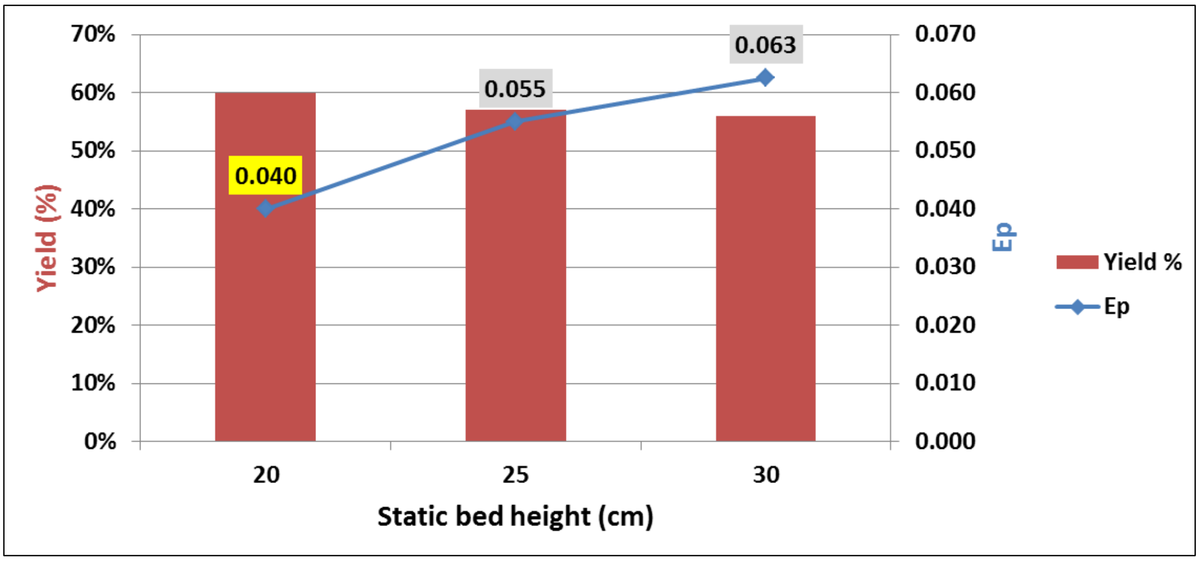

Figure 4-8: Beneficiation using magnetite – effect of bed height

It can be seen from Figure 4-8 above that the separation efficiency and the yield generally decrease with increasing static bed height. The magnetite sample used in this study was earlier described as a Group B material according to the Geldart's classification. Therefore, when fluidized, the bed is expected to experience bubbling and the bubbles coalesce as they rise up the bed. This rising bubbles would increase in size to become larger bubbles with strong wake turbulence, strong enough to drag dense particles (supposed to report to sinks) upwards resulting in back mixing, a phenomenon that consequently results in decreased separation efficiency (Firdaus *et al.*, 2012). An investigation by Firdaus *et al.* (2012) produced similar results showing that increasing the static bed height had the effect of increasing bubble size and consequently back mixing which resulted in lower separation efficiencies. Based on the result of this test, it was established that a shallow bed depth of 20 cm would provide the most effective separation for this ADMFB.

4.4.2 Effect of blending two solid medium

Using a static bed height of 20 cm as established in section 4.4.1, an investigation was carried out on the influence of replacing the magnetite with pyrrhotite ore at different weight (%) ratio. The blend of pyrrhotite/magnetite was prepared using 20%, 25% and up to 50% pyrrhotite by weight of the total material in the bed. Beneficiation tests were carried out using seven different blends at a different residence times (15, 30, 60, 120, 240 and 600 seconds). According to Figure 4-9, the optimal residence time of the process reached steady state at approximately 30 seconds, and therefore, 30 seconds was used as the optimum residence time for the subsequent tests. The results for the other blends from 30% to 50% are shown in Appendix B, Figure B-36.

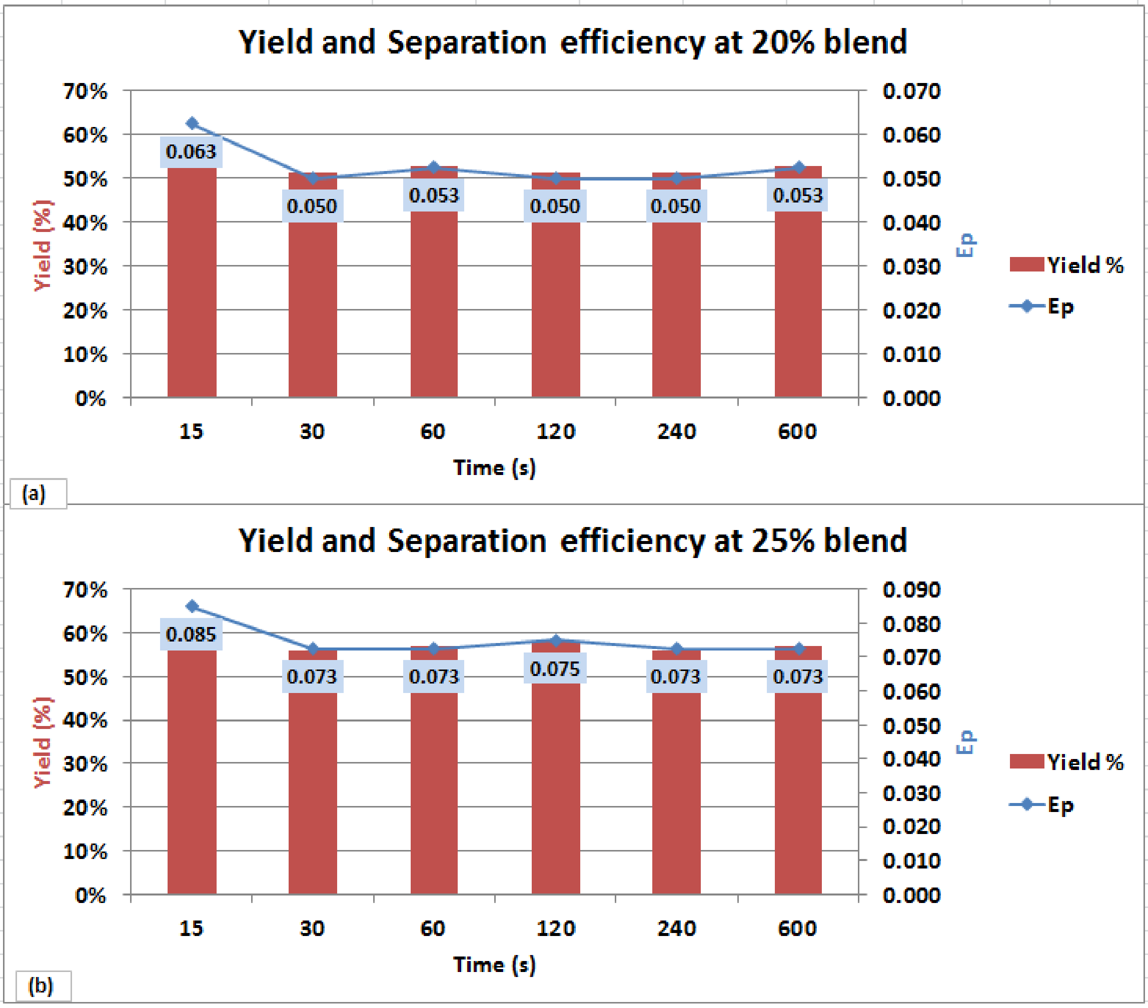

Figure 4-9: Beneficiation results at (a) 20% and (b) 25% blend ratios

For each blend ratio, the best separation results from the set optimum conditions were selected and the results plotted in Figure 4-10 as shown below. The amount of pyrrhotite in the blend was successfully increased to 40 wt% and a yield of 53 – 58% and probable error (Ep) of 0.053 – 0.073 was achieved. The optimum blend ratio was at 40 wt% pyrrhotite + 60 wt% magnetite beyond which the yield and separation efficiency began to decline.

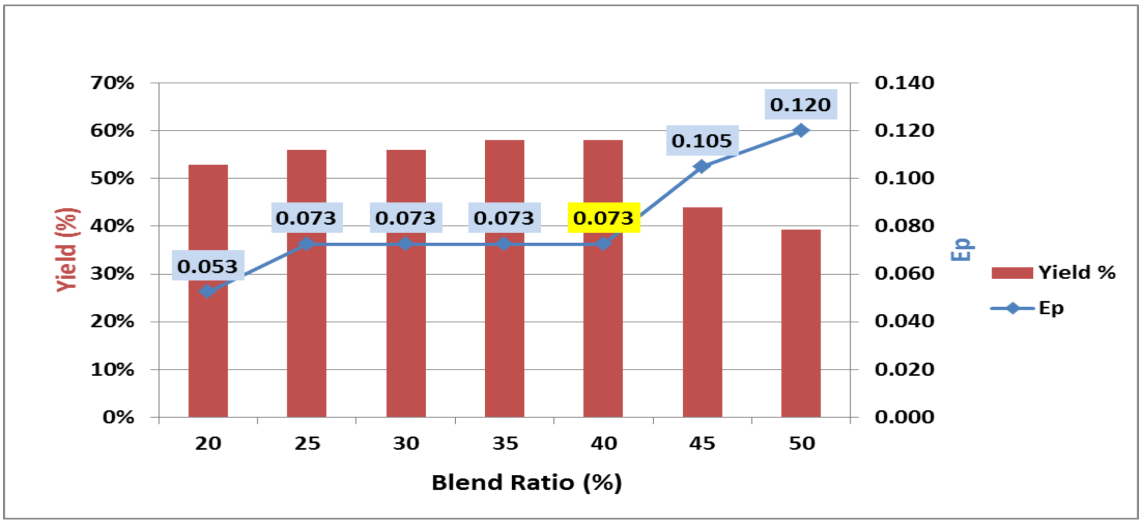

Figure 4-10: Coal beneficiation results at different blend ratios

Figure 4-11 below shows the existence of a relationship between the bed uniformity and stability, and the separation efficiency of the ADMFB separator. From the same figure, the bed density had a minimum fluctuation up to a blend of 40% pyrrhotite, with a CoV of the bed density in the range of 0.55 – 0.57%. The value of S_P was in the range of 4.4 – 4.7 kg/m^3 indicating a stable and uniform bed. However, when the blend ratio was increased beyond 40%, the bed became highly unstable and non-uniform with CoV and S_P increasing to 1.27% and 13.63 kg/m^3, respectively. This resulted in the poor separation efficiency of 0.105 and 0.120 at blend ratios of 45 and 50%, respectively.

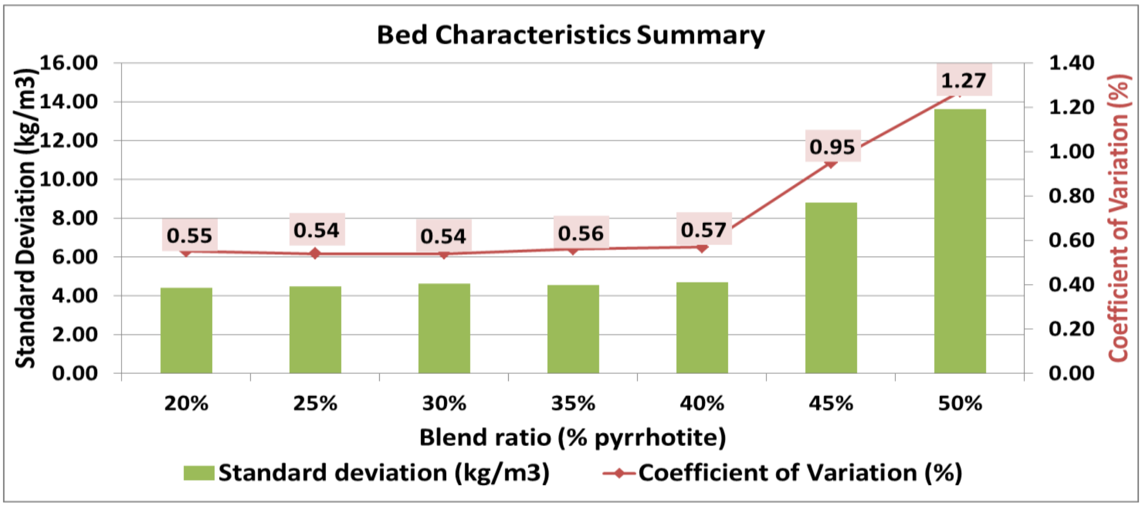

Figure 4-11: Bed stability characteristics at different blends

He *et al.* (2013) conducted a similar investigation using a blend of magnetite and paigeite ore to determine the bed's stability based on the bed density fluctuation. The author used a blend ratio up to 30 wt% and beyond that bed fluctuation increased rapidly and consequently compromised the efficiency of separation.

A comparison was made using 100 wt% magnetite and different blends of magnetite and pyrrhotite in the ADMFB separator for the beneficiation of density tracers. Figure 4-12 below shows the beneficiation results of 100 wt% magnetite (represented as 0 wt%) and the optimum blend ratio (40 wt%). The yield increased from 55% to 58% while the probable error (Ep), increased from 0.040 to 0.073 when the blend ratio was increased from 0 wt% to 40 wt% pyrrhotite. This proved that fairly comparable results could be accomplished by utilizing a blend of dense medium solids as an alternative to 100 wt% magnetite. This test established that the blend ratio of pyrrhotite could potentially be increased to 40 wt% and still achieves the same yield and separation efficiency as 100% magnetite bed.

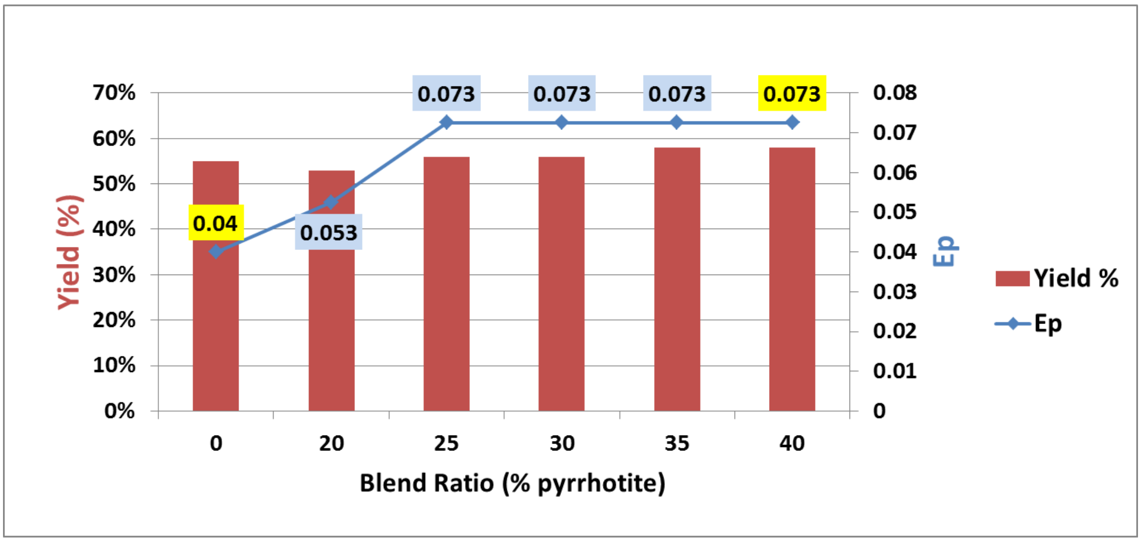

Figure 4-12: Comparison of beneficiation results for different blend ratios

4.4.3 Effect of particle size

In order to evaluate the effect of particle size on the separation efficiency of the ADMFB, density tracers with different particle size were used for the beneficiation tests under similar conditions. These coarser size tracers were dome shaped with a 16 mm diameter and 8 mm height. The results in Figure 4-13 (a) and (b) show that the separation efficiency decreased with a decrease in the feed particle size. The coarse size (8 × 16 mm) density tracers had a better probable error (Ep) and yield ranging 0.015 – 0.025 and 56 – 65%, respectively, compared to values of 0.040 – 0.073 and 53 – 58% for the fine size (6 – 13 mm) density tracers. This test supported the fact that coarse size particles are less prone to misplacement of particles caused by back mixing and bubbling effect of the fluidized bed.

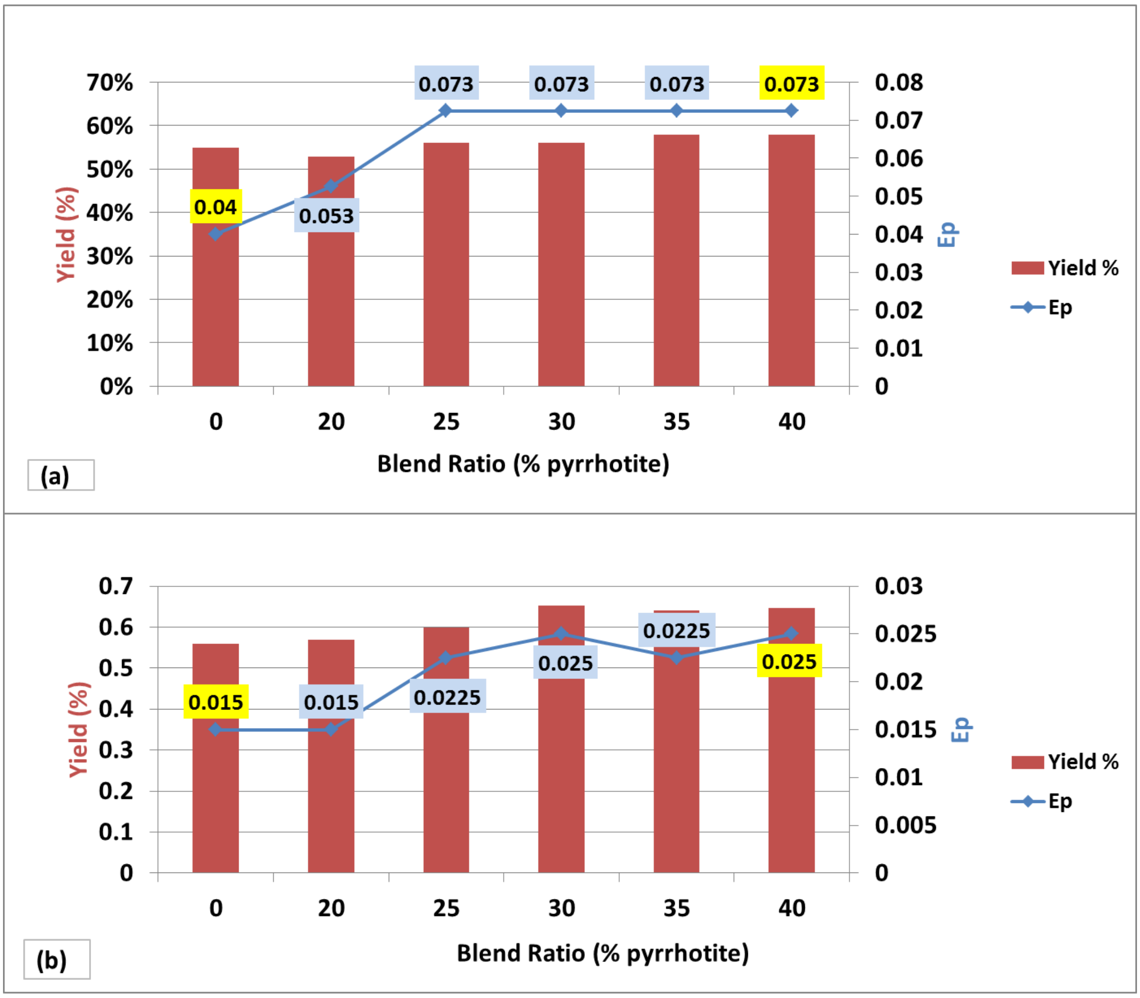

Figure 4-13: Beneficiation results using: (a) 6 – 13 mm; (b) 8 × 16 mm density tracers.

The effect of feed coal size on separation efficiency has been investigated by several authors (Chikerema and Moys, 2012; Firdaus *et al.*, 2012; Mohanta *et al.*, 2011) and the results obtained by these authors are found to be similar with findings in this study. Mohanta *et al.* (2011) developed a relationship showing that Ep decreases with increasing feed size until it becomes fairly constant and shows no size effect above 25 mm.

4.5 BENEFICIATION RESULTS (COAL)

The ROM coal was first subjected to a sink/float analysis in order to evaluate the potential of the ADMFB for cleaning coal without the utilization of water under different conditions. A 100 wt% magnetite fluidized bed at an optimum operating fluidization velocity $U_{of} \approx 1.4\ U_{mf}$ and 20 cm static bed height was utilized to beneficiate the ROM coal. The same coal was also beneficiated under the same condition with the blend of pyrrhotite/magnetite. From the sink and float analysis, it can be seen in Table 4-9 below that a clean coal of 5.54 % ash with a yield of 1.18 % is obtainable at 1.3 RD. In addition, at an RD of 1.5, a clean coal with an ash content of 13.96% and yield of 23.81% was also achieved.

Table 4-9: Sink/Float analysis of RoM coal

Sample		Ash %	CV MJ/kg	VM %	Yield %	S %
Feed		39.32	18.76	19.80	100	2.49
Float and Sink Test	F @ 1.30	5.54	31.47	28.31	1.18	0.37
	F @ 1.40	8.29	30.47	26.72	13.99	
	F @ 1.50	13.96	27.70	23.06	23.81	0.71
	F @ 1.60	22.05	24.10	22.00	10.04	
	F @ 1.70	32.06	19.83	18.60	6.90	
	F @ 1.80	38.56	17.73	18.84	6.55	
	F @ 1.86	42.79	15.81	16.14	2.45	
	S @ 1.86	76.53	4.08	10.70	35.08	

* CV: Calorific Value; VM: Volatile Matter; S: Sulphur

4.5.1 Beneficiation results for 40 wt% pyrrhotite bed

Five lab runs were carried out with each consisting of three (3) beneficiation tests, making a total of fifteen different beneficiation tests, and with the respective products and discards collected from the fluidized bed separator. The three (3) products and three (3) discards for each lab run were combined to give a bulk product and bulk discards sample, respectively. Float and sink tests were carried out on both bulk product and discard fractions of each lab run. The data collected which includes the total mass of feed; the total mass of sinks; the total mass of floats; yields; percentage (%) reconstituted feed; percentage (%) sinks and nominal specific density was calculated and recorded as shown in Table 4-10 for Run 1. The results for the rest of the lab run are shown in Appendix A. The data were used to plot the partition curves for each lab run.

Table 4-10: Partition data illustration for Run 1

Specific gravity fraction	Floats analysis (wt. %)	Sinks analysis (wt. %)	Floats % of feed	Sinks % of feed	Reconstituted feed (%)	Nominal S.G	Partition coefficient
<1.30	6.28	0.00	3.33	0.00	3.33		0.00
1.30-1.40	25.40	0.76	13.47	0.36	13.83	1.35	2.58
1.40-1.50	41.27	2.54	21.89	1.20	23.08	1.45	5.18
1.50-1.60	17.24	3.59	9.14	1.69	10.83	1.55	15.57
1.60-1.70	6.53	9.39	3.46	4.41	7.87	1.65	56.01
1.70-1.80	2.75	9.81	1.46	4.61	6.07	1.75	75.94
1.80-1.86	0.53	2.98	0.28	1.40	1.68	1.83	83.17
>1.86	0.00	70.92	0.00	33.31	33.31		100.00
Total	**100**	**100**	**52.04**	**47.96**	**100**		

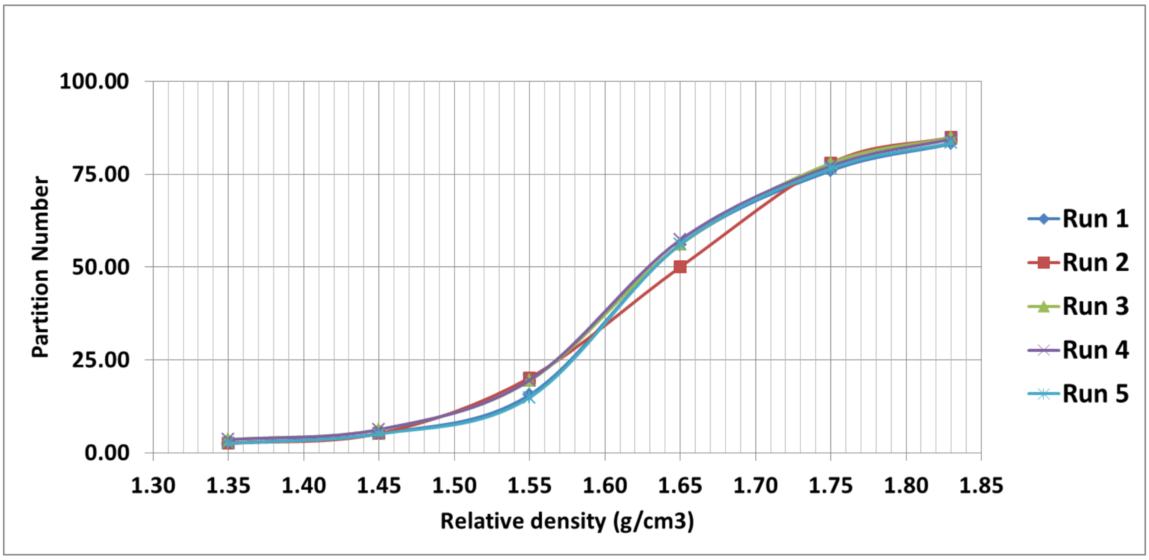

Figure 4-14: Partition curves representing each lab run

Figure 4-14 above shows the partition curves generated from the float and sink tests of the different products of each lab run. For each lab run the ρ_{25} and ρ_{75} were interpolated from the graphs and used to calculate the probable error (Ep) to give an indication of the separation efficiency. The yield was also determined from the mass of product recovered using Equation 3-14. The yield and probable error calculated from data provided in Figure 4-14 and Table 4-8 was used to plot the chart on Figure 4-15, which provides a comparison of results from each run.

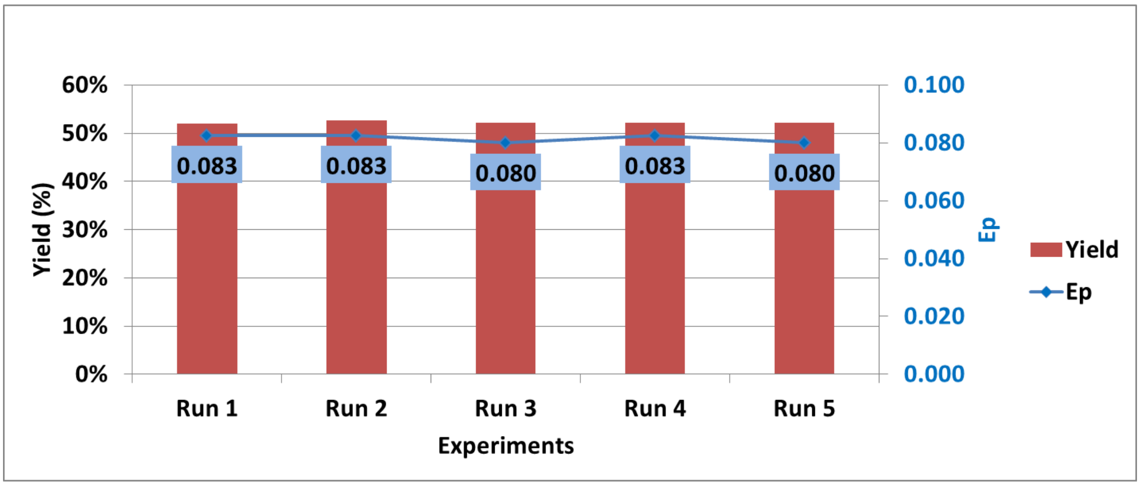

Figure 4-15: Yield and separation efficiency results for 40 wt% pyrrhotite blend

It can be seen from Figure 4-15 above that a dense medium of 40 wt% pyrrhotite + 60 wt% magnetite blend produces a clean coal product with a probable error (Ep) and yield ranging between 0.080 – 0.083 and 52.04 – 52.67%, respectively. The bed's cut-point/separation density (ρ_{50}) was at 1.63 – 1.64 g/cm^3, and a general consistency in the overall efficiency of the fluidized bed was achieved.

4.5.2 Beneficiation results for 100 wt% magnetite bed

A total of nine beneficiation tests were conducted with coal using 100% magnetite bed.

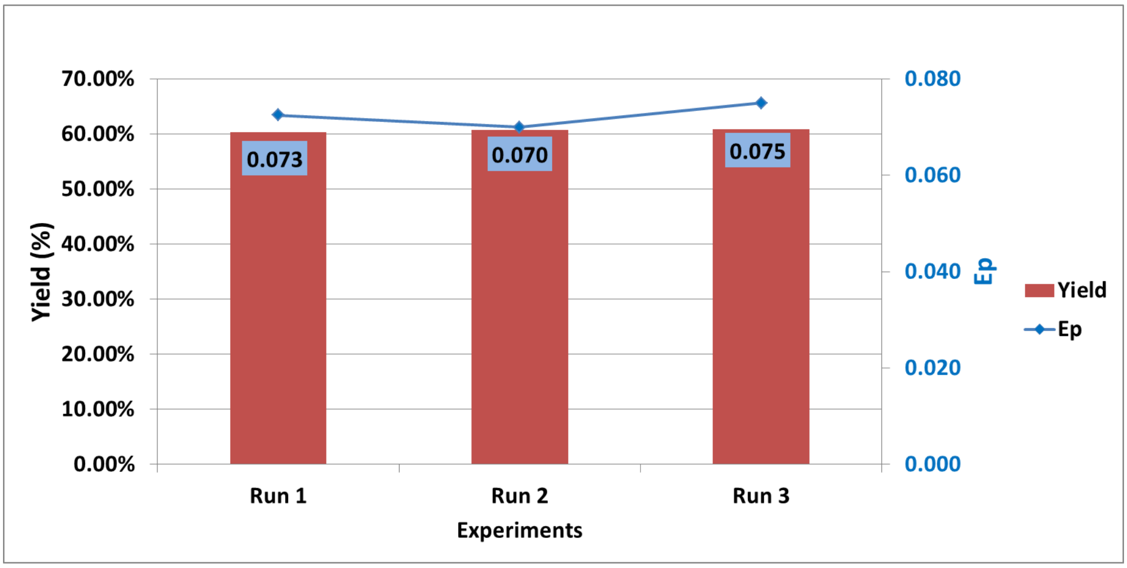

Figure 4-16: Yield and separation efficiency results for 100 wt% magnetite

The results in Figure 4-16 above show that a consistent yield ranging between 60.26 – 60.89% could be achieved at probable error (Ep) of 0.070 – 0.075 and at cut-point/separation density (ρ_{50}) of about 1.81 – 1.82 g/cm^3 for the 100 wt% magnetite bed.

Figure 4-17 below presents a comparison between the beneficiation results for the 40 wt% pyrrhotite + 60 wt% magnetite bed and 100 wt% magnetite bed. The average results for the 100 wt% magnetite lab run show that there was higher yield and separation efficiency for the 100 wt% magnetite bed compared to the 40 wt% pyrrhotite blend. The higher yield obtained was attributed to the higher cut density achieved for the 100 wt% magnetite bed.

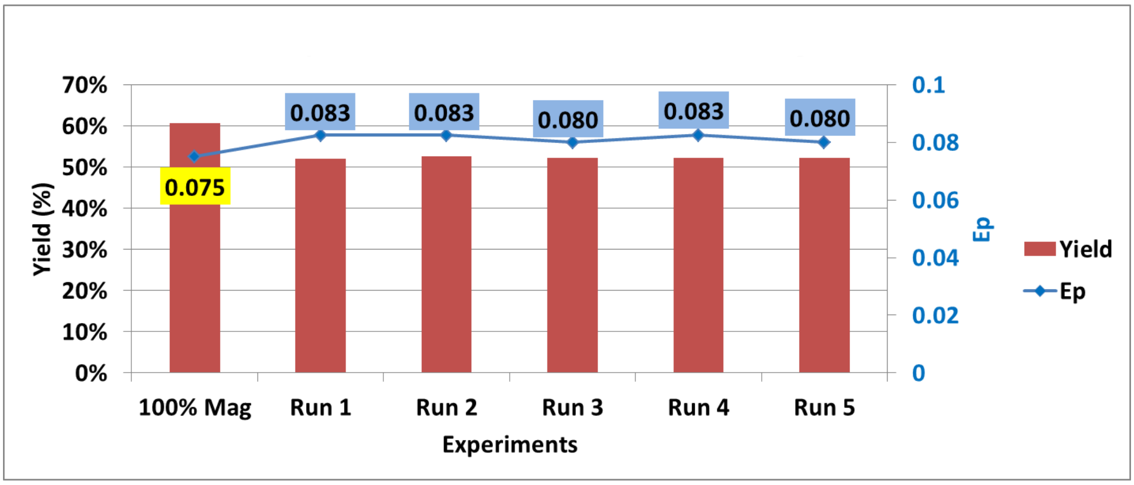

Figure 4-17: Comparison of 40 wt% blend and 100 wt% magnetite beneficiation

A detailed discussion on the effect of the cut-point density on quality of products obtained from the two beds, (i.e. the 100 wt% magnetite and the 40 wt% pyrrhotite + 60 wt% magnetite bed) is provided in section 4.5.3.

4.5.3 Product analysis

Table 4-11 below shows the properties of the products and discards recovered from the fluidized bed (ADMFB) using 40 wt% pyrrhotite + 60 wt% magnetite bed and 100 wt% magnetite as the dense medium material. The table presented the result from the proximate analysis, total sulphur and calorific value of the feed coal, discards and the cleaned products. Table 4-9 below shows that the ash content of the feed coal was reduced from 39.32% to 14.21 – 14.75% ash with a calorific value of 26.77 – 27.58 MJ/kg. The overall ash reduction was 62.49 – 63.86%, while the feed sulphur content was reduced from 2.49% to 0.41 – 0.42% using the dense medium of 40% pyrrhotite + 60% magnetite blend.

Table 4-11: Comparison of 40% blend and 100% magnetite beneficiation products

Sample		**Ash %**	**CV MJ\kg**	**VM %**	**Yield %**	**Ash reduction %**	**S %**
Feed		39.32	18.76	19.80	100	0.00	2.49
ADMFB 40% pyrrhotite	Product 1	14.75	27.60	24.14	52.36	62.49	0.42
	Product 2	14.21	26.77	23.55	52.18	63.86	0.41
	Product 3	14.54	27.58	25.09	52.20	63.12	0.42
	Discard 1	61.08	9.66	14.77	47.64	0.00	3.58
	Discard 2	62.06	8.84	14.28	47.82		
	Discard 3	61.52	8.80	14.76	47.80		
ADMFB 100% magnetite	Product 1	19.60	25.46	22.50	60.26	50.15	
	Product 2	20.20	25.24	21.99	60.67	48.63	
	Product 3	20.95	25.01	22.24	60.89	46.72	
	Discard 1	63.14	8.31	14.14	39.74	0.00	
	Discard 2	63.05	8.70	13.84	39.33		
	Discard 3	64.06	7.95	13.77	39.11		
Float and Sink Test	F @ 1.30	5.54	31.47	28.31	1.18		
	F @ 1.40	8.29	30.47	26.72	13.99		
	F @ 1.50	13.96	27.70	23.06	23.81		
	F @ 1.60	22.05	24.10	22.00	10.04		
	F @ 1.70	32.06	19.83	18.60	6.90		
	F @ 1.80	38.56	17.73	18.84	6.55		
	F @ 1.86	42.79	15.81	16.14	2.45		
	S @ 1.86	76.53	4.08	10.70	35.08		

* CV: Calorific Value; VM: Volatile Matter; S: Sulphur

According to Table 4-11, a clean coal product with an ash content of 19.60 – 20.95% and calorific value of 25.01 – 25.46 MJ/kg was also produced for the 100 wt% magnetite bed. The lower ash products obtained under the 40 wt% pyrrhotite + 60 wt% magnetite bed were as a result of the lower ρ_{50} (1.63 – 1.64 g/cm^3) of the bed compared to 100 wt% magnetite bed with ρ_{50} of 1.81 – 1.82 g/cm^3. The 40 wt% pyrrhotite bed, according to Table 4-11 above, produces cleaner coal products with similar ash content and with the yield as twice as that of the float/sink product at RD of 1.5 (shown in Table 4-11). A similar investigation by He *et al.* (2013) showed that a blend of paigeite ore at 25 – 35% + magnetite (75 – 65%) reduces a feed coal ash from 33.43% to 11.63% with an Ep and recovery efficiency at 0.07 and

98.59%, respectively. Further analysis was carried out on the products of the ADMFB 40% pyrrhotite bed and the results are depicted in Table 4-12 below.

Table 4-12: Ultimate analysis results of ADMFB 40 wt% pyrrhotite bed products

Sample		**C%**	**H%**	**N%**	**S%**	**O%**
Feed		49.40	2.57	1.20	2.49	2.06
ADMFB 40% pyrrhotite	Product 1	73.1	3.79	1.73	0.42	3.09
	Product 2	72.1	3.81	1.73	0.41	4.67
	Product 3	71.8	3.80	1.73	0.42	4.62
	Discard 2	25.1	1.61	0.71	3.58	3.89

* C: Carbon; H: Hydrogen; N: Nitrogen; S: Sulphur; O: Oxygen by difference [100-(H+C+N+Ash+H_20+S)]

These results indicate that pyrrhotite ore, which is normally dumped as tailings, has a potential to be used as mixed solid media for ADMFB beneficiation. This test also shows that the blending of some ores which have the required fluidization characteristics could improve the quality of the product obtained from an ADMFB process.

4.5.4 Effect of moisture

In order to determine the effect of moisture on the process, beneficiation tests using the same coal sample but with increased moisture content from 2.11% to 3.13% total moisture (48% higher than the other feed coal samples) was utilized.

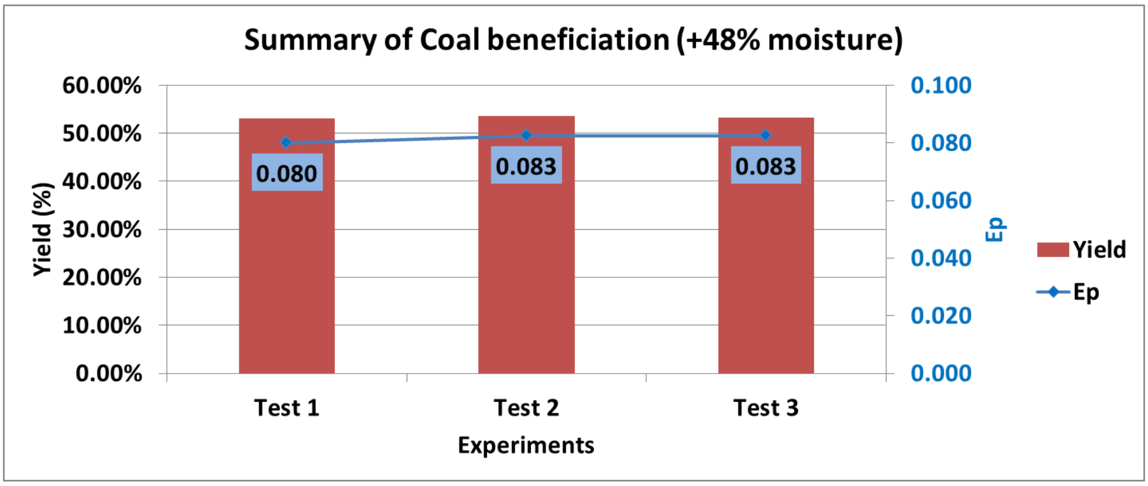

Figure 4-18: Beneficiation test results for coal with increased moisture content.

Figure 4-18 above shows the summary results of the beneficiation tests carried out with increased moisture in the sample. It can be seen that the probable error (Ep) and yield obtained were 0.080 – 0.083 and 53.04 – 53.67%, respectively. These results were within the range achieved for lab runs 1 – 4 (Figure 4-15), indicating that an increase in moisture content of the feed coal by 48% has no negative effects on the process in terms of yield and separation efficiency.

4.5.5 Organic efficiency

The efficiency of this ADMFB separator for beneficiating coal was determined by calculating the organic efficiency of the process using Equation 3-15. The organic efficiency is a ratio of actual yield of desired product to the theoretical yield at the same ash content. Using the washability curves as illustrated in Figure 4-1, it was established that the theoretical yield of approximately 14% ash product was 53%. The average yield from the lab runs (Figure 4-15) was in the range 52.04 – 52.67% and therefore, the organic efficiency ranged from 98.20 – 99.30%.

The potential of different blend ratio of pyrrhotite as a dense medium for coal beneficiation has been illustrated with respect to the quality and yield of clean coal products that can be obtained. However, it is also important to establish the cost impact of this alternative media for partial replacement of magnetite in an ADMFB process. The cost evaluation of the proposed potential dense medium material for use in dry coal beneficiation is presented in section 4.6

4.6 COST EVALUATION OF PYRRHOTITE AS DENSE SOLID MEDIUM

It was established in this study that a blend of pyrrhotite and magnetite could potentially be used as a dense medium material for coal beneficiation in an ADMFB separator. The economic impact of this novel medium (40 wt% pyrrhotite) as a supplement to 60 wt% magnetite on beneficiating coal was established and outlined based on the product quality and yield, compared to that from magnetite solely. The recent study from the modularized and commercial ADMFB separator by Zhao *et al*. (2016) was used as a basis for evaluating the cost of beneficiating coal from this system. The decision to use the approach applied by Zhao *et al*. (2016) in this study is due to the fact that there are no commercial ADMFB operating in South Africa, therefore this documented investigation was utilized.

4.6.1 Industrial modularized ADMFB Separator

The industrial modularized ADMFB dry coal separator used by Zhao *et al*. (2016) has a modest footprint of (25 × 8) m^2 and 11 m high, which would be suitable for junior coal miners in South Africa. All the critical sections on this separator are under one platform, i.e. the raw coal pre-treatment, dense medium recovery, air supply and dust removal. The technical parameters of the system are shown in Table 4-13.

Table 4-13: Technical parameters of the ADMFB Separator (Source: Zhao et al., 2016)

Parameter	Unit	Value
Capacity	t/hr	50
Dense medium loss rate	kg/t (feed coal)	5
Dense medium circulation rate	1 ton coal/t	2

The following reasons support the use of this plant as a case study:

1. The ADMFB separator currently uses a binary (blend) dense medium of magnetite and fine coal with a blend ratio of magnetite (100-75%): fine coal (0-25%). Therefore, the plant is already adaptable to a blend medium material such as the pyrrhotite/magnetite blend
2. Zhao *et al*. (2016) states that the separation density of the separator is adjustable by automatic bed density control system which adjusts the fine coal content. Hence the bed can separate different coal which has different washability characteristics for example the high ash SA coal tested in this study
3. This system also processes a feed coal size range of -100+6 mm which is within the size range of the coal tested (-13+6 mm) in this study. The wide feed size range of the separator also allows for different coal size products to be achieved.

4.6.2 Cost benefit of using pyrrhotite-magnetite blend

In order to develop a preliminary cost benefit analysis for the blend of pyrrhotite and magnetite, a basis for the calculations was also developed using a number of parameters as shown in Table 4-14 below. In addition, some assumptions as seen in section 4.6.2.2 were made.

4.6.2.1 Basis for calculations

In order to perform the cost evaluation, a basis was chosen for certain key operating parameters used. Table 4-14 shows parameters used and their values.

Table 4-14: Basis for calculation of dense medium operating costs

Index	Value
Operation cycle (hours/day)	20
Operation cycle (days/month)	30
Dense medium loss rate (kg/t feed coal)	5
Plant capacity (ton/hour)	50
Blend ratio (pyrrhotite weight %)	40%
Magnetite price per ton (ZAR)	2 400.00
Pyrrhotite price per ton (ZAR)	0.00

4.6.2.2 Assumptions

1. The plant used is the same as that used by Zhao *et al.* (2016) for the beneficiation of Chinese coal and with similar throughput.
2. Pyrrhotite-magnetite blend was used as the solid medium instead of magnetite only on the modularized plant with the same operating parameters as applied to the beneficiation of Chinese coal.
3. The dense medium material loss rate was constant even when the medium has changed to a blend (pyrrhotite/magnetite) and not magnetite/fine coal.
4. The pyrrhotite used is 100% magnetic, i.e. the 30% magnetic fraction highlighted in the Davis tube test (Table 4-3). Therefore, uniform dense medium loss between the pyrrhotite and magnetite is expected.

5. The cost of the ADMFB plant was not considered; the focus was on magnetite and pyrrhotite as the dense medium material and the cost of the clean coal product based on grade considered.
6. The cost of pyrrhotite is negligible and equated to zero as it is currently a reject material and is not sold by the mine in South Africa.

4.6.2.3 Comparison of dense medium costs for 100 wt% magnetite and 40:60 blend

According to the information provided by Zhao *et al.* (2016), along with the operating parameters and the basis provided in Tables 4-13 and 4-14 above, the operating cost of medium that could achieve clean coal products ranging from 27.60 to 25.01 MJ/Kg for a typical modularized plant (ADMFB) was calculated for South Africa application. Table 4-15 below shows the expected costs related to dense medium material for the plant using magnetite only and 40 wt% pyrrhotite + 60 wt% magnetite as a dense medium material. The monthly dense medium loss for the ADMFB separator is 150 tons as calculated from the dense medium loss rate of 5 kg per ton of raw coal (Table 4-14) regardless of the dense medium used (section 4.6.2.2: assumption 3).

Table 4-15: Monthly dense medium costs for magnetite only and blend

Index	**ADMFB separator dense medium**	
	100% magnetite	**40% pyrr + 60% magnetite**
Daily throughput (t)	1 000	
Monthly throughput (t)	30 000	
Monthly dense medium loss rate (kg)	150 000	
Monthly magnetite loss rate (kg)	150 000	90 000
Monthly dense medium cost (ZAR)	**360 000.00**	**216 000.00**

*pyrr: Pyrrhotite

However, based on section 4.6.2.2: assumption 6, the actual dense medium value loss is of magnetite since pyrrhotite cost is zero. Therefore, the monthly dense medium (magnetite) loss for the 100 wt% magnetite and the 40 wt% pyrrhotite + 60 wt% magnetite bed is 150 tons and 90 tons, respectively (section 4.6.2.2: assumption 4). If a blend of 40 wt% pyrrhotite + 60 wt% magnetite was utilized as the dense medium material for this modularized ADMFB separator, the expected costs would be as shown in Table 4-15 above. It can be seen that even with partial blending of up to 40 wt% pyrrhotite there are savings that can be achieved by using pyrrhotite as a dense medium material. The magnetite consumption could decrease from 150 tons to 90 tons and consequently reduce the cost from ZAR 360 000 to ZAR 216 000 when a 40 wt% pyrrhotite blend is used. This is coupled with a higher quality product that can be achieved using the 40 wt% pyrrhotite + 60 wt% magnetite compared to the 100 wt% magnetite dense medium materials (Table 4-11).

The blend ratio may be adjusted downwards from 40 wt% but in all instances a saving proportionate to the amount of pyrrhotite used will be achieved. Figure 4-19 below shows how the cost saving on dense medium material will increase with increasing blend ratio. In this study the increase in blend ratio was up to a limit of 40 wt% for an effective and yield were maintained within reasonable values.

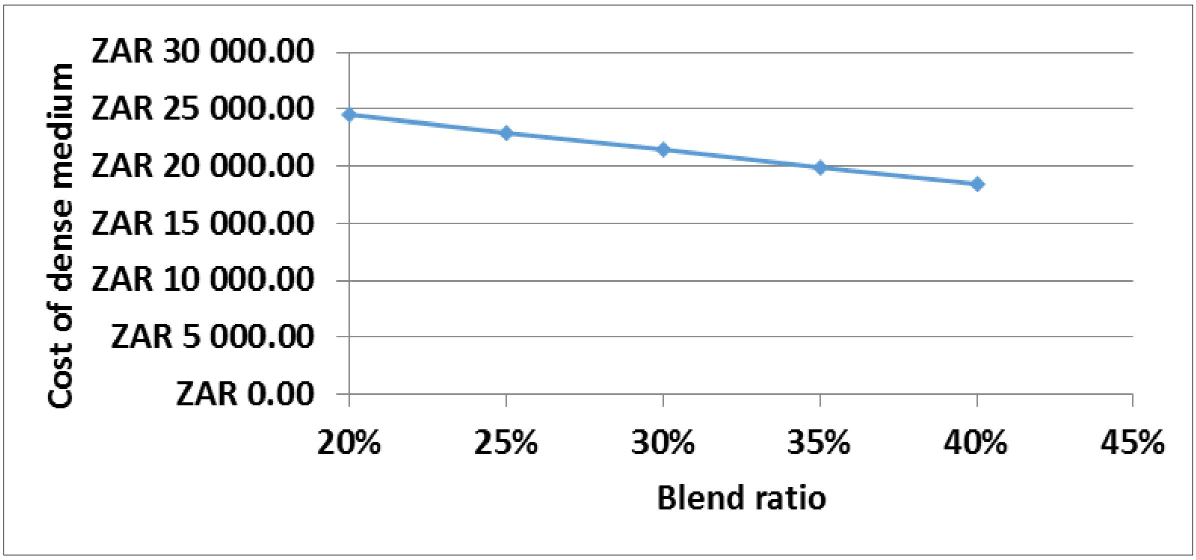

Figure 4-19: Effect of blending on dense medium costs

4.6.2.4 Comparison of product income for 100% magnetite and 40:60 blend

In order to give a full picture of the profitability of using a 40 wt% pyrrhotite + 60 wt% magnetite blend, a comparison of the revenue potential for the two dense media options was also carried out. The results of product grades highlighted in Table 4-11ranging from 27.60 to 25.01MJ/Kg above were used. The revenue from the two coal products was calculated based on the following:

I. Coal prices (Prevost, 2017),
II. Plant technical parameters (Zhao *et al.*, 2016),
III. Operating parameters in Tables 4-11, 4-13, 4-14 and 4-15.

Table 4-16: Monthly income analysis for 100 wt% magnetite and 40 wt% pyrr + 60 wt% magnetite

Index	**ADMFB separator dense medium**	
	100% magnetite	**40% pyrr + 60% magnetite**
Daily throughput (t)	1 000	
Monthly throughput (t)	30 000	
Recovery (average) %	60	53
Clean coal product (t)	18 000	15 900
Product price per ton (ZAR)	600	790
Monthly revenue (ZAR)	**10 800 000**	**12 561 000**
Monthly dense medium cost (ZAR)	360 000	216 000
Expected 'Profit' (ZAR)	**10 440 000**	**12 345 000**

*pyrr: Pyrrhotite

Table 4-16 depicts the expected profit that could be generated from an ADMFB using two different media based on the average SA inland sized coal prices. The cost for a clean coal product, grades B and D are ZAR790 and ZAR600 respectively. Therefore, according to this study the 100% magnetite clean coal product and 40 wt% pyrrhotite + 60 wt% magnetite product are expected to be ZAR600 and ZAR790 per ton, respectively. Therefore, factoring in the yield and dense medium cost for each it can be seen that higher 'profits' can be expected for the latter because of the higher quality product.

The next and final chapter provides conclusions of the study along with the recommendations for any future studies and/or implementation of potential alternative dense medium material.

Chapter 5 : Conclusions and Recommendations

5.1. Conclusions

In this study, the potential of pyrrhotite, granulated blast furnace slag, silica sand and coal rejects were evaluated as alternative solid medium materials to magnetite, solely/mixed to expand the choice of dense medium suitable for ADMFB coal separation in South Africa. Material characterizations, fluidization characterizations, sink/float and ADMFB beneficiation tests were conducted, and different clean coal products were obtained. A cost evaluation was performed to determine the economic potential of using pyrrhotite as an alternative dense medium material for concept of screening.

The following conclusions were drawn from this study:

1. All the solid medium materials tested were classified as Geldart Group B materials (40 – 500 µm and density 1 400 – 4 000 kg/cm^3), with the potential for creating a bed with good fluidization characteristics.

2. According to the results obtained from the Davis tube test, pyrrhotite was the only medium out of the four proposed media that has a magnetic and non-magnetic material of about 30% and 70%, respectively.

3. The fluidization characterization tests showed that the most stable and uniform beds in descending order were, magnetite, pyrrhotite, GBFS, silica sand and coal rejects.

4. Magnetite, pyrrhotite and GBFS exhibited the most uniform and stable beds at 20 cm bed height with a coefficient of variation (CoV) that was less than 0.7%, compared to silica sand and coal rejects with CoV of 0.85 – 1.18%.

5. An investigation using 100 wt% magnetite bed and density tracers showed that the probable error (Ep) reduces from 0.063 to 0.040 with a decreased static bed height from 30 to 20 cm.

6. The beneficiation tests conducted using density tracers and a bed of pyrrhotite-magnetite blend at 40 wt% pyrrhotite + 60 wt% magnetite produces products with yield ranging between 53 – 58% and probable error (Ep) 0.053 – 0.073. The optimum blend ratio was at 40 wt% pyrrhotite + 60 wt% magnetite, however, beyond which the yield and probable error began to decline.

7. The coarser particle tracers (8 × 16) mm had better Ep and yield of 0.015 – 0.025 and 56 – 65%, respectively, more than (6 – 13) mm tracers with an Ep ranging between 0.040 – 0.073 and yield of 53 – 58%.

8. The coal beneficiation test with 100 wt% magnetite bed produced coal products with yield and Ep of 60.26 – 60.89% and 0.070 – 0.075, respectively. Clean coal products with an ash content ranging between ***19.60 – 20.95%*** and calorific value (25.01 – 25.46) MJ/kg were produced at a cut-point/separation density (ρ_{50}) of about 1.81 – 1.82 g/cm^3.

9. A bed of 40 wt% pyrrhotite + 60 wt% magnetite blend produces clean coal products with an ash content ranging between ***14.21 – 14.75%*** and calorific value (26.77 – 27.58) MJ/kg from a feed coal of 39.32%. The Ep and yield achieved from the bed at a cut-point/separation density of 1.63 – 1.64 g/cm^3 ranging between 0.080 – 0.083 and 52.04 – 52.67%, respectively. The overall ash reduction was 62.49 – 63.86%, while the feed sulphur content was reduced from 2.49% to 0.41 – 0.42%.

10. From a cost perspective, the partial replacement or blending of the pyrrhotite ore, which is considered a reject with magnetite, might be of great impact in reducing the operating cost of a coal ADMFB process.

11. The superior product achieved by the 40 wt% pyrrhotite + 60 wt% magnetite bed has a higher market value per tonne of about ZAR790.00 compared to ZAR600.00 for the 100% magnetite bed. Therefore, there is potential for higher revenue generation if a blend is utilized as the dense medium material.

In summary, pyrrhotite proved to be the superior dense medium material amongst the other materials tested as alternative media to magnetite. The most uniform and stable bed density was achieved using a blend of pyrrhotite (40 wt%) and magnetite (60 wt%), rather than an individual medium. A cleaner coal product with less ash and sulphur content was obtained from this blend compared to using 100 wt% magnetite bed. From the 40 wt% pyrrhotite bed, feed ash content was reduced from 39.32% to about 14.50% ash and calorific value increased from 18.76 to 27.30 MJ/kg for the product coal. By way of contrast, a 100 wt% magnetite bed produced a product with an ash content of about 20.30% and calorific value of about 25.24 MJ/kg. This research has presented results that show that there is considerable potential for developing dry coal beneficiation using the AMDFB process in future for the South African coal market.

5.2. Recommendations

This study has successfully demonstrated that pyrrhotite can be used as a blend for the beneficiation of coal in an ADMFB application. Therefore, the following recommendations are made for further investigation based on the present results;

1. Pilot scale test using a blend of pyrrhotite and magnetite should be carried out in a continuous ADMFB plant to establish the separation efficiency of the system in continuous mode.

2. Techno-economic studies should be carried out to investigate the potential of a full scale pyrrhotite preparation plant that can produce pyrrhotite for use as a dense medium in dry coal processing.

3. Further investigation should be carried out to determine other suitable and low cost minerals which can be used as an alternative dense medium.

References

Anon ISO 13909-4:2016 - Hard Coal and Coke - Mechanical sampling - Part 4: Coal - Preparation of test samples. [online]. Available from: https://www.iso.org/standard/63910.html [Accessed November 23, 2017].

Anon ASTM D4239 - 05 Standard Test Methods for Sulfur in the Analysis Sample of Coal and Coke Using High Temperature Tube Furnace Combustion Methods. [online]. Available from: https://www.astm.org/DATABASE.CART/HISTORICAL/D4239-05.htm [Accessed November 23, 2017a].

Anon ASTM D5142 - 09 Standard Test Methods for Proximate Analysis of the Analysis Sample of Coal and Coke by Instrumental Procedures. [online]. Available from: https://www.astm.org/Standards/D5142.htm [Accessed November 23, 2017b].

Anon ASTM D5373 - 02 Standard Test Methods for Instrumental Determination of Carbon, Hydrogen, and Nitrogen in Laboratory Samples of Coal and Coke. [online]. Available from: https://www.astm.org/DATABASE.CART/HISTORICAL/D5373-02.htm [Accessed November 23, 2017c].

Anon ASTM D5865 - 04 Standard Test Method for Gross Calorific Value of Coal and Coke. [online]. Available from: https://www.astm.org/DATABASE.CART/HISTORICAL/D5865-04.htm [Accessed November 23, 2017d].

Anon ISO 13320:2009 - Particle Size Analysis -- Laser Diffraction Methods. [online]. Available from: https://www.iso.org/standard/44929.html [Accessed November 23, 2017e].

Anon ISO/TR 18336:2016 - Guidelines for good XRF laboratory practice for the iron ore industry. [online]. Available from: https://www.iso.org/standard/62200.html [Accessed November 23, 2017f].

Arnold, R.G. (1967) Range in Composition and Structure of 82 Natural Terrestrial Pyrrhotites. *The Canadian Mineralogist*. **9**(1), 31–50.

Azimi, E., Karimipour, S., Rahman, M., Szymanski, J., Gupta, R. (2013) Evaluation of the Performance of Air Dense Medium Fluidized Bed (ADMFB) for Low-Ash Coal Beneficiation. Part 1: Effect of Operating Conditions. *Energy & Fuels*. **27**(10), 5595–5606.

Bada, S.O., Falcon, L.M., Falcon, R.M.S., Bergmann, C.P. (2012) Feasibility Study on Triboelectrostatic Concentration of< 105 μm phosphate ore. *Journal of the Southern African Institute of Mining and Metallurgy*. **112**(5), 341–345.

Bada, S.O., Falcon, R.M.S., Falcon, L.M. (2010) The Potential of Electrostatic Separation in the Upgrading of South African Fine Coal Prior to Utilization–A Review. *The Journal of The Southern African Institute of Mining and Metallurgy*. **110**(11), 691–702.

Becker, M. (2009) *The Mineralogy and Crystallography of Pyrrhotite from Selected Nickel and PGE Ore Deposits and its Effect on Flotation Performance*. PhD Thesis. Pretoria, South Africa: University of Pretoria.

Bertaut, E.F. (1953) Contribution à l'étude des Structures Lacunaires: la Pyrrhotine. *Acta Crystallographica*. **6**(6), 557–561.

Boylu, F., Çinku, K., Çetinel, T., Karakaş, F., Güven, O., KaraağaçlIoğlu, I.E., Çelik, M.S. (2015) Effect of Coal Moisture on the Treatment of a Lignitic Coal through a Semi-Pilot-Scale Pneumatic Stratification Jig. *International Journal of Coal Preparation and Utilization*. **35**(3), 143–154.

Carpenter, R.H., Desborough, G.A. (1964) Range in solid solution and structure of naturallyoccurring troilite and pyrrhotite. *American Geologist*. **49**.

Chen, Q., Yang, Y. (2003) Development of Dry Beneficiation of Coal in China. *Coal Preparation*. **23**(1–2), 3–12.

Chikerema, P. (2011) *Effects of Particle Size, Shape and Density on the Performance of an Air Fluidized Bed in Dry Coal Beneficiation*. MSc Dissertation. Johannesburg, South Africa: University of the Witwatersrand.

Chikerema, P., Moys, M. (2012) Effects of Particle Size, Shape, and Density on the Performance of an Air Fluidized Bed in Dry Coal Beneficiation. *International Journal of Coal Preparation and Utilization*. **32**(2), 80–94.

Choung, J., Mak, C., Xu, Z. (2006) Fine Coal Beneficiation using an Air Dense Medium Fluidized Bed. *Coal Preparation*. **26**(1), 1–15.

Çicek, T. (2008) Dry Cleaning of Turkish Coal. *Energy Sources, Part A: Recovery, Utilization, and Environmental Effects*. **30**(7), 593–605.

De Vasconcelo, S., Douglas, P., Amarante Mesquita, A.L. (2011) Minimum and Full Fluidization Velocity for Alumina used in the Aluminum Smelter. *International Journal of Engineering Business Management*. **3**(4), 7–13.

Department of Minerals and Energy (DME) (2001) *National Inventory Discard and Duff Coal: Summary report.*

Dwari, R.K., Rao, K.H. (2007) Dry Beneficiation Of Coal - A Review. *Mineral Processing and Extractive Metallurgy Review*. **28**(3), 177–234.

Fan, M., Chen, Q., Zhao, Y., Luo, Z. (2001) Fine Coal (6–1 Mm) Separation in Magnetically Stabilized Fluidized Beds. *International Journal of Mineral Processing*. **63**(4), 225–232.

Fan, M., Chen, Q., Zhao, Y., Luo, Z., Guan, Y. (2003) Fundamentals of a Magnetically Stabilized Fluidized Bed for Coal Separation. *Coal Preparation*. **23**(1–2), 47–55.

Firdaus, M., O'Shea, J.-P., Oshitani, J., Franks, G.V. (2012) Beneficiation of Coarse Coal Ore in an Air-Fluidized Bed Dry Dense-Medium Separator. *International Journal of Coal Preparation and Utilization*. **32**(6), 276–289.

Fraser, T., Yancey, H. (1926) Artificial Storm of Air-Sand Floats Coal on Its Upper Surface, Leaving Refuse to Sink. *Coal Age*, 325–327.

Fu, Z., Zhao, Y., Yang, X., Luo, Z., Zhao, J. (2016) Fine Coal Beneficiation via Air-Dense Medium Fluidized Beds with Improved Magnetite Powders. *International Journal of Coal Preparation and Utilization*. **36**(1), 55–68.

Geldart, D. (1973) Types of Gas Fluidization. *Powder Technology*. **7**(5), 285–292.

Hancox, P.J., Götz, A.E. (2014) South Africa's coalfields - A 2014 perspective. *International Journal of Coal Geology*. **132**, 170–254.

He, J., Zhao, Y., He, Y., Luo, Z., Duan, C. (2013) Fluidization Characteristics of the Dense Gas-Solid Fluidized Bed Separator Based on the Mixed-Medium Solids of Magnetite and Paigeite Powder. *International Journal of Coal Preparation and Utilization*. **33**(5), 225–241.

He, Y., Zhao, Y., Chen, Q. (2003) Fine Particle Behavior in Air Fluidized Bed Dense Medium Dry Separator. *Coal Preparation*. **23**(1–2), 33–45.

Hise, E., Holman, A., Friedlaender, F. (1981) Development of high-gradient and open-gradient magnet separation of dry fine coal. *IEEE Transactions on Magnetics*. **17**(6), 3314–3316.

Honaker, R.Q., Bimpong, C. (2009) Alternative Materials for Dense Medium Separations. *International Journal of Coal Preparation and Utilization*. **29**(4), 173–191.

Honaker, R.Q., Saracoglu, M., Thompson, E., Bratton, R., Luttrell, G.H., Richardson, V. (2008) Upgrading Coal Using a Pneumatic Density-Based Separator. *International Journal of Coal Preparation and Utilization*. **28**(1), 51–67.

ISO (2011) *SANS 3082: Iron ores - Sampling and Sample Preparation Procedures*. 1st ed. Pretoria, South Africa: SABS.

ISO (1989) *SABS 8833: Magnetite For Use in Coal Preparation - Test methods*. 1st ed. Pretoria, South Africa: SABS.

ISO (2011) *SANS 7936: Hard coal - Determination and Presentation of Float and Sink Characteristics - General Directions for Apparatus and Procedures*. 1st ed. Pretoria, South Africa: SABS.

ISO 13909-4 (2016) ISO 13909-4:2016 - Hard Coal and Coke -- Mechanical Sampling -- Part 4: Coal -- Preparation of Test Samples. [online]. Available from: https://www.iso.org/standard/63910.html [Accessed November 23, 2017].

Jiao, H.-G., Cui, J.-Y., Liu, P., Chen, Q.-R., Tie, Z.-X. (2009) Experimental Study of Magnetic Property and Dry Magnetic Separation of Fine Coal. *Zhongguo Kuangye Daxue Xuebao/Journal of China University of Mining and Technology*. **38**(1), 131–134+148.

Korte (2014) *Dry Processing of Coal – Status update*. COALTECH.

Kretzschmar, S. (2010) *Dry beneficiation of coal using an air dense-medium fluidised bed separator*.

Le Roux, A. (2014) *Opportunity for Electricity Generation from Discard Coal at the Witbank Coalfields*. Thesis. Stellenbosch : Stellenbosch University.

Luo, Z., Fan, M., Zhao, Y., Tao, X., Chen, Q., Chen, Z. (2008) Density Dependent Separation of Dry Fine Coal in aVibrated Fluidized Bed. *Powder Technology*. **187**(2), 119–123.

Luo, Z., Zhao, Y., Tao, X., Fan, M., Chen, Q., Wei, L. (2003) Progress in Dry Coal Cleaning Using Air-Dense Medium Fluidized Beds. *Coal Preparation*. **23**(1–2), 13–20.

LUO, Z., ZHU, J., FAN, M., ZHAO, Y., TAO, X. (2007) Low Density Dry Coal Beneficiation Using an Air Dense Medium Fluidized Bed. *Journal of China University of Mining and Technology*. **17**(3), 306–309.

Mohanta, S., Chakraborty, S., Meikap, B.C. (2011) Influence of Coal Feed Size on the Performance of Air Dense Medium Fluidized Bed Separator Used for Coal Beneficiation. *Industrial & Engineering Chemistry Research*. **50**(18), 10865–10871.

Mohanta, S., Chakraborty, S., Meikap, B.C. (2013) Optimization Process of an Air Dense Medium Fluidized Bed Separator for Treating High-Ash Non-coking Indian Coal. *Mineral Processing and Extractive Metallurgy Review*. **34**(4), 240–248.

Mohanta, S., Daram, A.B., Chakraborty, S., Meikap, B.C. (2012) Characteristics of Minimum Fluidization Velocity for Magnetite Powder used in An Air Dense Medium Fluidized Bed for Coal Beneficiation. *Particle and Particle Systems Characterization*. **29**(4), 228–237.

Mohanta, S., Rao, C.S., Daram, A.B., Chakraborty, S., Meikap, B.C. (2013) Air Dense Medium Fluidized Bed for Dry Beneficiation of Coal: Technological Challenges for Future. *Particulate Science and Technology*. **31**(1), 16–27.

Özbay, E., Erdemir, M., Durmuş, H.İ. (2016) Utilization and Efficiency of Ground Granulated Blast Furnace Slag on Concrete Properties – A review. *Construction and Building Materials*. **105**, 423–434.

Patil, D.P., Parekh, B.K. (2011) Beneficiation of Fine Coal Using the Air Table. *International Journal of Coal Preparation and Utilization*. **31**(3–4), 203–222.

Perry, R.H., Green, D.W., Maloney, J.O. (1997) *Perry's Chemical Engineers' Handbook*. McGraw-Hill.

Prevost, X.M. (2015) Coal in the Global and Southern African Context.

Prevost, X. (2017) SA Inland sized coal prices.

Richardson, J.F., Harker, J.H., Coulson, J.M. (2008) *Particle Technology and Separation Processes*. 5. ed., reprinted. Oxford: Butterworth Heinemann.

Sahu, A.K., Biswal, S.K., Parida, A. (2009) Development of Air Dense Medium Fluidized Bed Technology For Dry Beneficiation of Coal – A Review. *International Journal of Coal Preparation and Utilization*. **29**(4), 216–241.

Sahu, A.K., Tripathy, A., Biswal, S.K. (2013) Study on Particle Dynamics in Different Cross Sectional Shapes of Air Dense Medium Fluidized Bed Separator. *Fuel*. **111**, 472–477.

Sahu, A.K., Tripathy, A., Biswal, S.K., Parida, A. (2011) Stability Study of an Air Dense Medium Fluidized Bed Separator for Beneficiation of High-Ash Indian Coal. *International Journal of Coal Preparation and Utilization*. **31**(3–4), 127–148.

Sampaio, C.H., Aliaga, W., Pacheco, E.T., Petter, E., Wotruba, H. (2008) Coal Beneficiation of Candiota Mine by Dry Jigging. *Fuel Processing Technology*. **89**(2), 198–202.

Song, S., Zhao, Y., Luo, Z., Tang, L. (2012) Motion Behavior of Particles in Air–Solid Magnetically Stabilized Fluidized Beds for Separation. *International Journal of Mining Science and Technology*. **22**(5), 725–729.

Wang, T.-J., Jin, Y., Tsutsumi, A., Wang, Z., Cui, Z. (2000) Energy Transfer Mechanism in a Vibrating Fluidized Bed. *Chemical Engineering Journal*. **78**(2), 115–123.

Wang, Y., Luo, Z., Huang, G., Ren, B. (2016) Effect of Agitation on the Characteristics of Air Dense Medium Fluidization. *International Journal of Mining Science and Technology*. **26**(3), 383–387.

Wei, L., Chen, Q., Zhao, Y. (2003) Formation of Double-Density Fluidized Bed and Application in Dry Coal Beneficiation. *Coal Preparation*. **23**(1–2), 21–32.

Wills, B.A. (2011) *Wills' Mineral Processing Technology: An Introduction to the Practical Aspects of Ore Treatment and Mineral Recovery*. Butterworth-Heinemann.

Wyckoff, R.W.G. (1963) *Crystal Structures - Volume 1*. New York: Interscience Publishers.

Xin-xi, Z., Dai-yong, D., Bing, T., Jin-song, W., Feng, D., Hai-sheng, L., Rui-xin, M. (2009) Research on the Triboelectrostatic Separation of Minerals from Coal. *Procedia Earth and Planetary Science*. **1**(1), 845–850.

Yang, W. ed. (2003) *Handbook of Fluidization and Fluid-Particle Systems*. New York: Marcel Dekker.

Yang, X., Zhao, Y., Luo, Z., Song, S., Duan, C., Dong, L. (2013) Fine Coal Dry Cleaning Using a Vibrated Gas-Fluidized Bed. *Fuel Processing Technology*. **106**, 338–343.

Zhao, Y., Fu, Z., Yang, X., Luo, Z., Duan, C., Song, S., Cai, L. (2015) Fine Coal Dry Cleaning using an Air Dense Medium Fluidized Bed with Improved Magnetite Medium. *Procedia Engineering*. **102**, 1133–1141.

Zhao, Yue-min, Li, G., Luo, Z., Liang, C., Tang, L., Chen, Z., Xing, H. (2011) Modularized Dry Coal Beneficiation Technique Based on Gas-Solid Fluidized Bed. *Journal of Central South University of Technology*. **18**(2), 374–380.

Zhao, Y., Li, G., Luo, Z., Zhang, B., Dong, L., Liang, C., Duan, C. (2016) Industrial Application of a Modularized Dry-Coal-Beneficiation Technique Based on a Novel Air Dense Medium Fluidized Bed. *International Journal of Coal Preparation and Utilization*, 1–14.

Zhao, Y., Tang, L., Luo, Z., Liang, C., Xing, H., Wu, W., Duan, C. (2010) Experimental and Numerical Simulation Studies of The Fluidization Characteristics of A Separating Gas–Solid Fluidized Bed. *Fuel Processing Technology*. **91**(12), 1819–1825.

Zhao, Y., Yang, X., Luo, Z., Duan, C., Song, S. (2014) Progress in Developments of Dry Coal Beneficiation. *International Journal of Coal Science & Technology*. **1**(1), 103–112.

Zhao, Y. M., Liu, X.J., Liu, K.L., Luo, Z.F., Wu, W.C., Song, S.L., Tang, L.G. (2011) Fluidization Characteristics of a Gas-Paigeite-Powder Bed to be Utilized for Dry Coal Beneficiation. *International Journal of Coal Preparation and Utilization*. **31**(3–4), 149–160.

Zhenfu, L., Qingru, C. (2001) Dry Beneficiation Technology of Coal with an Air Dense-Medium Fluidized Bed. *International Journal of Mineral Processing*. **63**(3), 167–175.

Zhenfu, L., Qingru, C., Yaomin, Z. (2002) Dry Beneficiation of Coarse Coal Using an Air Dense Medium Fluidized Bed (ADMFB). *Coal Preparation*. **22**(1), 57–64.

Appendices

APPENDIX A: BED DENSITY DISTRIBUTION, WASHABILITY DATA AND PARTITION DATA

Table A-1: Bed uniformity and stability of magnetite 25cm

	Density (kg/m³)					
Sampling Point	**0 cm**	**5 cm**	**10 cm**	**15 cm**	**20 cm**	**25 cm**
A	1751	1770	1825	1864	1903	1945
B	1739	1781	1823	1860	1930	1939
C	1748	1765	1826	1846	1911	1942
D	1740	1786	1830	1864	1910	1938
E	1755	1789	1822	1865	1913	1918
F	1743	1775	1826	1864	1918	1930
G	1720	1762	1800	1838	1885	1912
H	1749	1787	1826	1865	1920	1931
I	1748	1790	1844	1880	1925	1957
CoV (%)	**0.59**	**0.60**	**0.62**	**0.66**	**0.69**	**0.71**
S_P (kg/m³)	**3.42**	**3.56**	**3.79**	**4.07**	**4.42**	**4.59**

Table A-2: Bed uniformity and stability of magnetite 30 cm

	Density (kg/m³)						
Sampling Point	**0 cm**	**5 cm**	**10 cm**	**15 cm**	**20 cm**	**25 cm**	**30 cm**
A	833	1028	1202	1376	1550	1725	1899
B	843	1021	1194	1368	1545	1714	1920
C	841	1016	1191	1346	1539	1737	1893
D	830	1010	1181	1369	1531	1748	1935
E	831	1009	1181	1353	1533	1708	1891
F	835	1013	1190	1367	1545	1730	1899
G	845	1024	1202	1374	1560	1718	1891
H	838	1020	1199	1359	1520	1720	1897
I	835	1010	1186	1361	1540	1706	1887
CoV (%)	**0.63**	**0.66**	**0.69**	**0.72**	**0.76**	**0.79**	**0.83**
SP (kg/m3)	**1.75**	**2.24**	**2.73**	**3.28**	**3.89**	**4.56**	**5.28**

Table A-3: Bed uniformity and stability of pyrrhotite 20 cm

Sampling Point	Density (kg/m³)				
	0 cm	**5 cm**	**10 cm**	**15 cm**	**20 cm**
A	1201	1292	1373	1455	1543
B	1195	1281	1366	1452	1538
C	1198	1284	1363	1433	1528
D	1188	1278	1382	1450	1529
E	1198	1291	1364	1446	1516
F	1202	1282	1361	1441	1520
G	1207	1295	1373	1455	1536
H	1199	1281	1362	1439	1521
I	1201	1290	1370	1454	1534
CoV (%)	**0.44**	**0.47**	**0.50**	**0.55**	**0.59**
S_P (kg/m³)	**1.75**	**2.03**	**2.29**	**2.37**	**2.52**

Table A-4; Bed uniformity and stability of pyrrhotite 30 cm

Sampling Point	Density (kg/m³)						
	0 cm	**5 cm**	**10 cm**	**15 cm**	**20 cm**	**25 cm**	**30 cm**
A	1344	1390	1447	1482	1527	1573	1619
B	1325	1370	1422	1471	1520	1548	1617
C	1336	1381	1425	1450	1508	1549	1596
D	1348	1393	1439	1485	1504	1577	1623
E	1338	1384	1430	1476	1522	1567	1591
F	1327	1375	1417	1473	1525	1571	1620
G	1347	1393	1439	1485	1531	1585	1593
H	1335	1377	1423	1472	1535	1573	1622
I	1345	1395	1438	1484	1540	1580	1623
CoV (%)	**0.64**	**0.65**	**0.70**	**0.75**	**0.77**	**0.82**	**0.86**
S_P (kg/m³)	**2.85**	**3.02**	**3.34**	**3.67**	**3.92**	**4.29**	**4.62**

Table A-5: Bed uniformity and stability of GBFS 20 cm

	Density (kg/m^3)				
Sampling Point	**0 cm**	**5 cm**	**10 cm**	**15 cm**	**20 cm**
A	811	919	1031	1135	1244
B	801	906	1011	1130	1240
C	810	918	1026	1121	1242
D	808	916	1024	1132	1237
E	807	915	1024	1138	1228
F	808	916	1024	1132	1240
G	815	922	1030	1146	1260
H	809	917	1025	1137	1241
I	808	916	1024	1132	1245
CoV (%)	**0.46**	**0.48**	**0.55**	**0.60**	**0.68**
S_P (kg/m^3)	**1.23**	**1.45**	**1.89**	**2.25**	**2.39**

Table A-6: Bed uniformity and stability of GBFS 25 cm

	Density (kg/m^3)					
Sampling Point	**0 cm**	**5 cm**	**10 cm**	**15 cm**	**20 cm**	**25 cm**
A	855	917	960	1016	1104	1160
B	856	912	954	1009	1093	1140
C	859	904	953	1007	1082	1145
D	852	915	971	1020	1102	1150
E	854	916	962	1025	1102	1163
F	845	906	967	1023	1090	1151
G	858	920	959	1024	1089	1155
H	850	913	955	1011	1093	1142
I	845	920	963	1018	1101	1141
CoV (%)	**0.60**	**0.61**	**0.64**	**0.66**	**0.70**	**0.73**
S_P (kg/m^3)	**1.71**	**1.87**	**2.04**	**2.24**	**2.57**	**2.78**

Table A-7: Bed uniformity and stability of silica sand 20 cm

	Density (kg/m³)				
Sampling Point	**0 cm**	**5 cm**	**10 cm**	**15 cm**	**20 cm**
A	837	955	1094	1233	1385
B	835	940	1096	1244	1389
C	847	955	1102	1219	1398
D	837	957	1086	1231	1384
E	842	963	1113	1240	1390
F	833	957	1088	1220	1383
G	845	950	1096	1226	1361
H	837	955	1102	1235	1398
I	847	957	1097	1218	1384
CoV (%)	**0.64**	**0.67**	**0.73**	**0.76**	**0.79**
S_P (kg/m³)	**1.79**	**2.13**	**2.68**	**3.13**	**3.65**

Table A-8: Bed uniformity and stability of silica sand 25 cm

	Density (kg/m³)					
Sampling Point	**0 cm**	**5 cm**	**10 cm**	**15 cm**	**20 cm**	**25 cm**
A	1214	1243	1269	1287	1311	1312
B	1198	1222	1245	1269	1292	1332
C	1193	1215	1237	1250	1282	1306
D	1196	1219	1243	1266	1293	1313
E	1194	1216	1239	1260	1280	1306
F	1197	1215	1235	1253	1270	1310
G	1196	1222	1243	1264	1287	1336
H	1200	1223	1247	1270	1293	1337
I	1180	1211	1240	1269	1299	1325
CoV (%)	**0.73**	**0.76**	**0.81**	**0.85**	**0.91**	**0.97**
S_P (kg/m³)	**2.89**	**3.09**	**3.37**	**3.60**	**3.91**	**4.28**

Table A-9: Bed uniformity and stability of silica sand 30 cm

	Density (kg/m³)						
Sampling Point	**0 cm**	**5 cm**	**10 cm**	**15 cm**	**20 cm**	**25 cm**	**30 cm**
A	1076	1056	1103	1152	1201	1250	1299
B	1081	1040	1104	1152	1210	1267	1324
C	1093	1045	1106	1146	1201	1253	1303
D	1079	1036	1113	1150	1217	1265	1322
E	1069	1050	1108	1154	1210	1290	1345
F	1096	1037	1133	1168	1182	1249	1327
G	1075	1042	1129	1175	1222	1256	1311
H	1091	1048	1118	1168	1194	1239	1296
I	1075	1024	1120	1180	1222	1259	1315
CoV (%)	**0.87**	**0.89**	**0.97**	**1.06**	**1.11**	**1.15**	**1.18**
S_P (kg/m³)	**3.13**	**3.10**	**3.59**	**4.09**	**4.45**	**4.81**	**5.18**

Table A-10; Bed uniformity and stability of coal rejects 20 cm

	Density (kg/m³)				
Sampling Point	**0 cm**	**5 cm**	**10 cm**	**15 cm**	**20 cm**
A	526	648	790	898	1008
B	528	641	795	908	1019
C	529	642	798	899	999
D	531	647	805	903	1010
E	525	650	804	909	1005
F	532	657	807	895	997
G	534	652	794	894	992
H	524	651	805	913	1004
I	523	650	794	912	995
CoV (%)	**0.72**	**0.76**	**0.78**	**0.82**	**0.85**
S_P (kg/m³)	**1.27**	**1.64**	**2.08**	**2.46**	**2.84**

Table A-11: Bed uniformity and stability of coal rejects 25 cm

	Density (kg/m^3)					
Sampling Point	**0 cm**	**5 cm**	**10 cm**	**15 cm**	**20 cm**	**25 cm**
A	944	871	840	823	826	769
B	930	879	838	827	827	776
C	946	872	835	825	835	778
D	943	873	825	815	816	788
E	935	870	849	827	820	784
F	946	875	834	829	829	775
G	954	889	840	834	823	769
H	937	879	828	839	809	776
I	948	888	841	834	826	790
CoV (%)	**0.77**	**0.81**	**0.84**	**0.86**	**0.93**	**0.98**
S_P (kg/m^3)	**2.41**	**2.37**	**2.34**	**2.36**	**2.55**	**2.54**

Table A-12: Bed uniformity and stability of coal rejects 30 cm

	Density (kg/m^3)						
Sampling Point	**0 cm**	**5 cm**	**10 cm**	**15 cm**	**20 cm**	**25 cm**	**30 cm**
A	957	910	862	814	766	718	678
B	970	927	879	829	783	725	687
C	960	916	852	832	775	719	684
D	954	927	860	828	759	715	673
E	967	915	863	811	769	707	675
F	947	919	859	813	772	712	689
G	959	910	862	814	766	718	670
H	966	927	873	824	775	720	687
1	950	907	861	821	781	733	688
CoV (%)	**0.82**	**0.86**	**0.91**	**0.96**	**0.99**	**1.02**	**1.07**
S_P (kg/m^3)	**2.62**	**2.64**	**2.62**	**2.64**	**2.55**	**2.45**	**2.43**

Table A-13: Float and sink test results for feed coal

Specific gravity fraction	**Wt.%**	**Ash%**	**Ash Product**	**Separating Density (g/cm3)**	**Cumulative Float (Clean coal)**			**Cumulative Sink (Discard)**		
					Wt.%	**Ash Product**	**Ash%**	**Wt.%**	**Ash Product**	**Ash%**
<1.3	1.18	5.54	6.55	1.30	1.18	6.55	5.54	98.82	3933.22	39.80
1.3-1.4	13.99	8.29	115.98	1.40	15.17	122.52	8.08	84.83	3817.24	45.00
1.4-1.5	23.81	13.96	332.36	1.50	38.98	454.89	11.67	61.02	3484.88	57.11
1.5-1.6	10.04	22.05	221.37	1.60	49.02	676.26	13.80	50.98	3263.50	64.01
1.6-1.7	6.90	32.06	221.11	1.70	55.92	897.37	16.05	44.08	3042.39	69.01
1.7-1.8	6.55	38.56	252.68	1.80	62.47	1150.05	18.41	37.53	2789.71	74.33
1.8-1.86	2.45	42.79	104.68	1.83	64.92	1254.72	19.33	35.08	2685.04	76.53
>1.86	35.08	76.53	2685.04	1.86	100.00	3939.76	39.40	0.00	0.00	0.00
Total	**100**	**39.40**	**3939.76**							

Table A-14; Partition for Run 2

Specific gravity fraction	Floats analysis (Wt. %)	Sinks analysis (Wt.%)	Floats % of feed	Sinks % of feed	Reconstituted feed (%)	Nominal S.G	Partition coefficient
<1.30	7.28	0.00	3.91	0.00	3.91		0.00
1.30-1.40	25.99	0.77	13.95	0.36	14.30	1.35	2.49
1.40-1.50	40.71	2.57	21.85	1.19	23.04	1.45	5.18
1.50-1.60	16.08	4.71	8.63	2.18	10.81	1.55	20.18
1.60-1.70	7.27	8.42	3.90	3.90	7.81	1.65	50.00
1.70-1.80	2.16	8.85	1.16	4.10	5.26	1.75	77.97
1.80-1.86	0.53	3.44	0.28	1.60	1.88	1.83	84.95
>1.86	0.00	71.23	0.00	33.00	33.00		100.00
Total	**100**	**100**	**52.67**	**47.33**	**100**		

Table A-15: Partition data for Run 3

Specific gravity fraction	Floats analysis (wt.%)	Sinks analysis (wt.%)	Floats % of feed	Sinks % of feed	Reconstituted feed (%)	Nominal S.G	Partition coefficient
<1.30	7.37	0.00	3.92	0.00	3.92		0.00
1.30-1.40	26.21	1.10	13.95	0.51	14.46	1.35	3.55
1.40-1.50	41.06	3.11	21.85	1.46	23.31	1.45	6.25
1.50-1.60	16.22	4.44	8.63	2.08	10.71	1.55	19.41
1.60-1.70	6.41	9.30	3.41	4.35	7.76	1.65	56.07
1.70-1.80	2.17	8.76	1.16	4.10	5.25	1.75	77.98
1.80-1.86	0.55	3.52	0.29	1.65	1.94	1.83	84.84
>1.86	0.00	69.77	0.00	32.64	32.64		100.00
Total	**100**	**100**	**52.21**	**47.79**	**100**		

Table A-16; Partition data for Run 4

Specific gravity fraction	Floats analysis (wt. %)	Sinks analysis (wt. %)	Floats % of feed	Sinks % of feed	Reconstituted feed (%)	Nominal S.G	Partition coefficient
<1.30	7.26	0.00	3.86	0.00	3.86		0.00
1.30-1.40	26.55	1.09	14.11	0.51	14.62	1.35	3.49
1.40-1.50	41.34	3.12	21.97	1.46	23.44	1.45	6.24
1.50-1.60	15.88	4.37	8.44	2.05	10.49	1.55	19.53
1.60-1.70	6.14	9.35	3.26	4.38	7.64	1.65	57.29
1.70-1.80	2.27	8.72	1.21	4.09	5.29	1.75	77.19
1.80-1.86	0.55	3.42	0.29	1.60	1.89	1.83	84.44
>1.86	0.00	69.93	0.00	32.76	32.76		100.00
Total	**100**	**100**	**52.15**	**47.85**	**100**		

Table A-17: Partition data for Run 5

Specific gravity fraction	Floats analysis (wt. %)	Sinks analysis (wt. %)	Floats % of feed	Sinks % of feed	Reconstituted feed (%)	Nominal S.G	Partition coefficient
<1.30	6.19	0.00	3.29	0.00	3.29		0.00
1.30-1.40	25.86	0.75	13.76	0.35	14.11	1.35	2.48
1.40-1.50	41.33	2.50	21.99	1.17	23.16	1.45	5.05
1.50-1.60	16.97	3.37	9.03	1.58	10.61	1.55	14.87
1.60-1.70	6.47	9.40	3.44	4.40	7.84	1.65	56.12
1.70-1.80	2.66	9.82	1.41	4.59	6.01	1.75	76.48
1.80-1.86	0.53	3.04	0.28	1.42	1.71	1.83	83.40
>1.86	0.00	71.12	0.00	33.28	33.28		100.00
Total	**100**	**100**	**52.20**	**47.80**	**100**		

APPENDIX B: CALIBRATIONS, REPEATABILITY, FLUDIZATION CHARACTERIZATION AND BENEFICIATION RESULTS

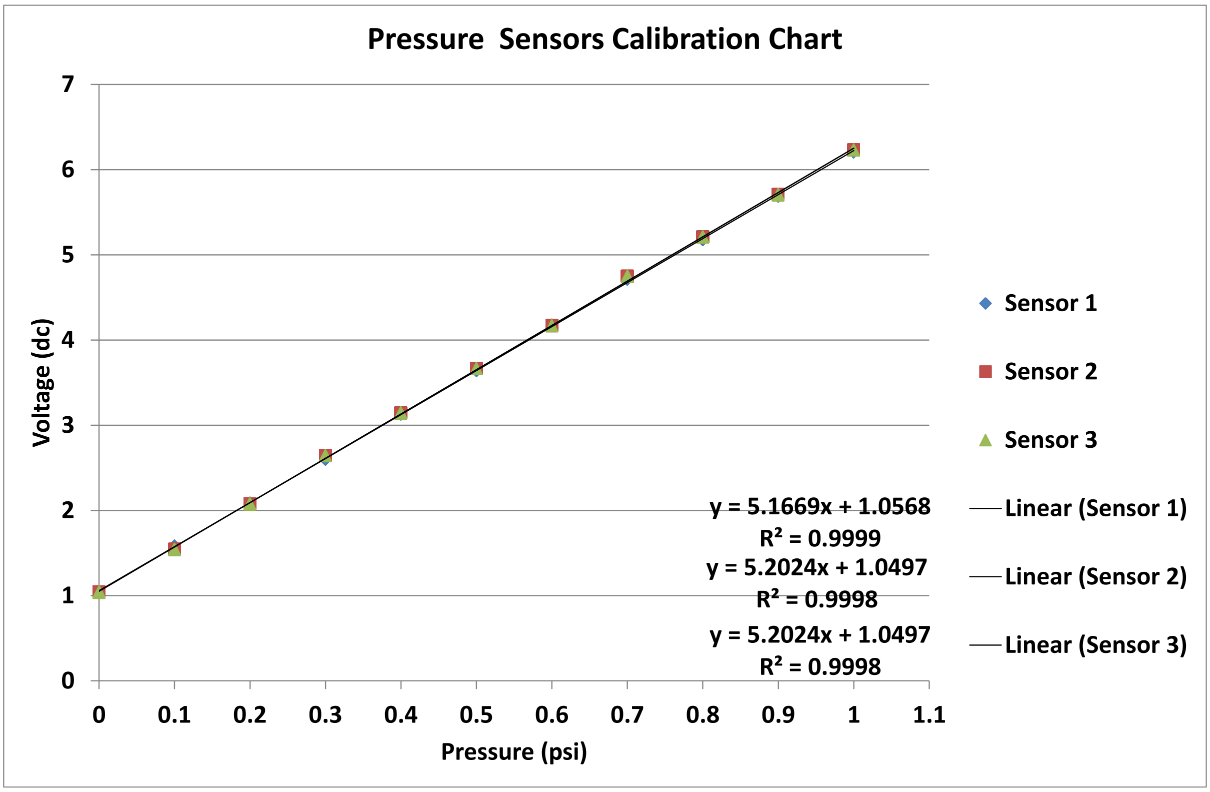

Figure B-1: Pressure sensors calibration chart

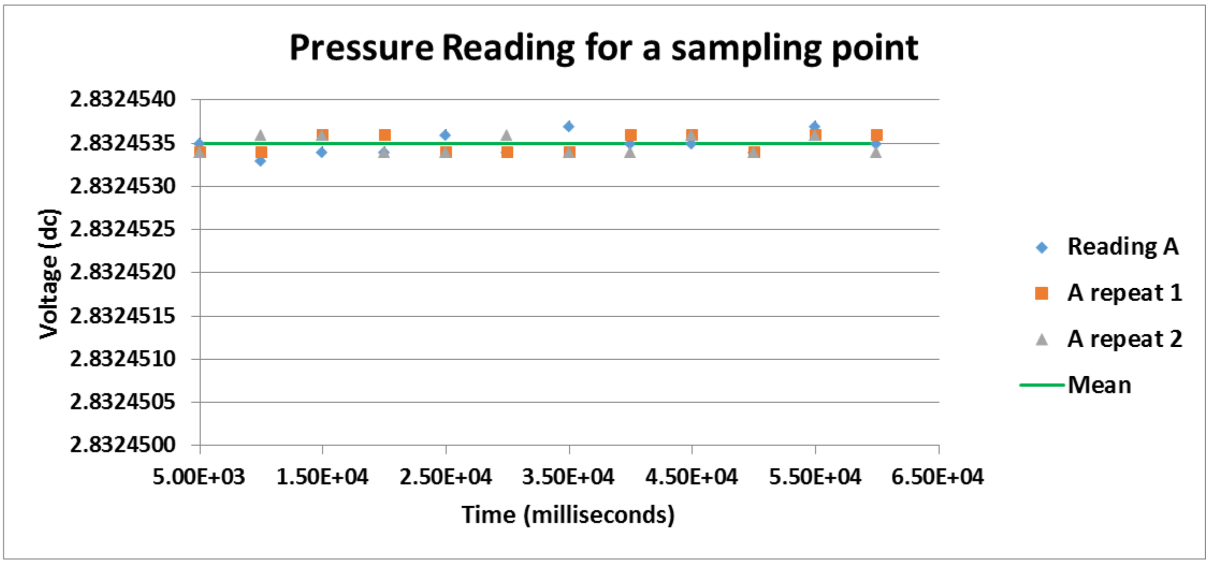

Figure B-0-2: Illustration of repeatability of pressure drop measurements

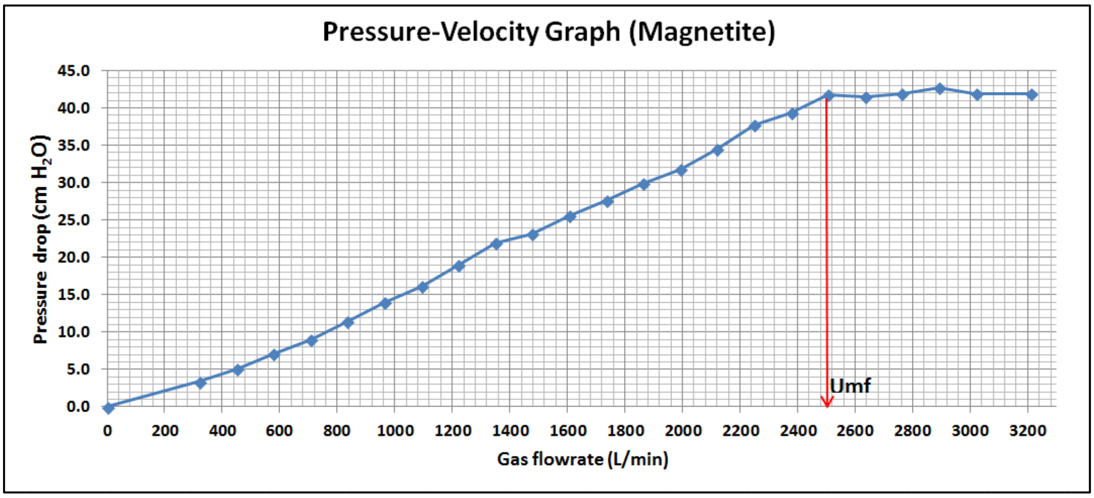

Figure B-3: Magnetite minimum fluidization velocity graph

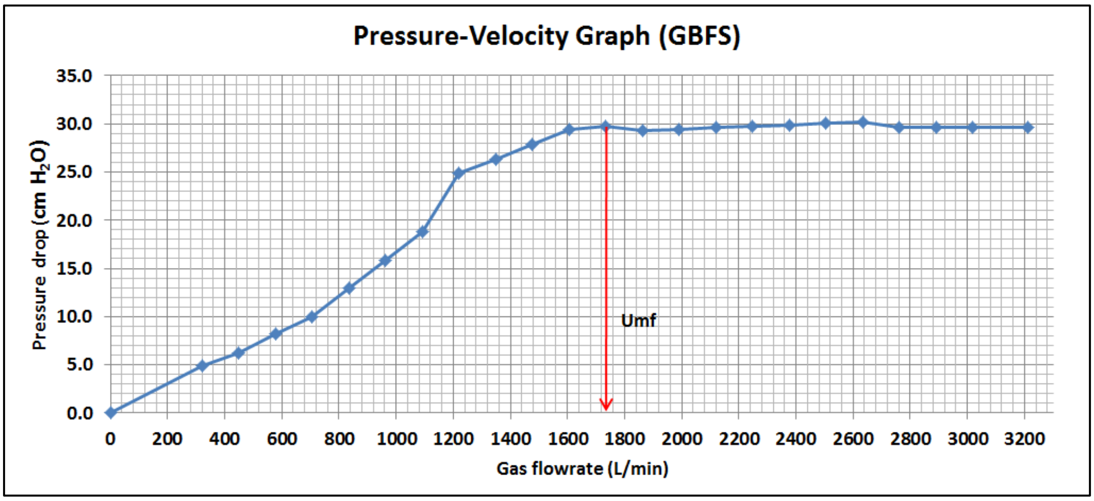

Figure B-4: Granulated blast furnace slag minimum fluidization velocity graph

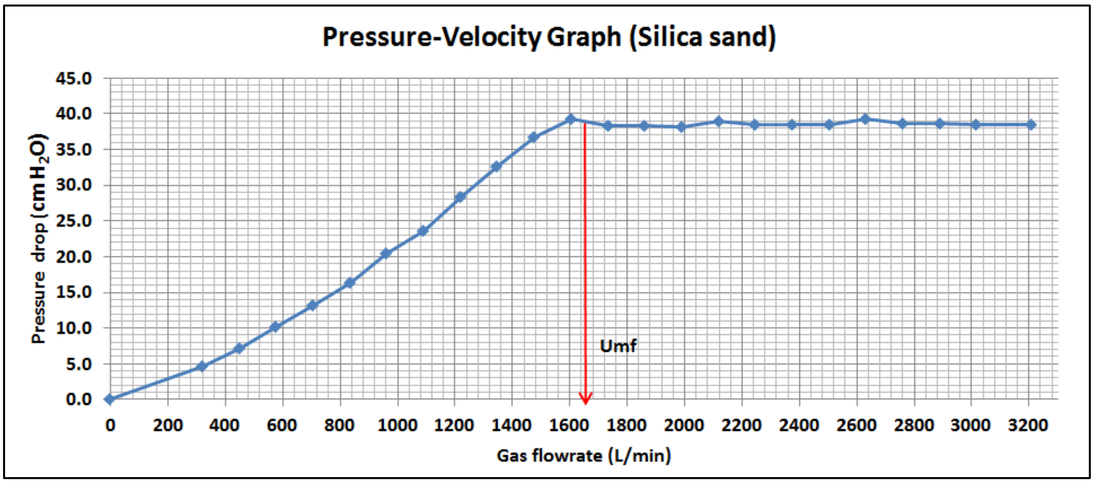

Figure B-5: Silica sand minimum fluidization velocity graph

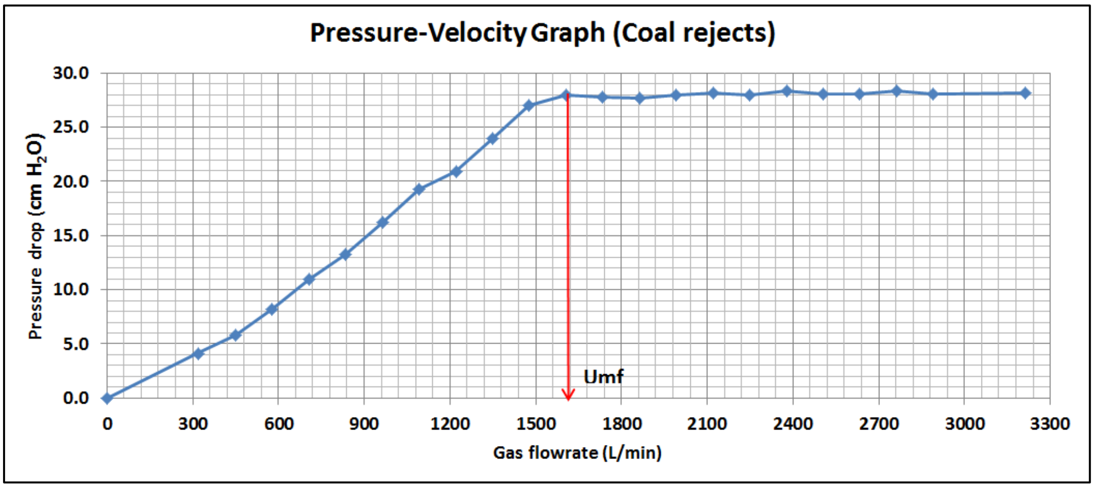

Figure B-6: Coal rejects minimum fluidization velocity graph

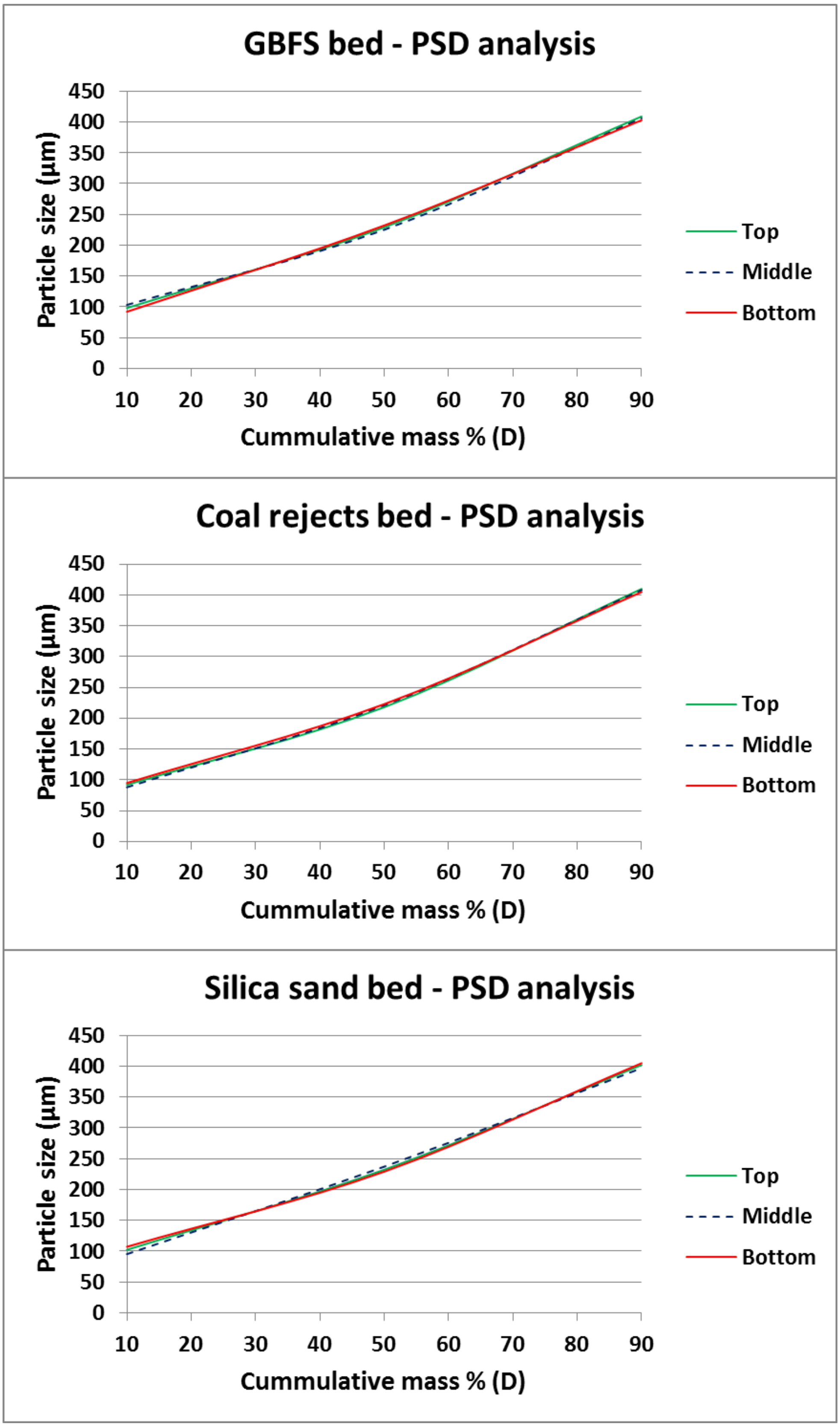

Figure B-7: PSD analysis illustrating segregation evaluation of the materials

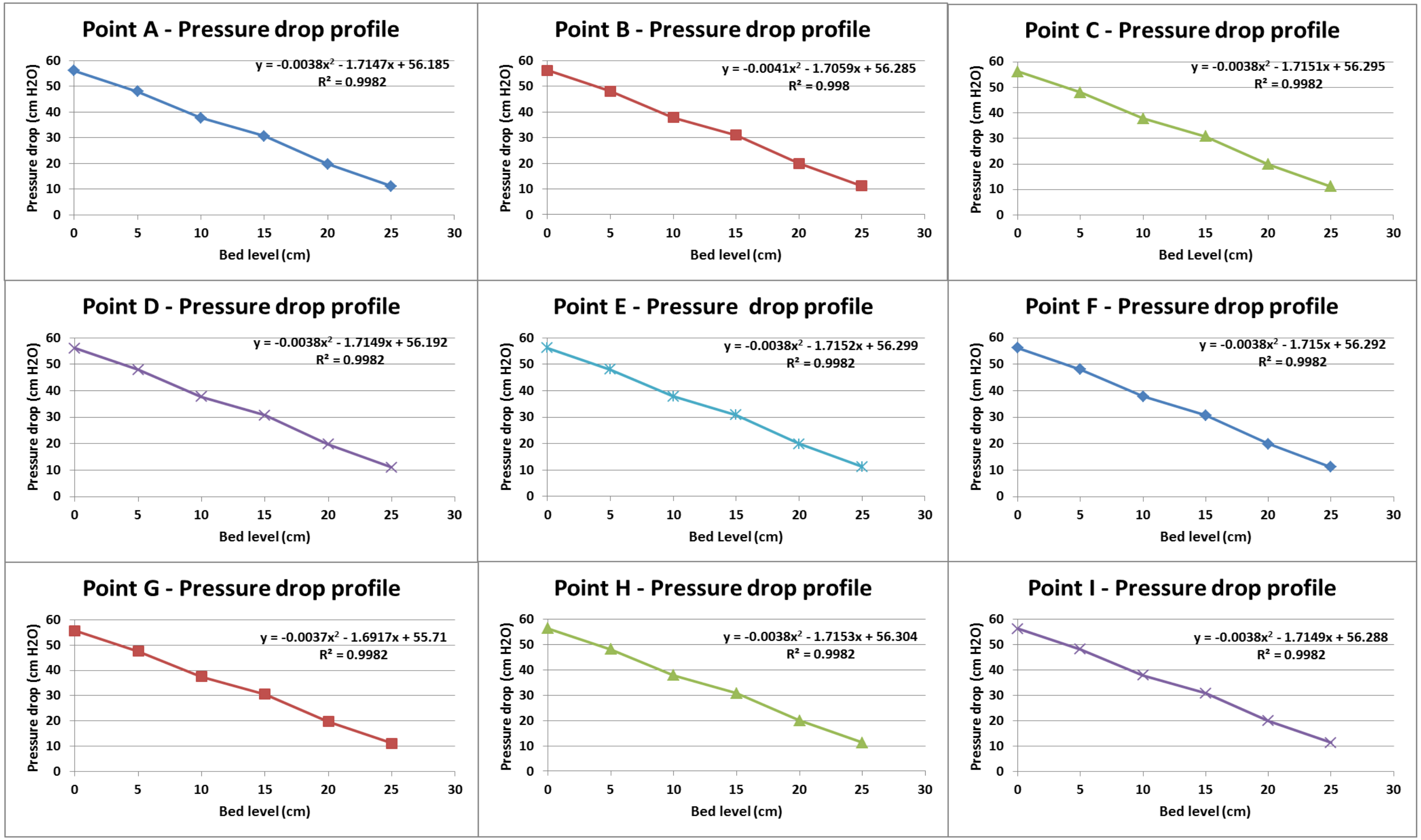

Figure B-8: Pressure drop profiles for magnetite 25cm static bed height

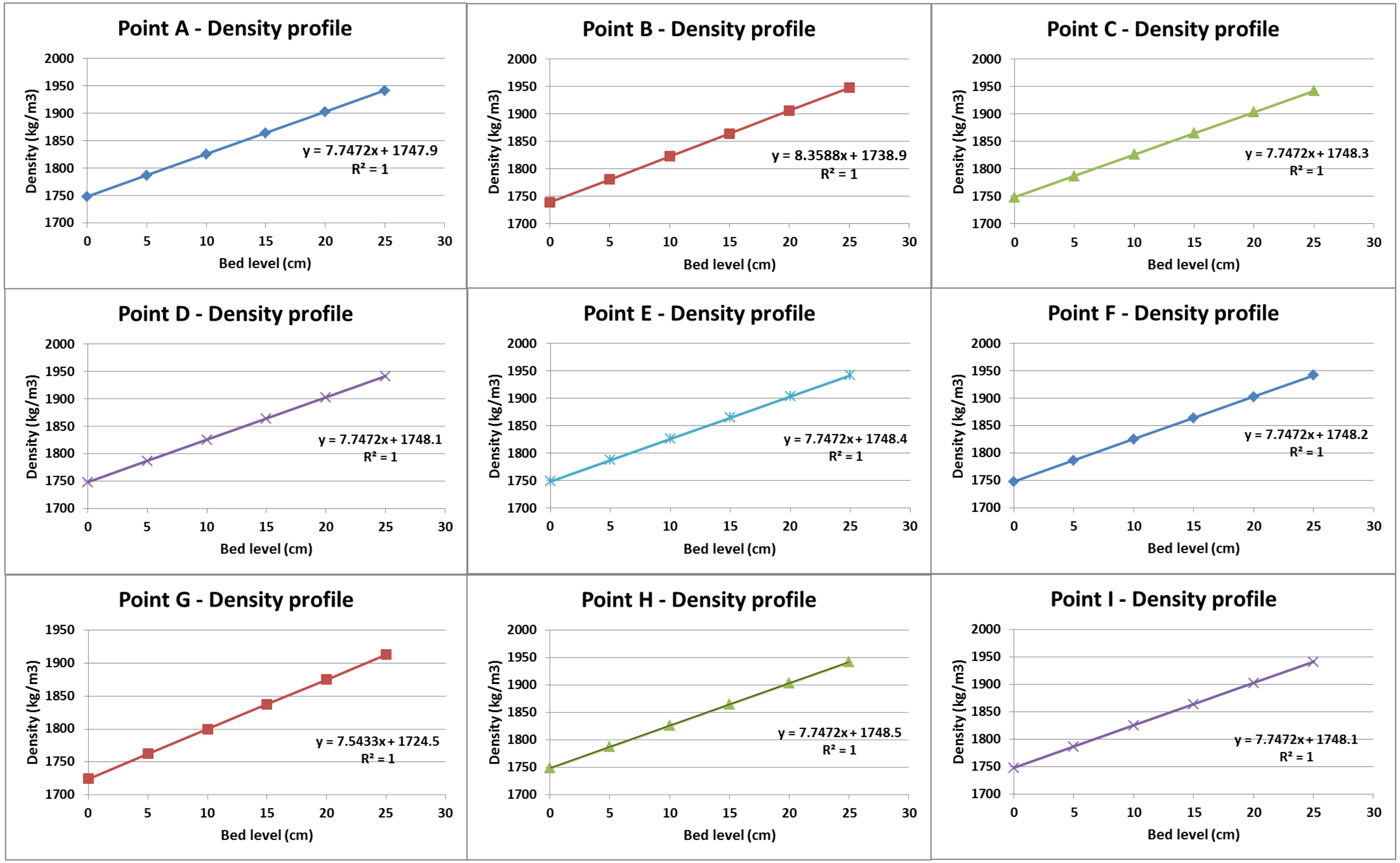

Figure B-9: Density profiles for magnetite 25cm static bed height

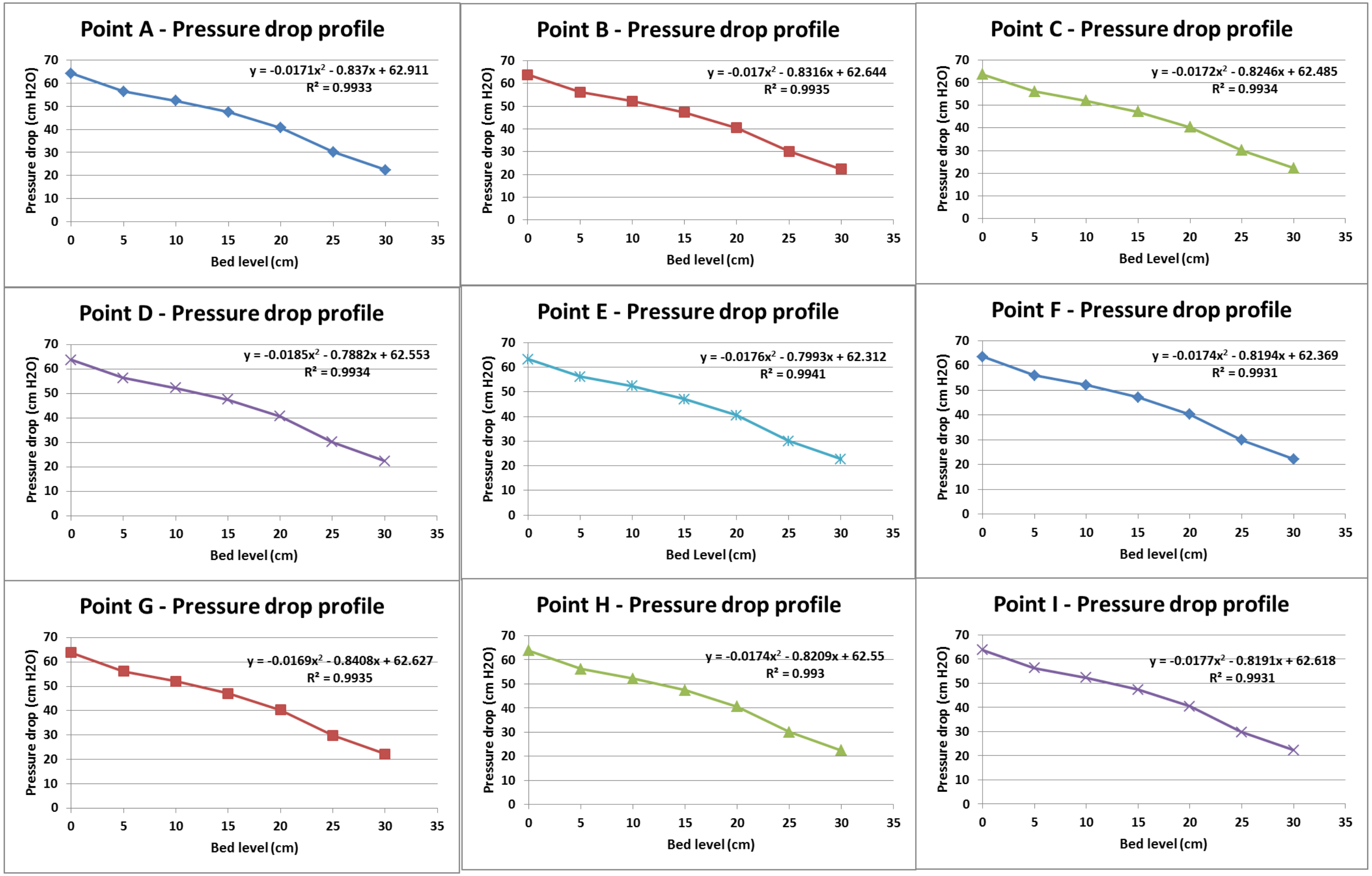

Figure B-10: Pressure drop profiles for magnetite 30 cm static bed height

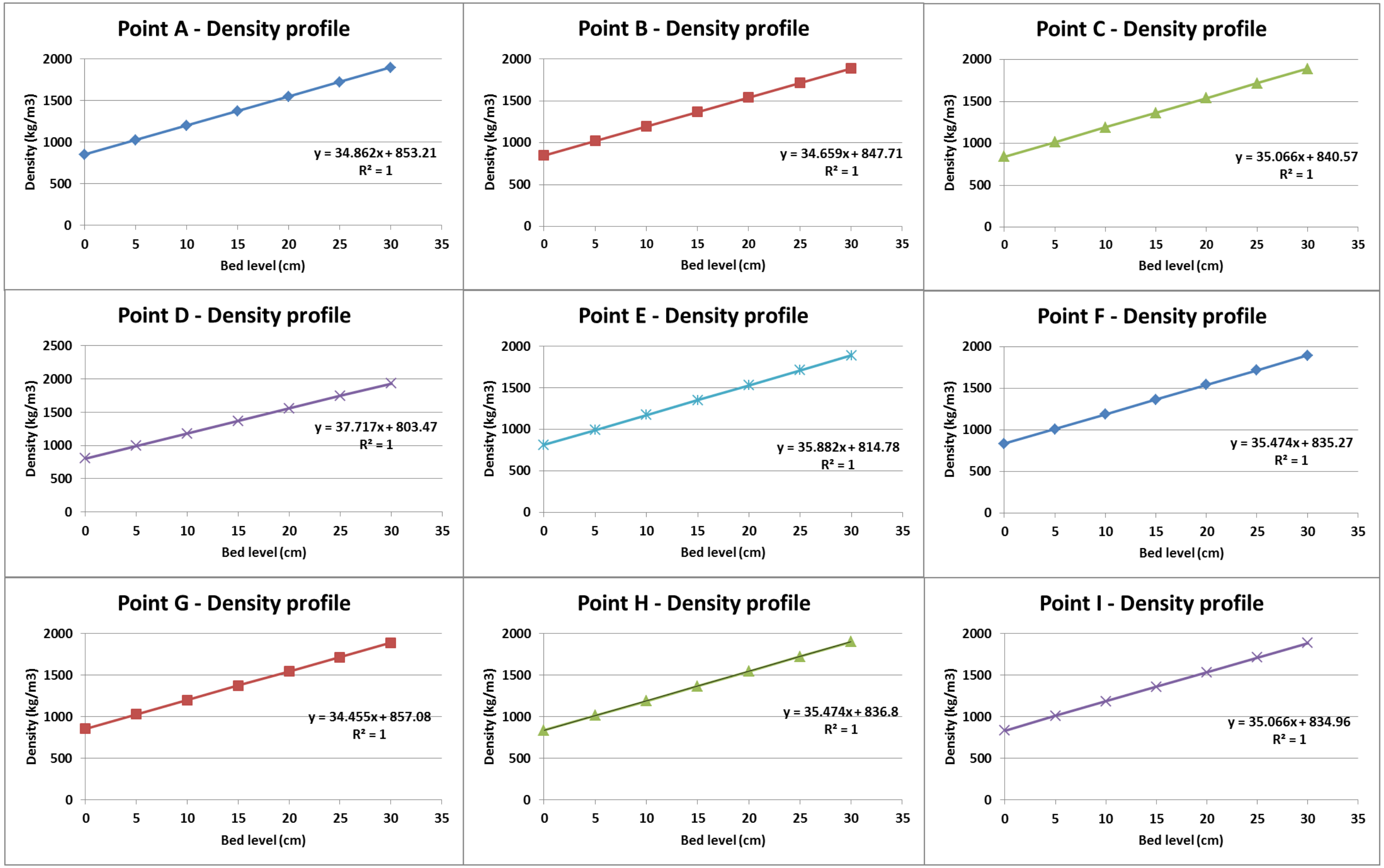

Figure B-11: Density profiles for magnetite 30 cm static bed height

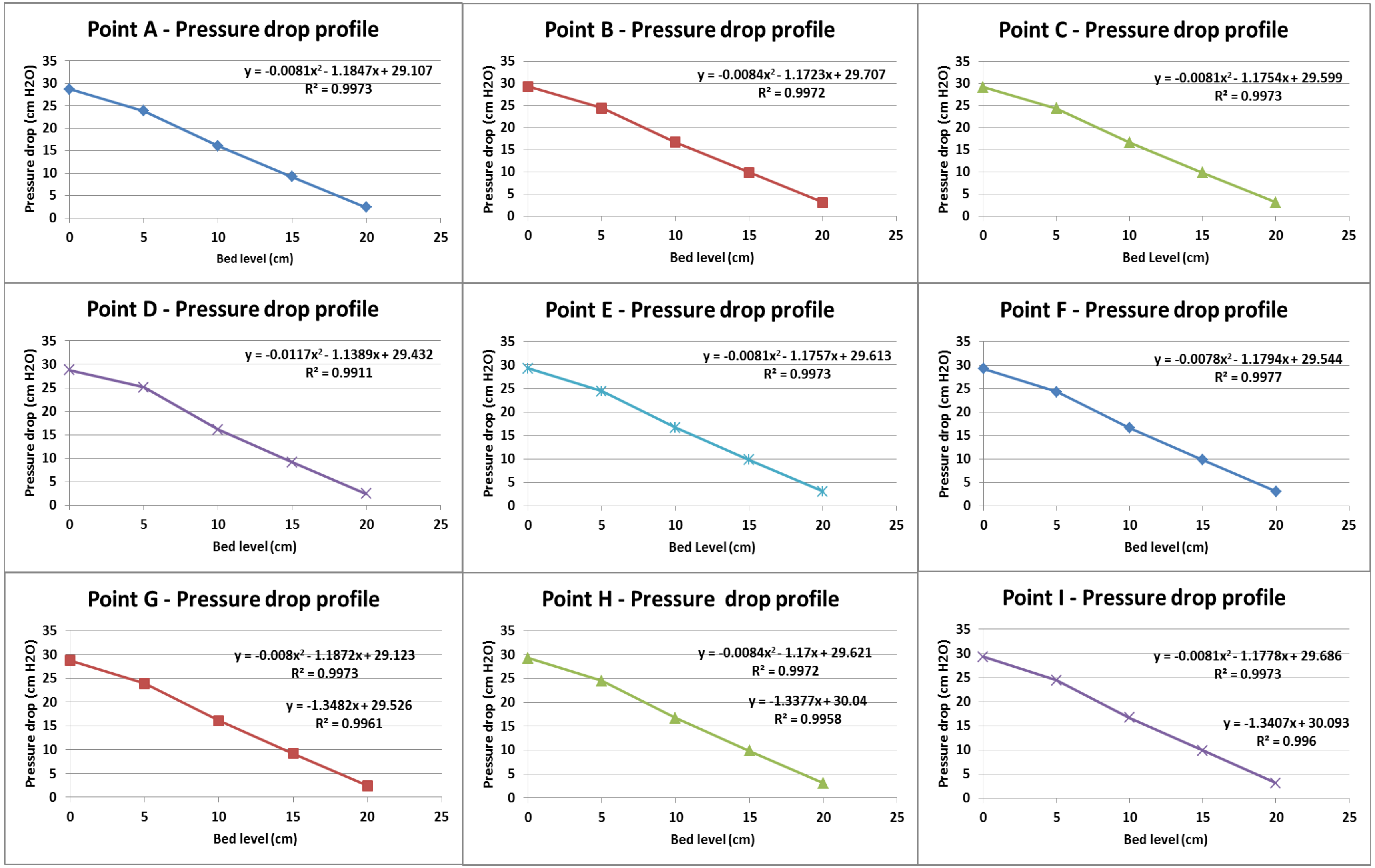

Figure B-12: Pressure drop profiles for pyrrhotite 20 cm static bed height

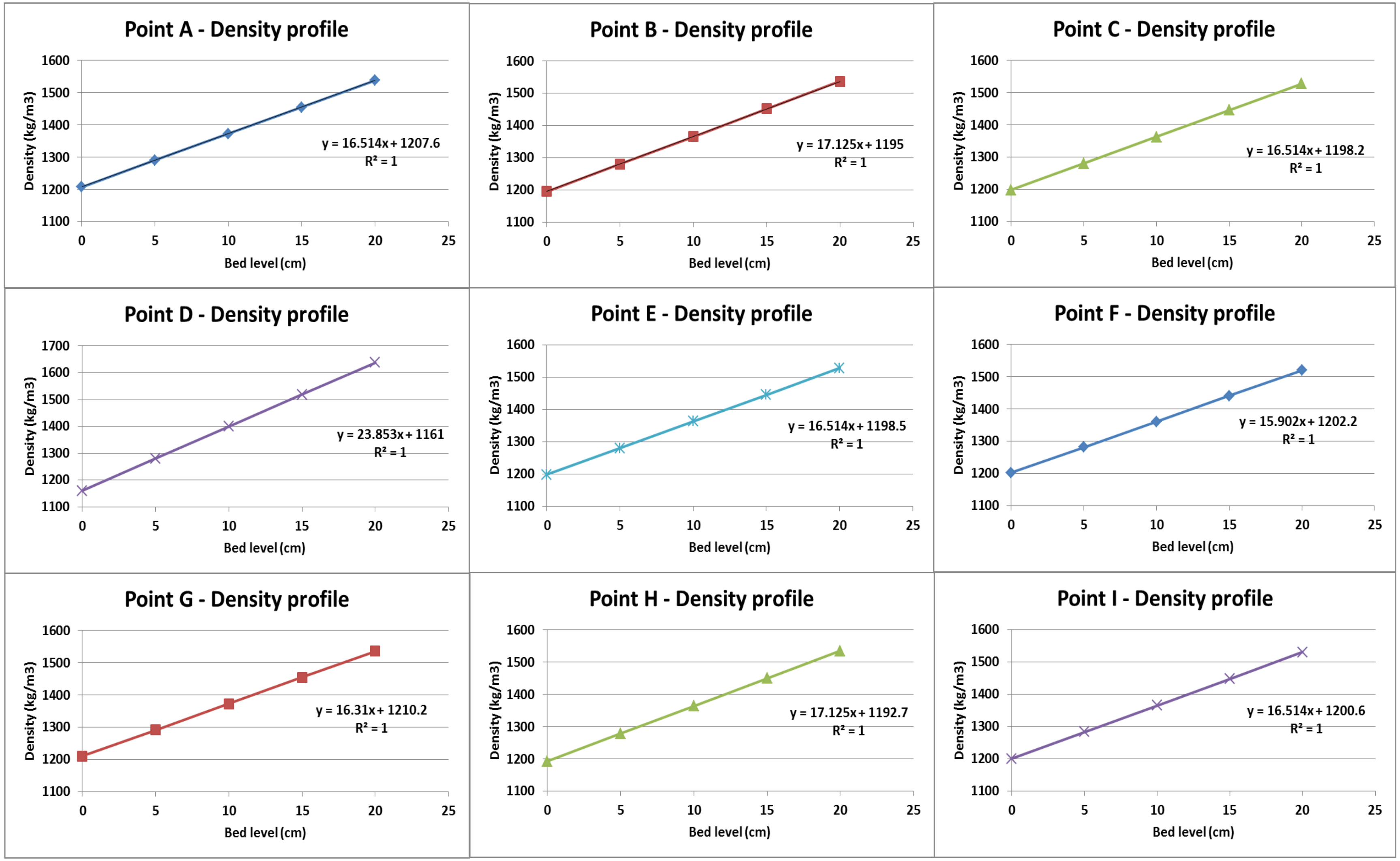

Figure B-13: Density profiles for pyrrhotite 20 cm static bed height

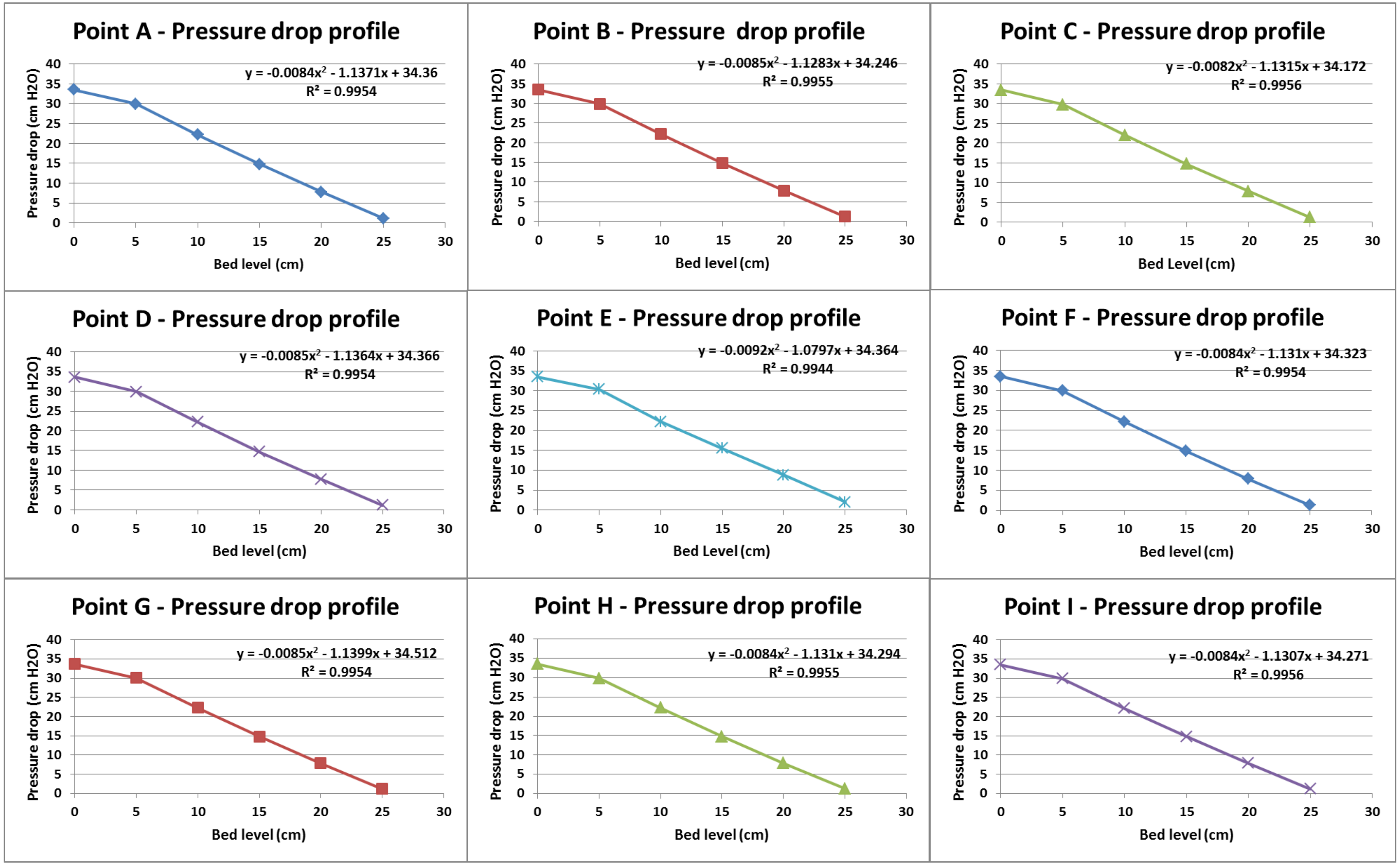

Figure B-14: Pressure drop profile for pyrrhotite 25 cm bed height

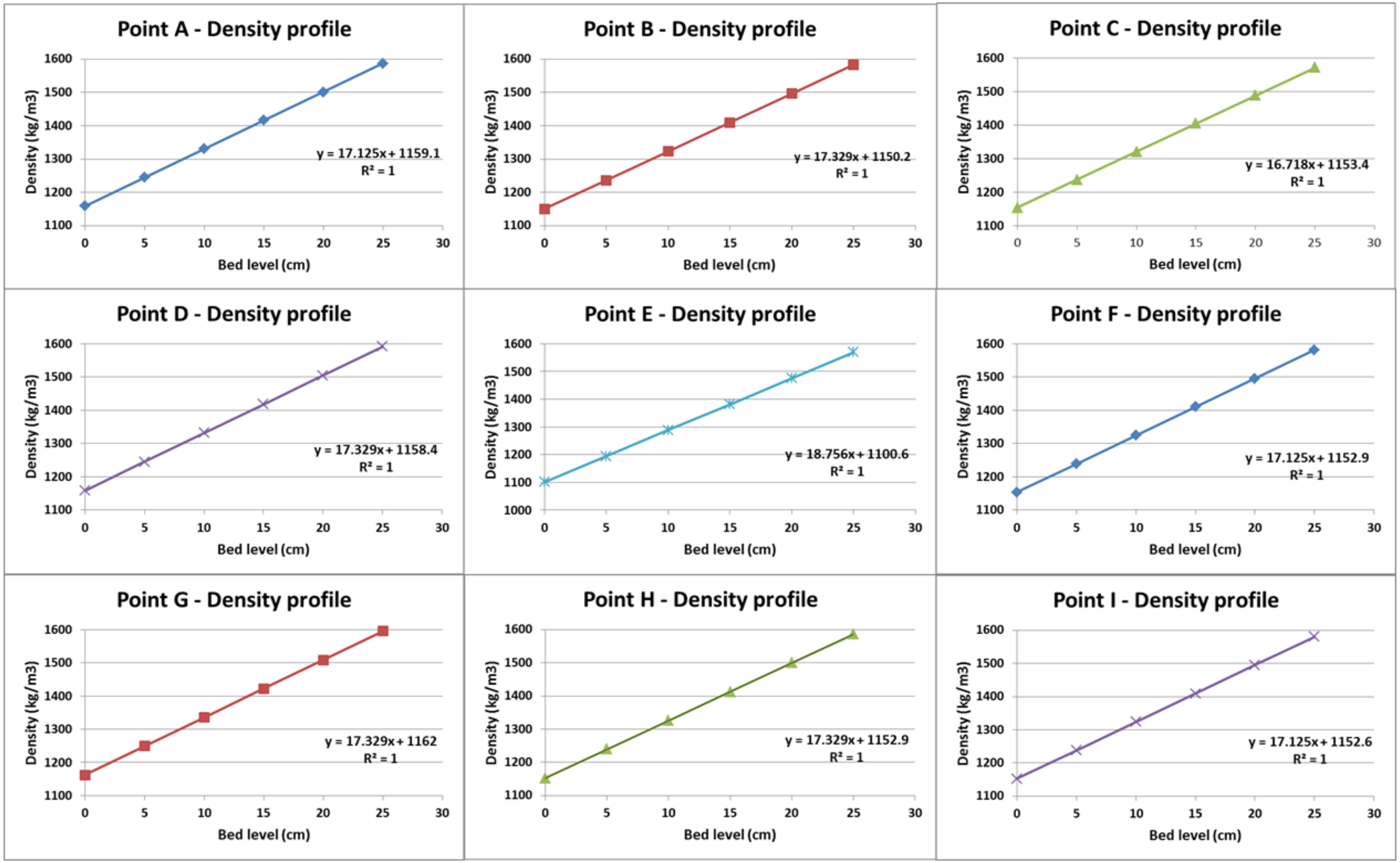

Figure B-15: Density profile for pyrrhotite 25 cm bed height

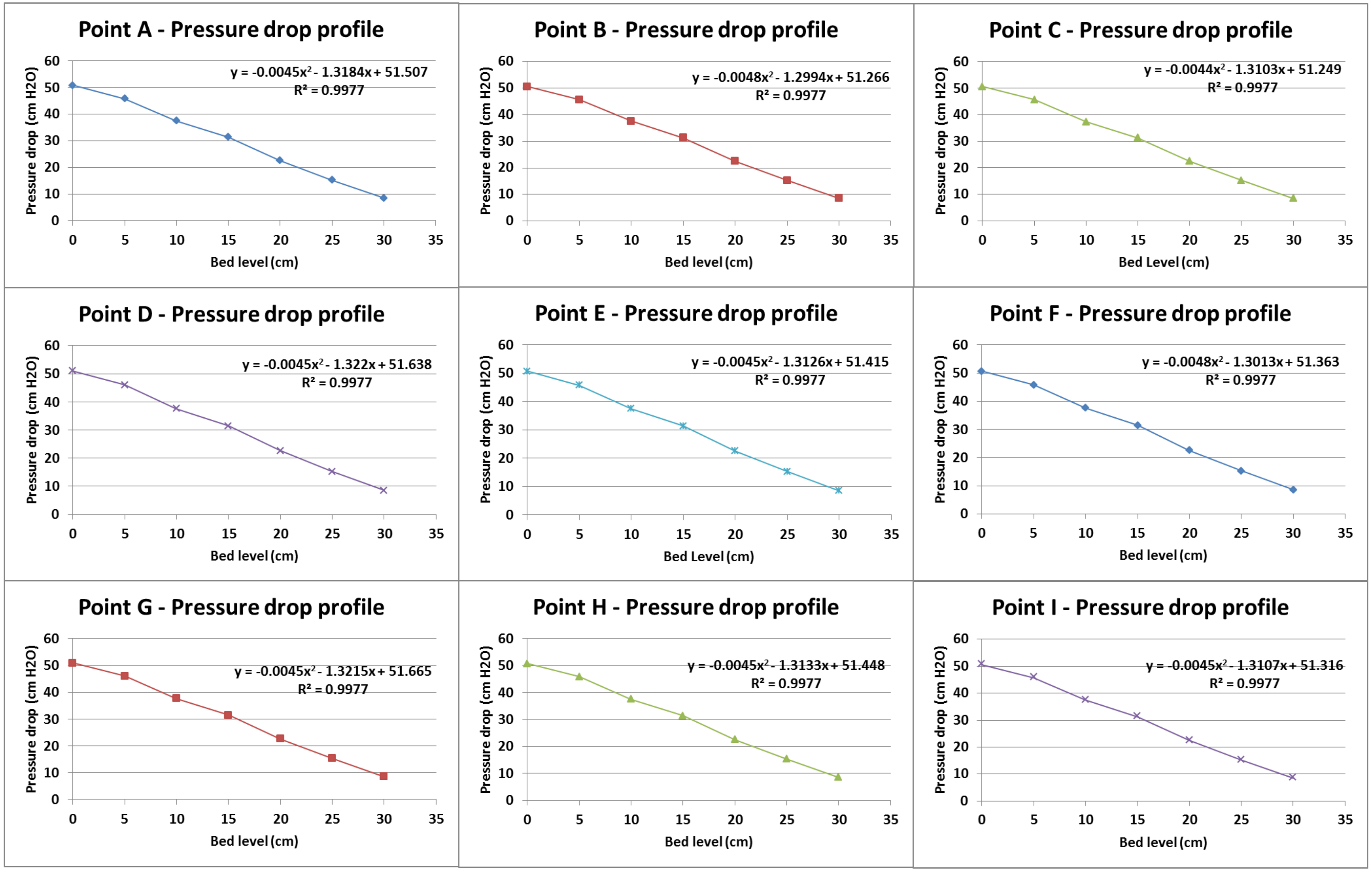

Figure B-16: Pressure drop profiles for pyrrhotite 30 cm static bed height

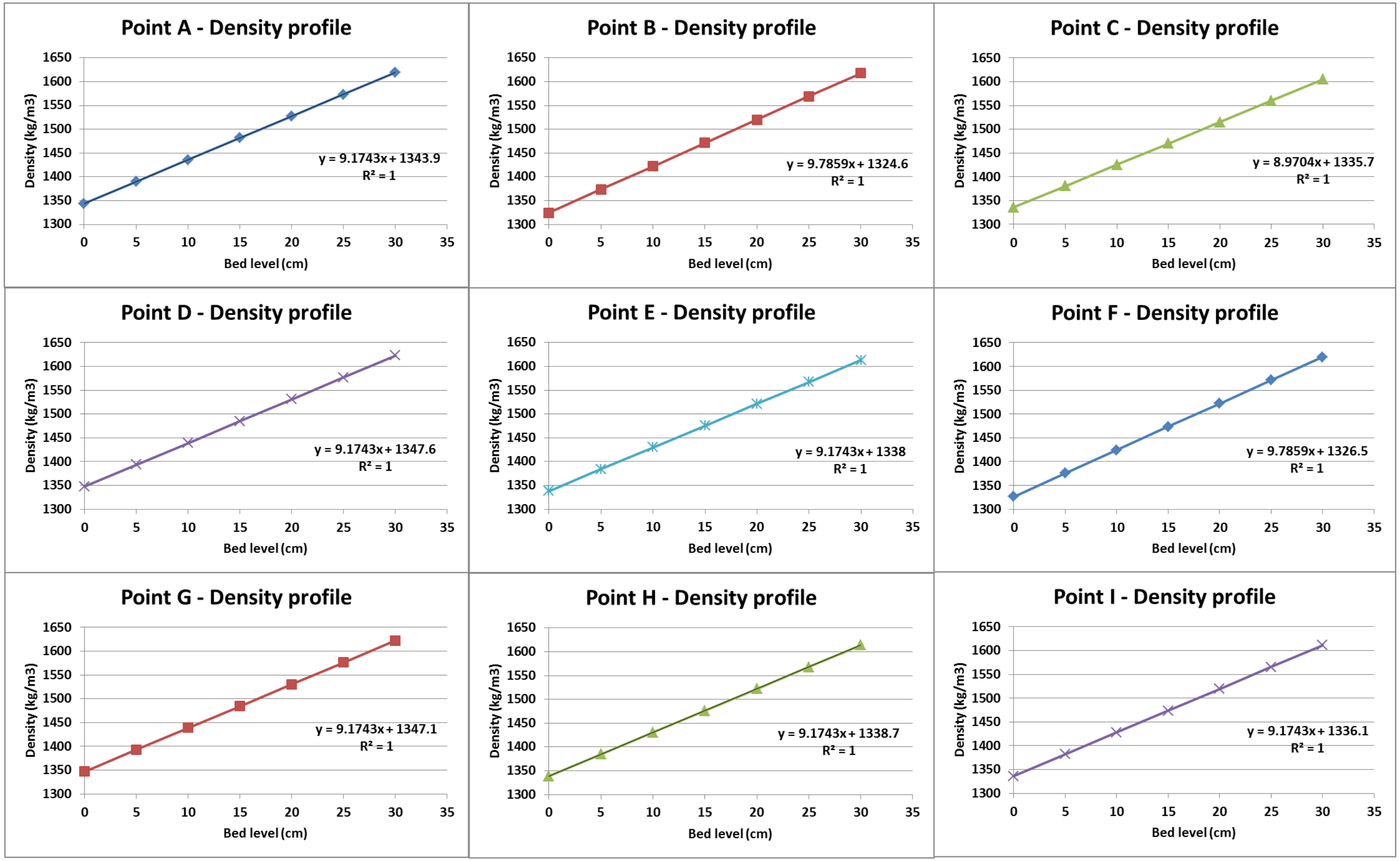

Figure B-17: Density profiles for pyrrhotite 30 cm static bed height

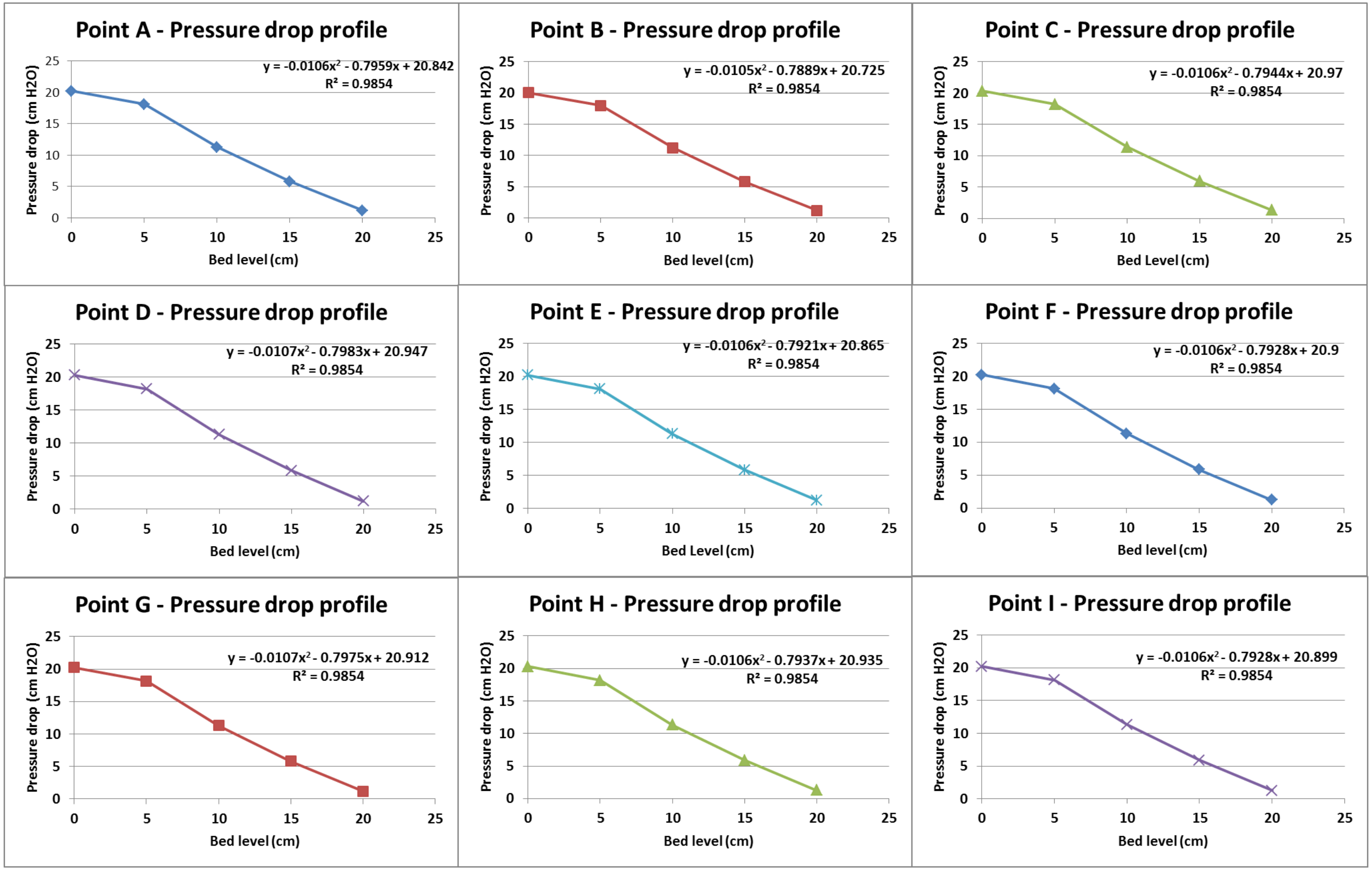

Figure B-18: Pressure drop profiles for GBFS 20 cm static bed height

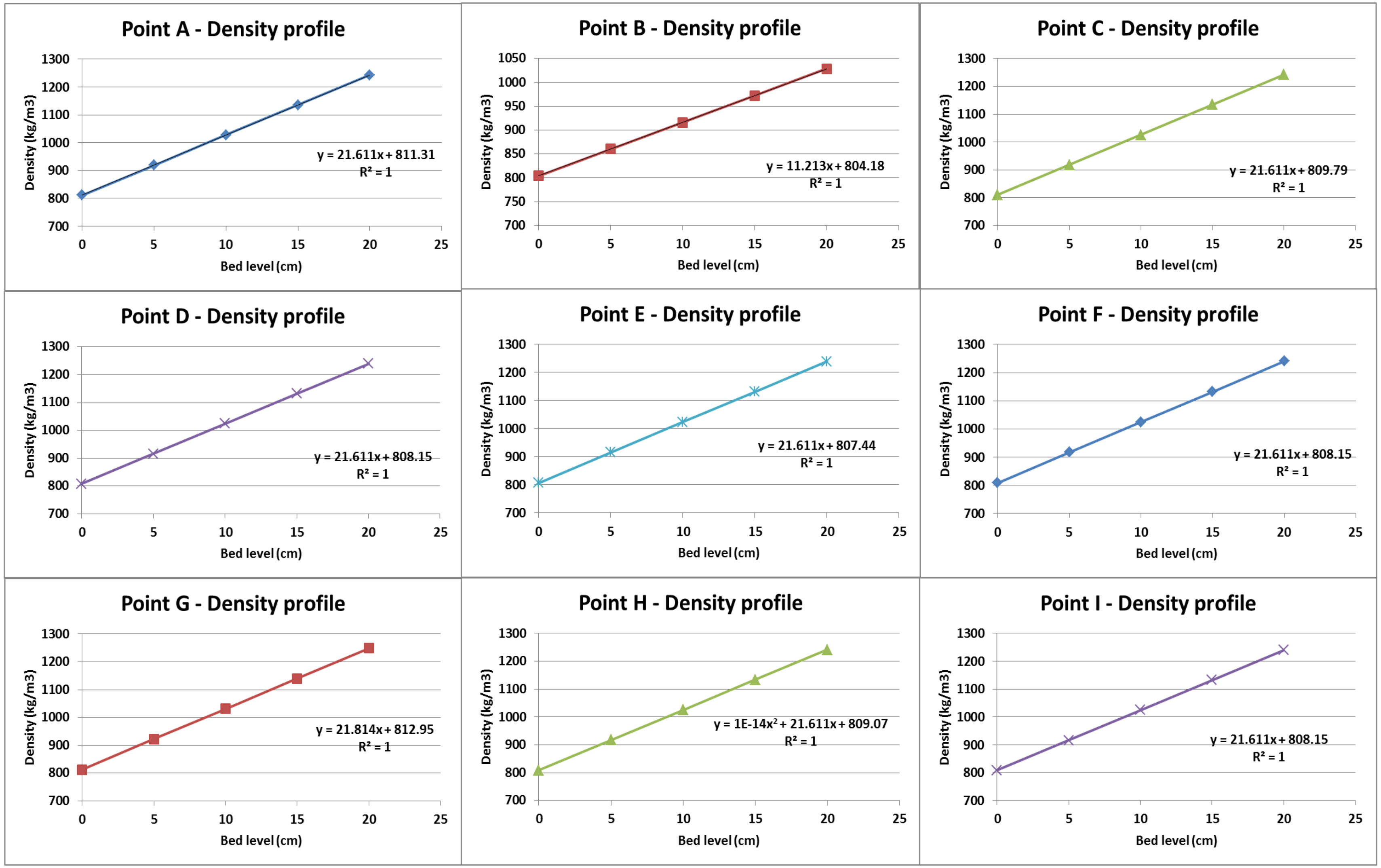

Figure B-19: Density profiles for GBFS 20 cm static bed height

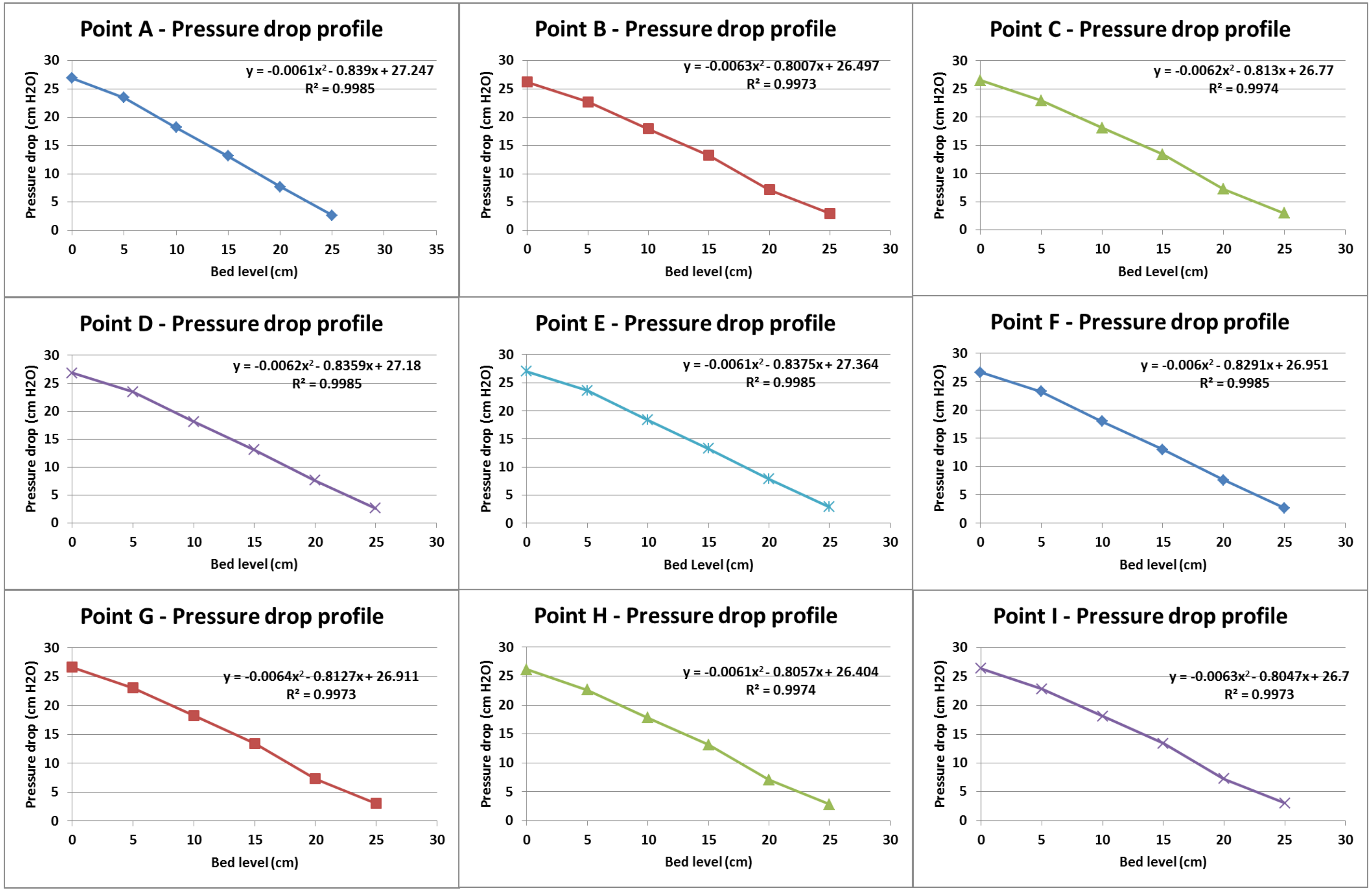

Figure B-20: Pressure drop profiles for GBFS 25 cm static bed height

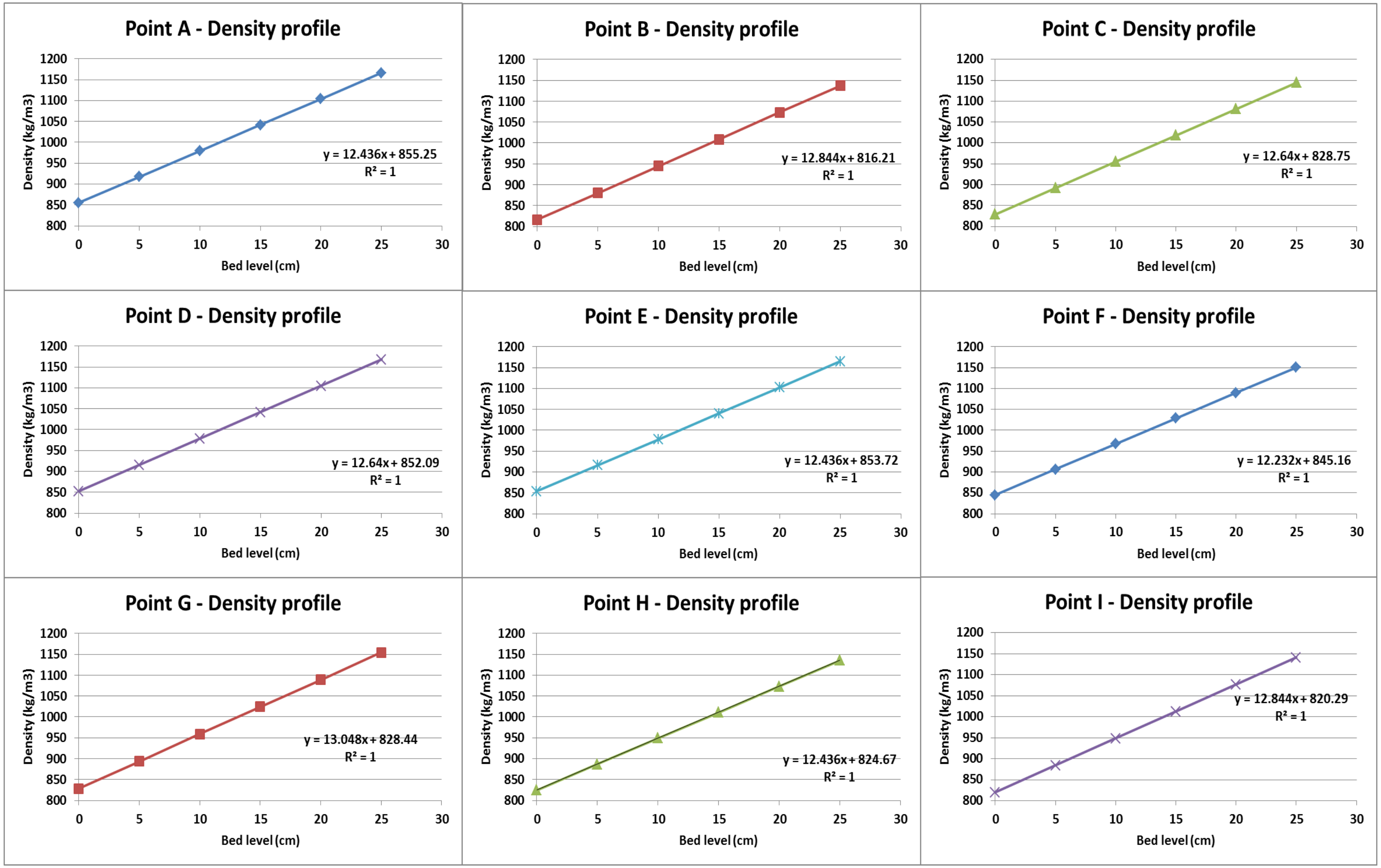

Figure B-21: Density profiles for GBFS 25 cm static bed height

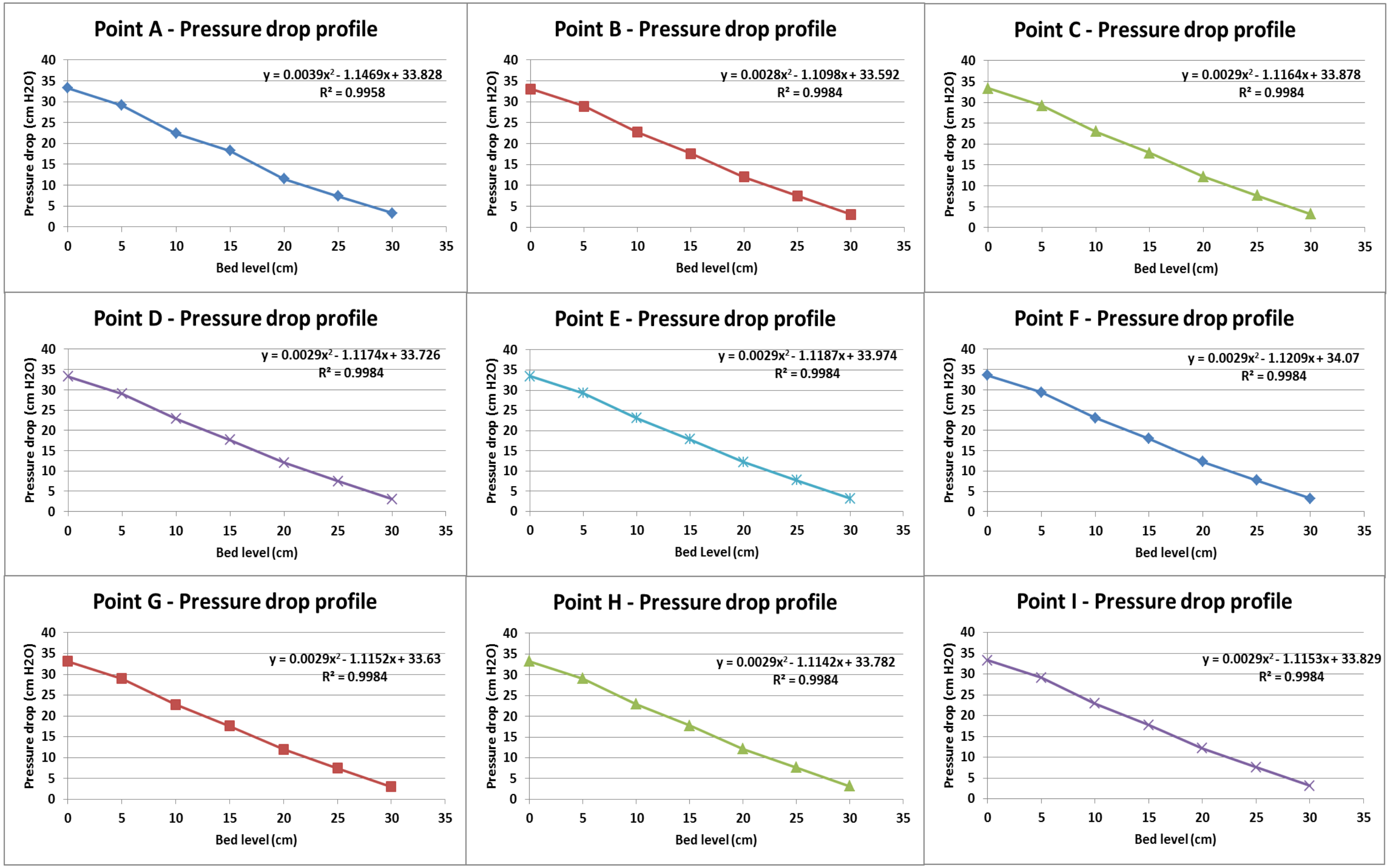

Figure B-22: Pressure drop profile for GBFS 30 cm bed height

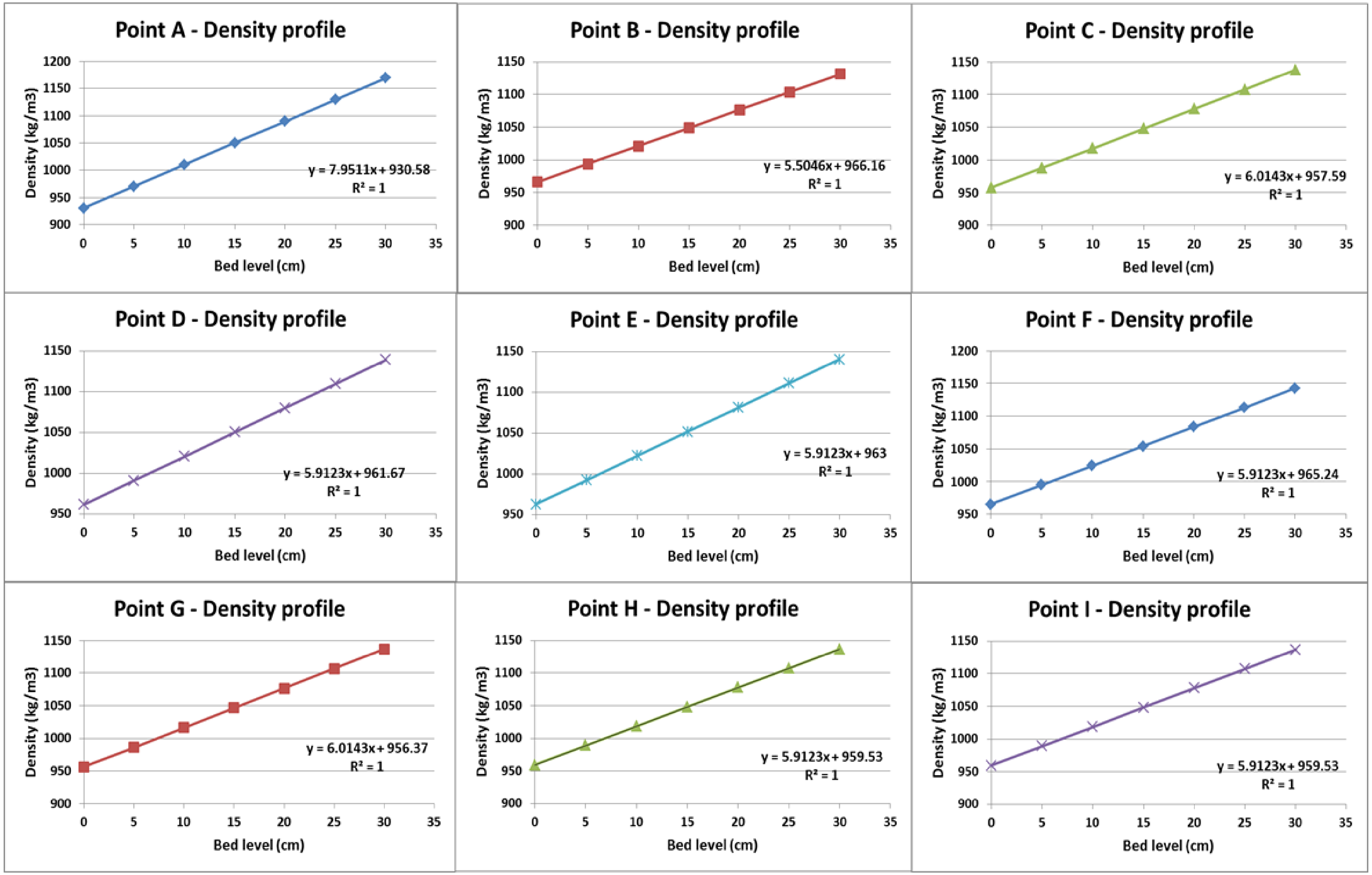

Figure B-23: Density profile for GBFS 30 cm bed height

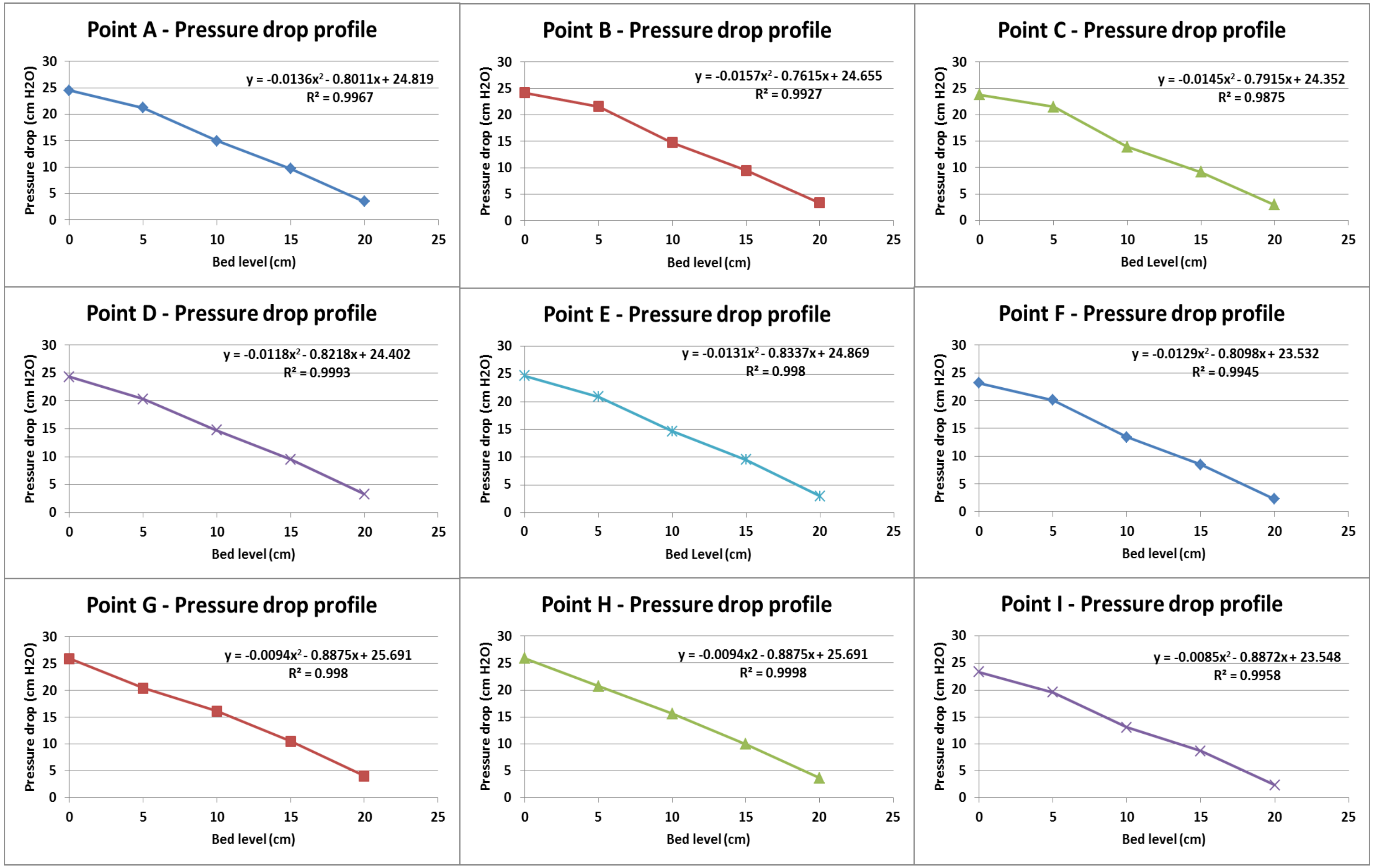

Figure B-24: Pressure drop profiles for silica sand 20 cm static bed height

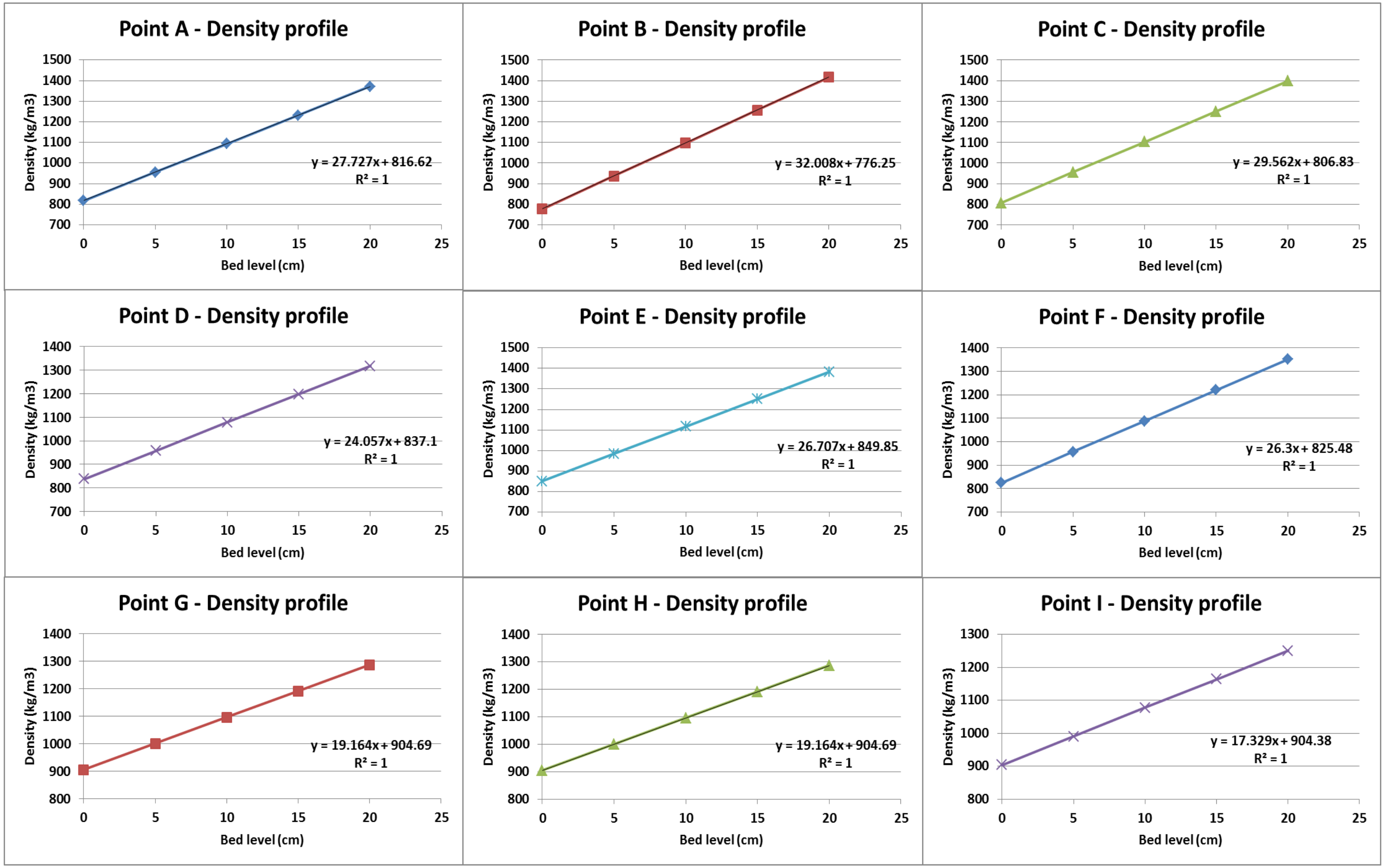

Figure B-25: Density profiles for silica sand 20 cm static bed height

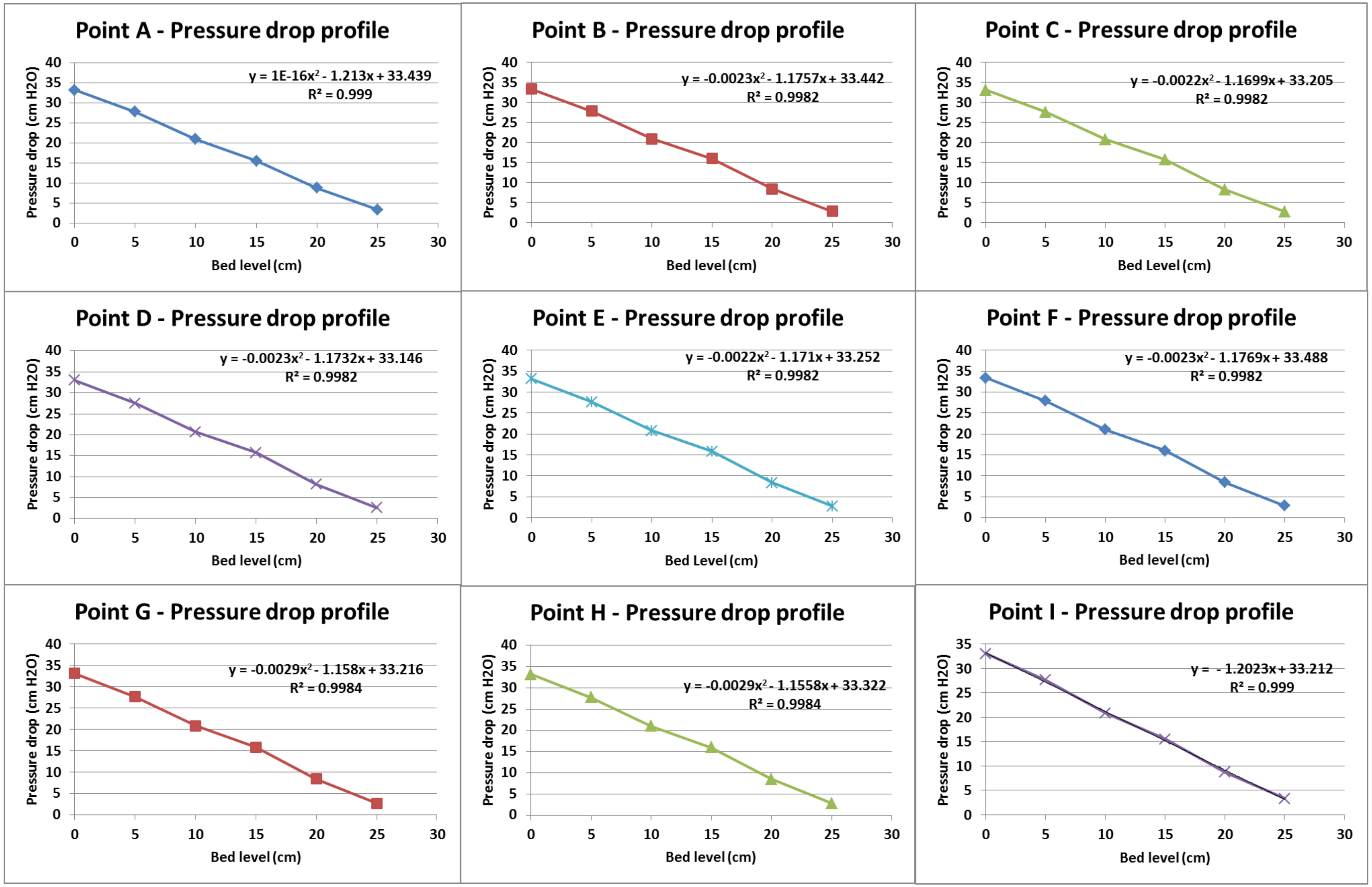

Figure B-26: Pressure drop profiles for silica sand 25 cm static bed height

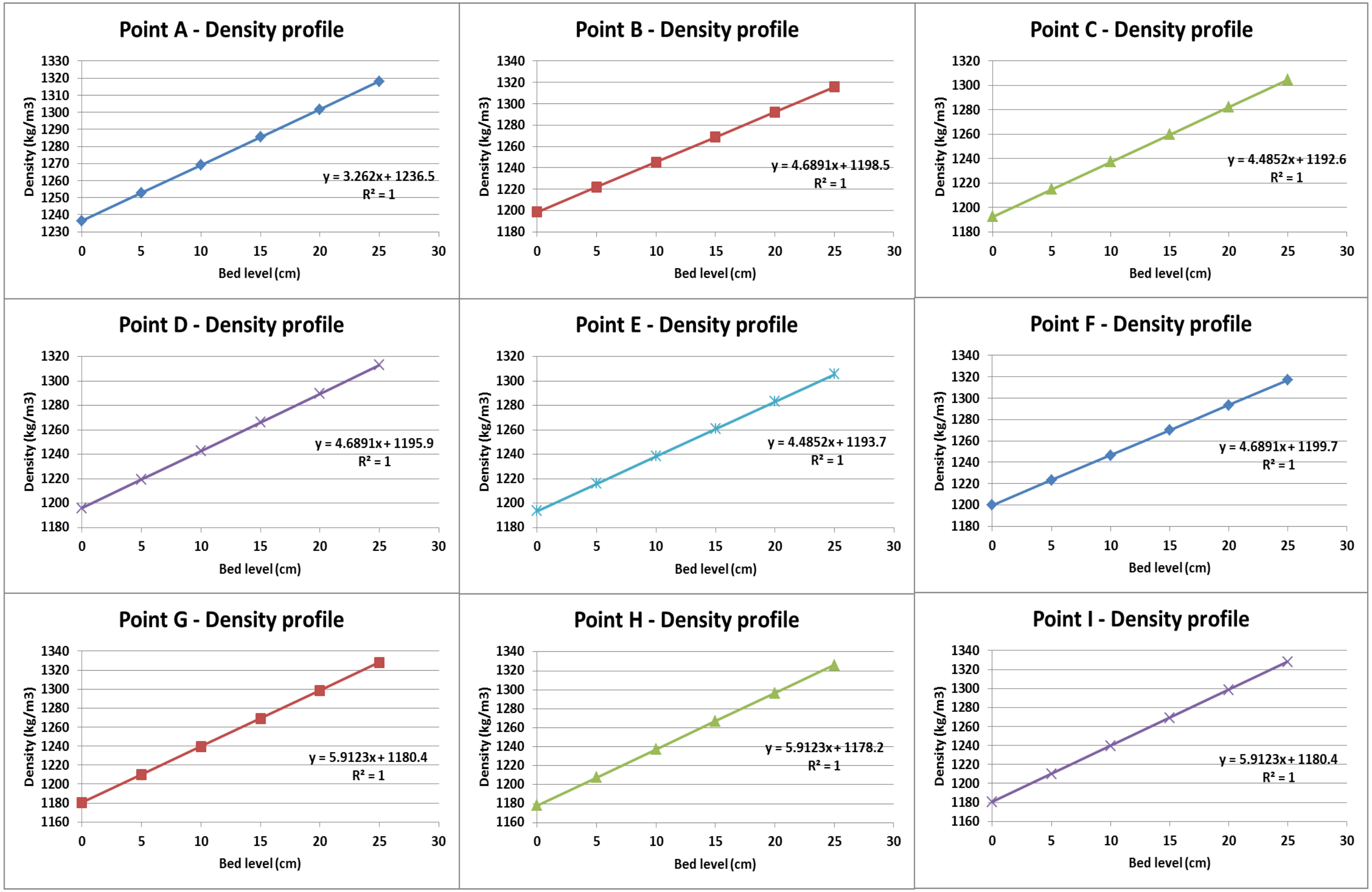

Figure B-27: Density profiles for silica sand 25 cm static bed heightFigure

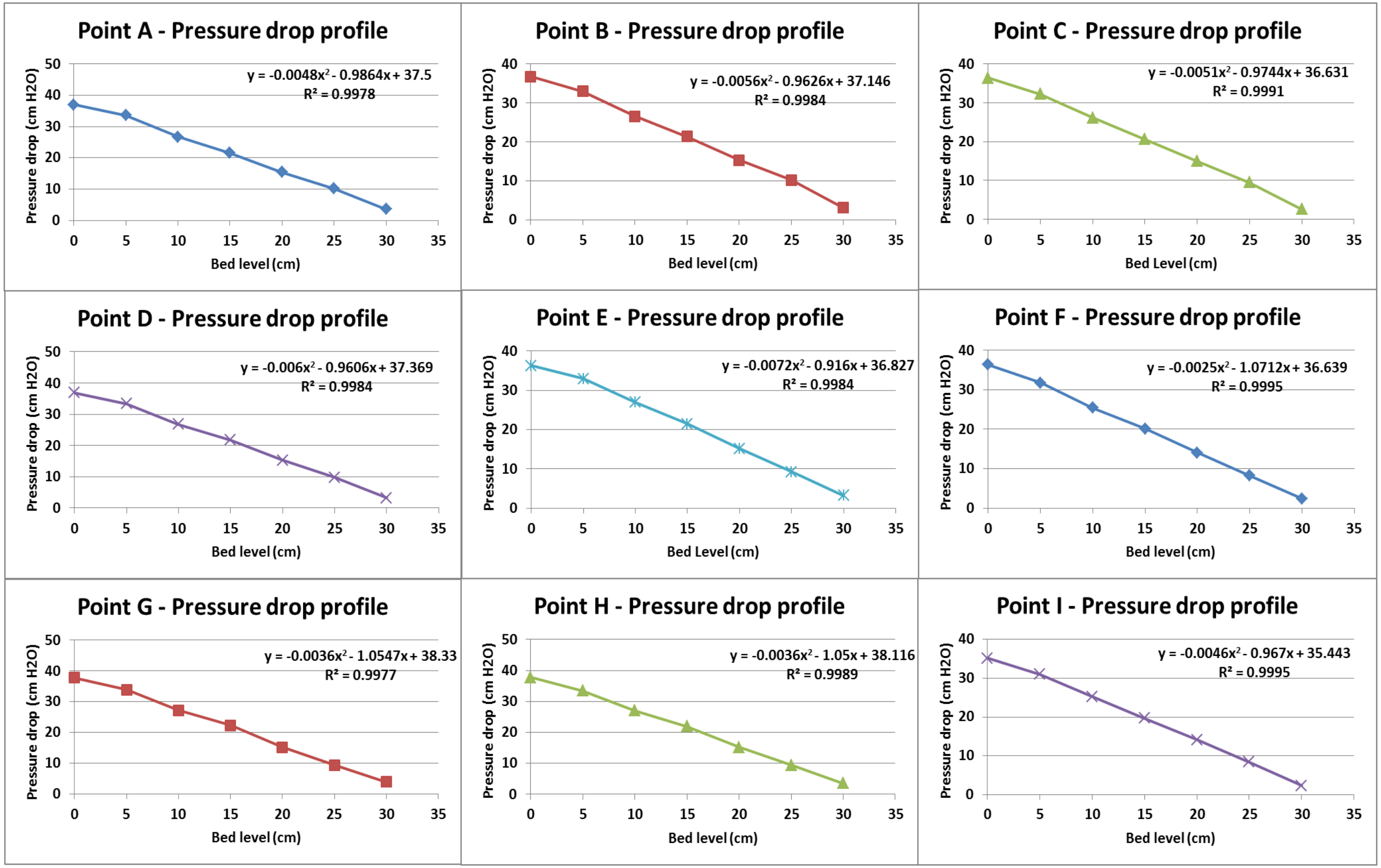

Figure B-28: Pressure drop profiles for silica sand 30 cm static bed height

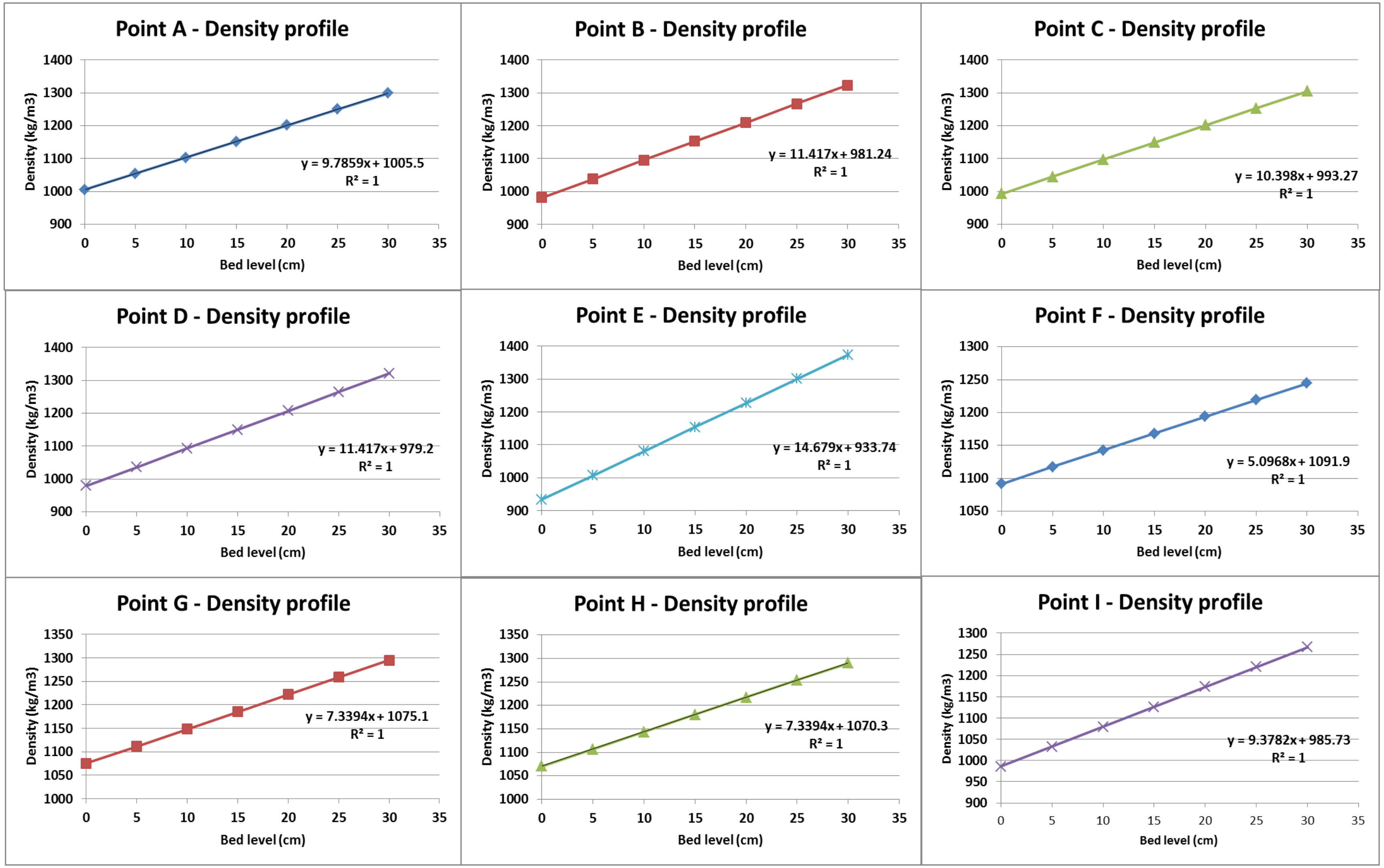

Figure B-29: Density profiles for silica sand 30 cm static bed height

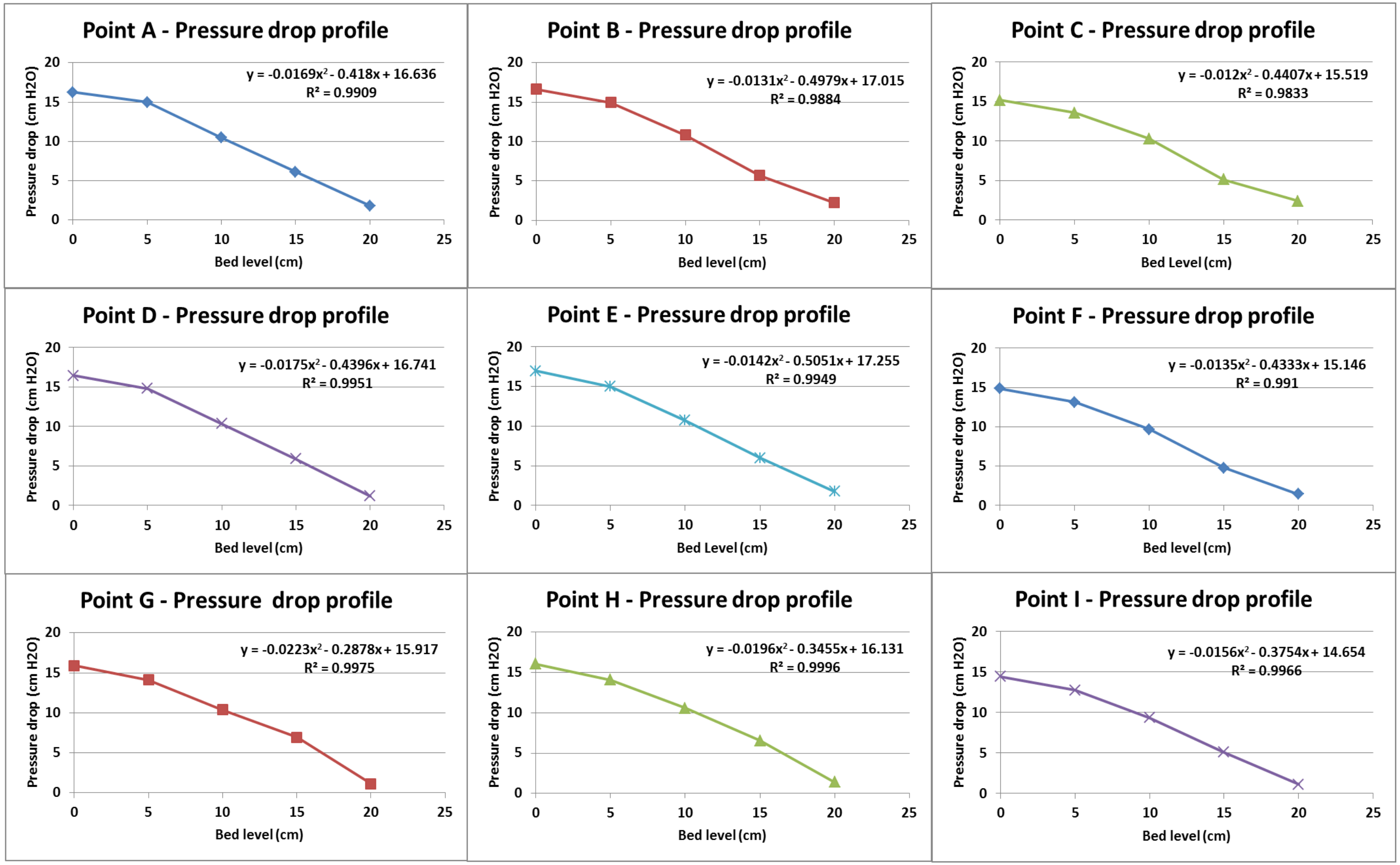

Figure B-30: Pressure drop profiles for coal rejects 20 cm static bed height

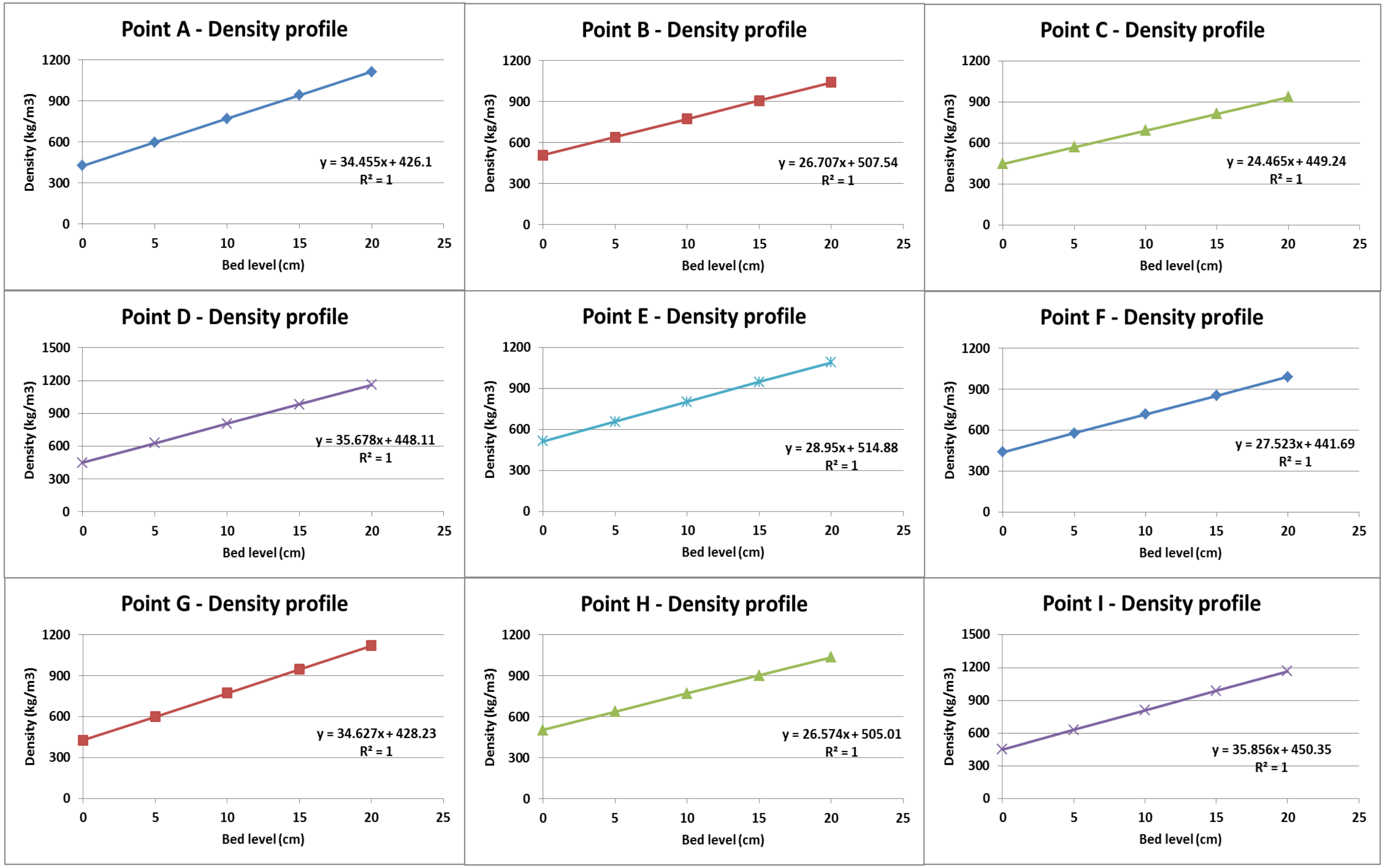

Figure B-31: Density profiles for coal rejects 20 cm static bed height

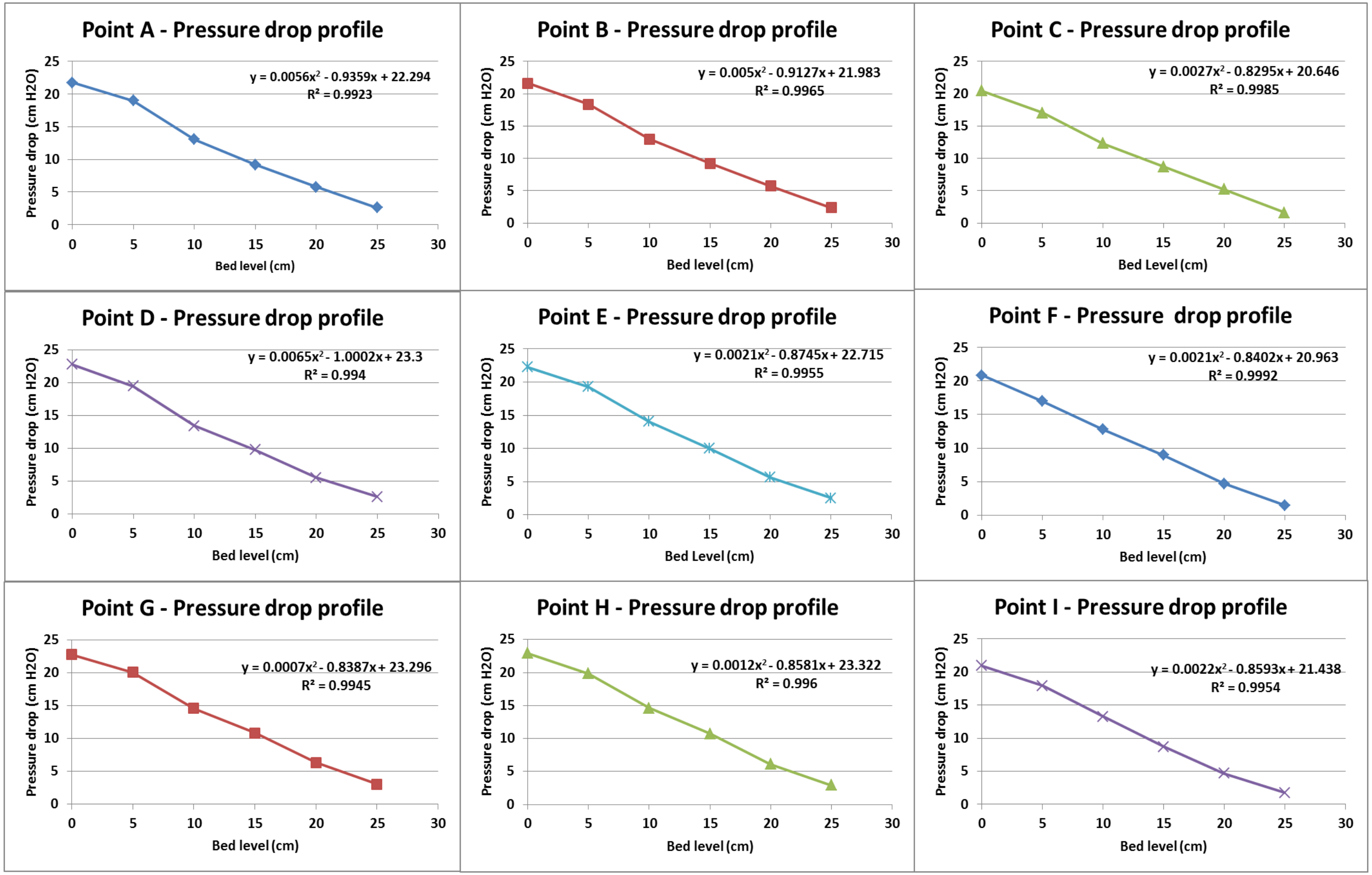

Figure B-32: Pressure drop profiles for coal rejects 25 cm static bed height

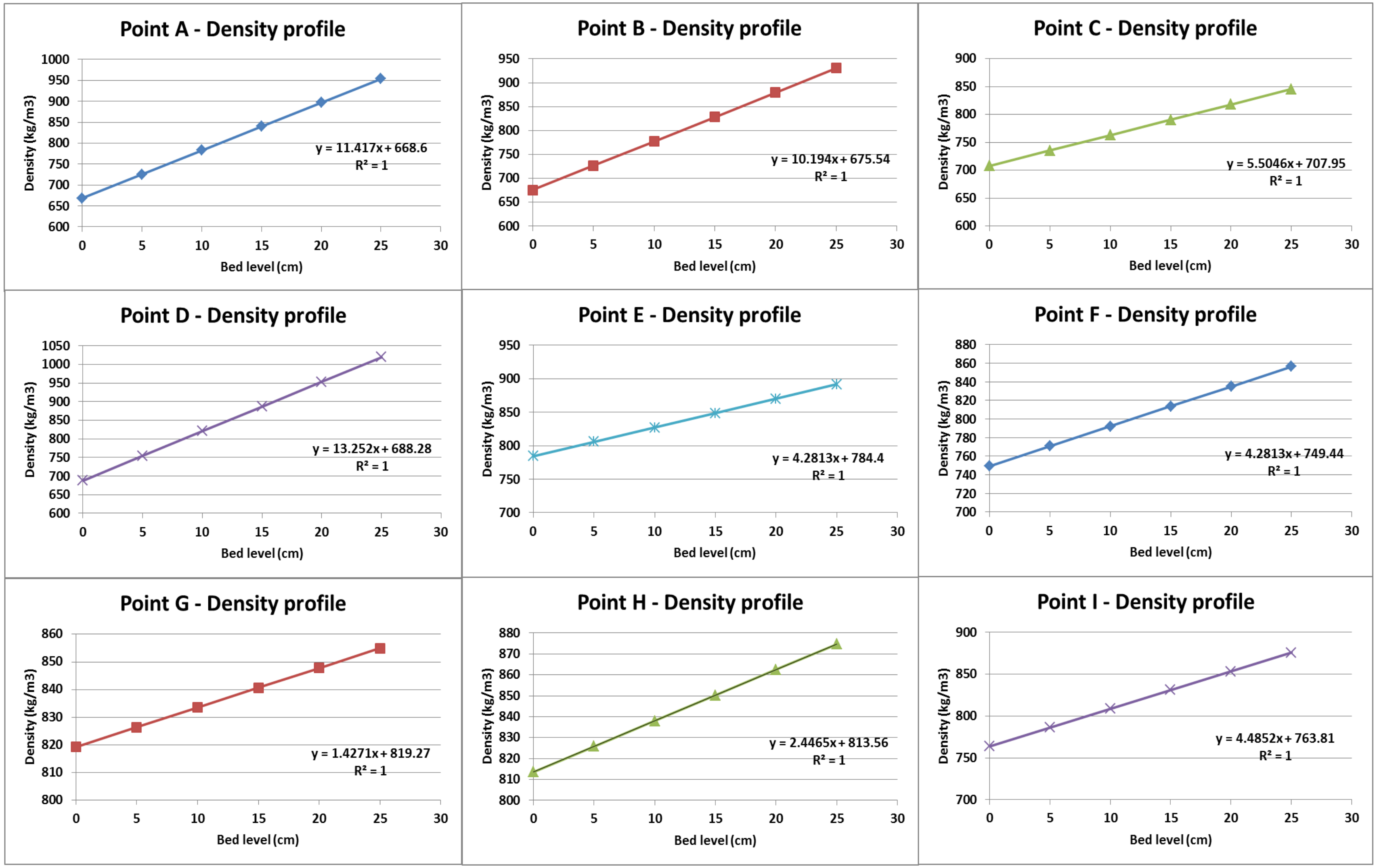

Figure B-33: Density profiles for coal rejects 25 cm static bed height

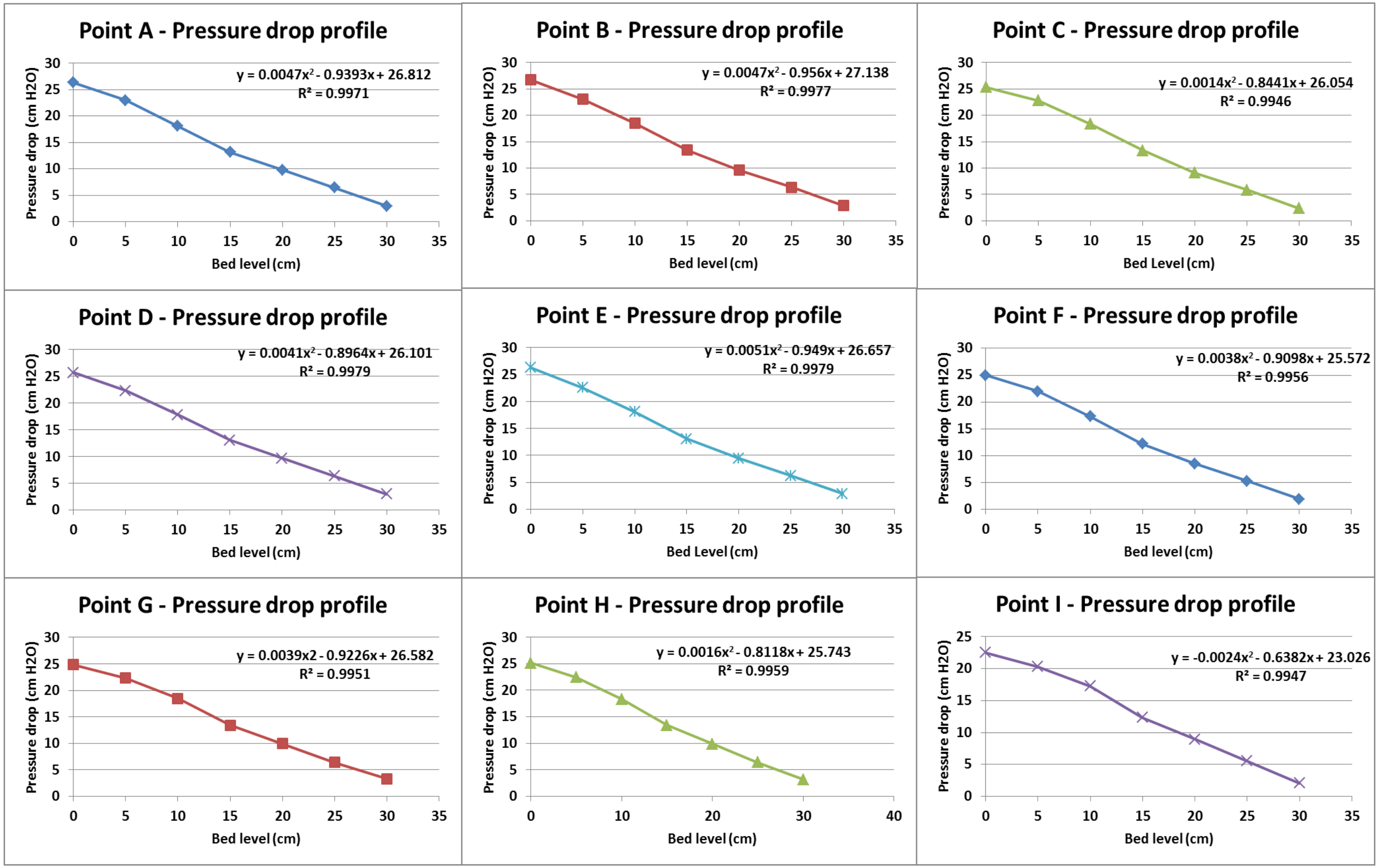

Figure B-34: Pressure drop profiles for coal rejects 30 cm static bed height

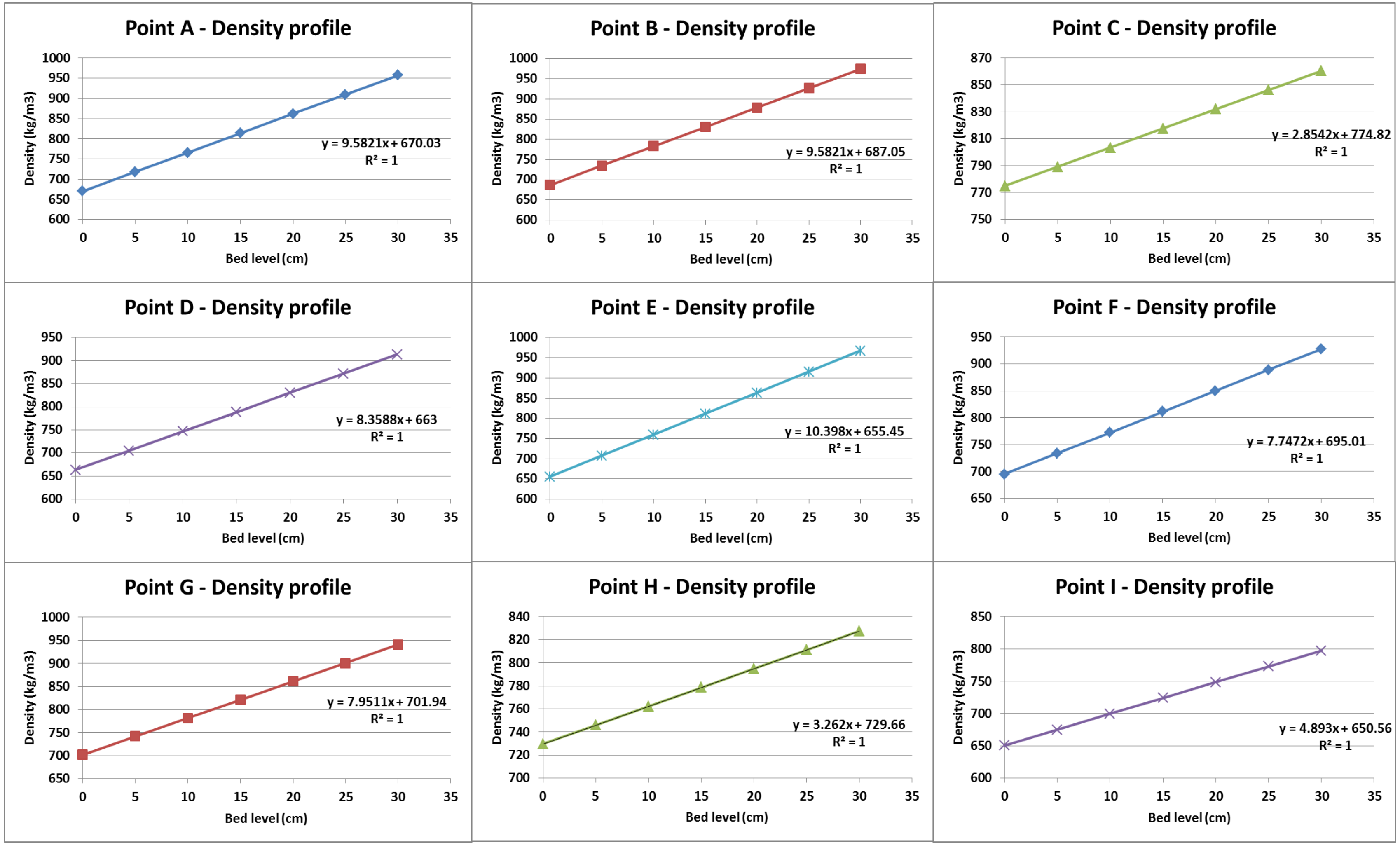

Figure B-35: Pressure drop profiles for coal rejects 30 cm static bed height

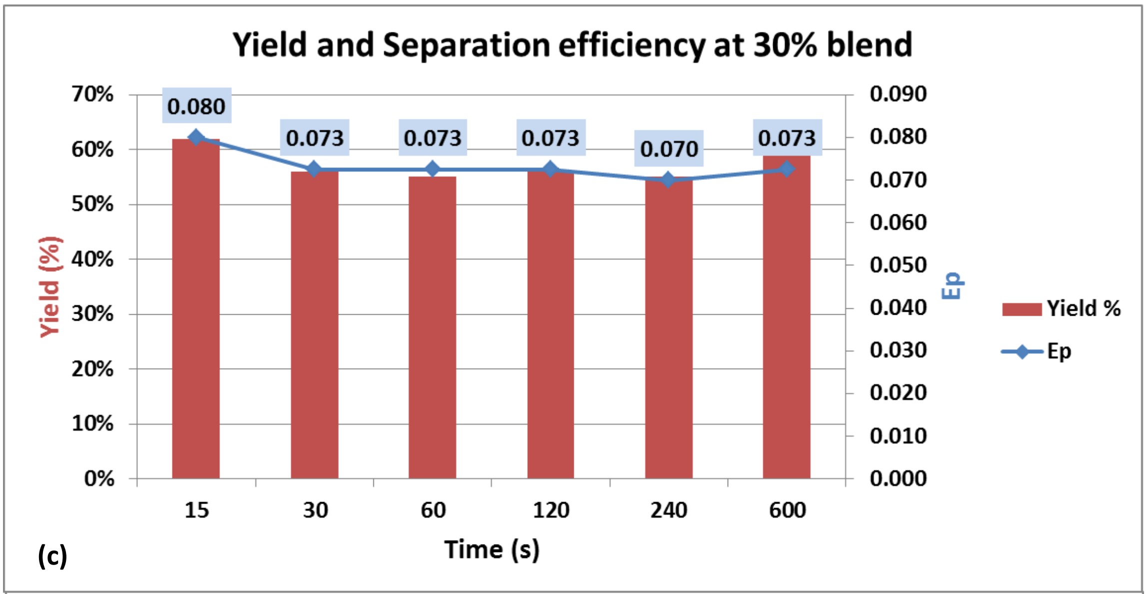
Yield and Separation efficiency at 30% blend
Yield (%)
70%
60%
50%
40%
30%
20%
10%
0%
0.080
0.073
0.073
0.073
0.070
0.073
0.090
0.080
0.070
0.060
0.050
0.040
0.030
0.020
0.010
0.000
Ep
Yield %
Ep
15
30
60
120
240
600
Time (s)
(c)

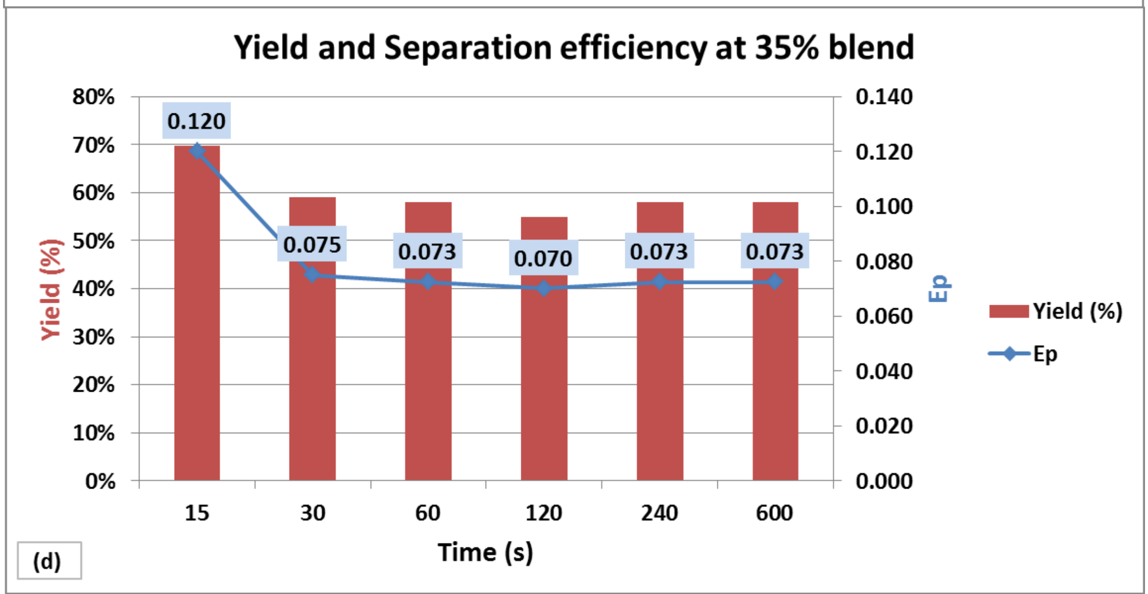
Yield and Separation efficiency at 35% blend
Yield (%)
80%
70%
60%
50%
40%
30%
20%
10%
0%
0.120
0.075
0.073
0.070
0.073
0.073
0.140
0.120
0.100
0.080
0.060
0.040
0.020
0.000
Ep
Yield (%)
Ep
15
30
60
120
240
600
Time (s)
(d)

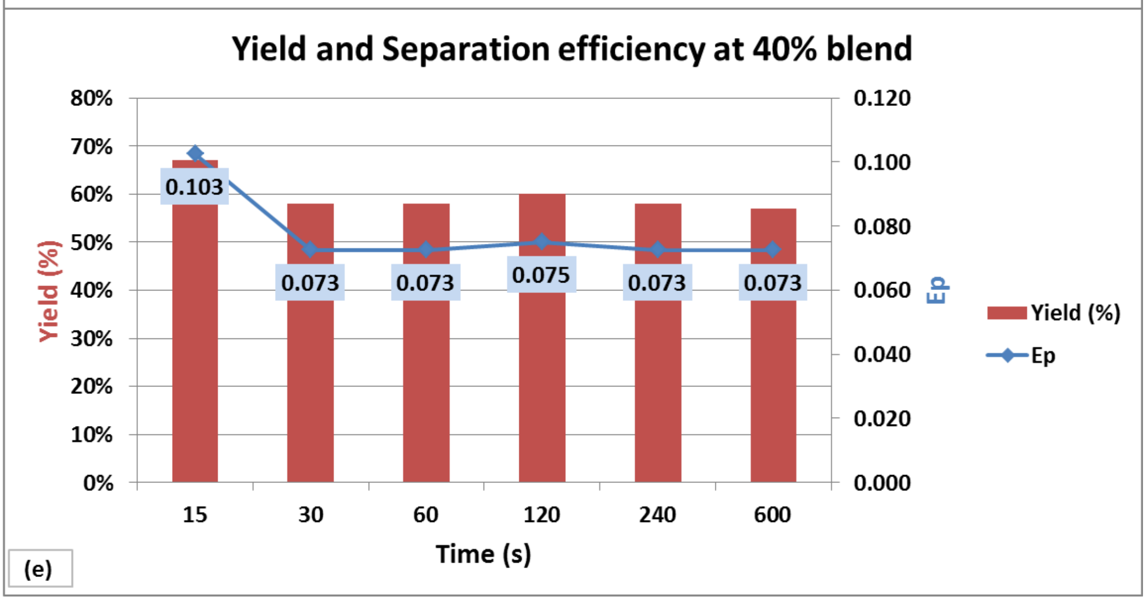
Yield and Separation efficiency at 40% blend
Yield (%)
80%
70%
60%
50%
40%
30%
20%
10%
0%
0.103
0.073
0.073
0.075
0.073
0.073
0.120
0.100
0.080
0.060
0.040
0.020
0.000
Ep
Yield (%)
Ep
15
30
60
120
240
600
Time (s)
(e)

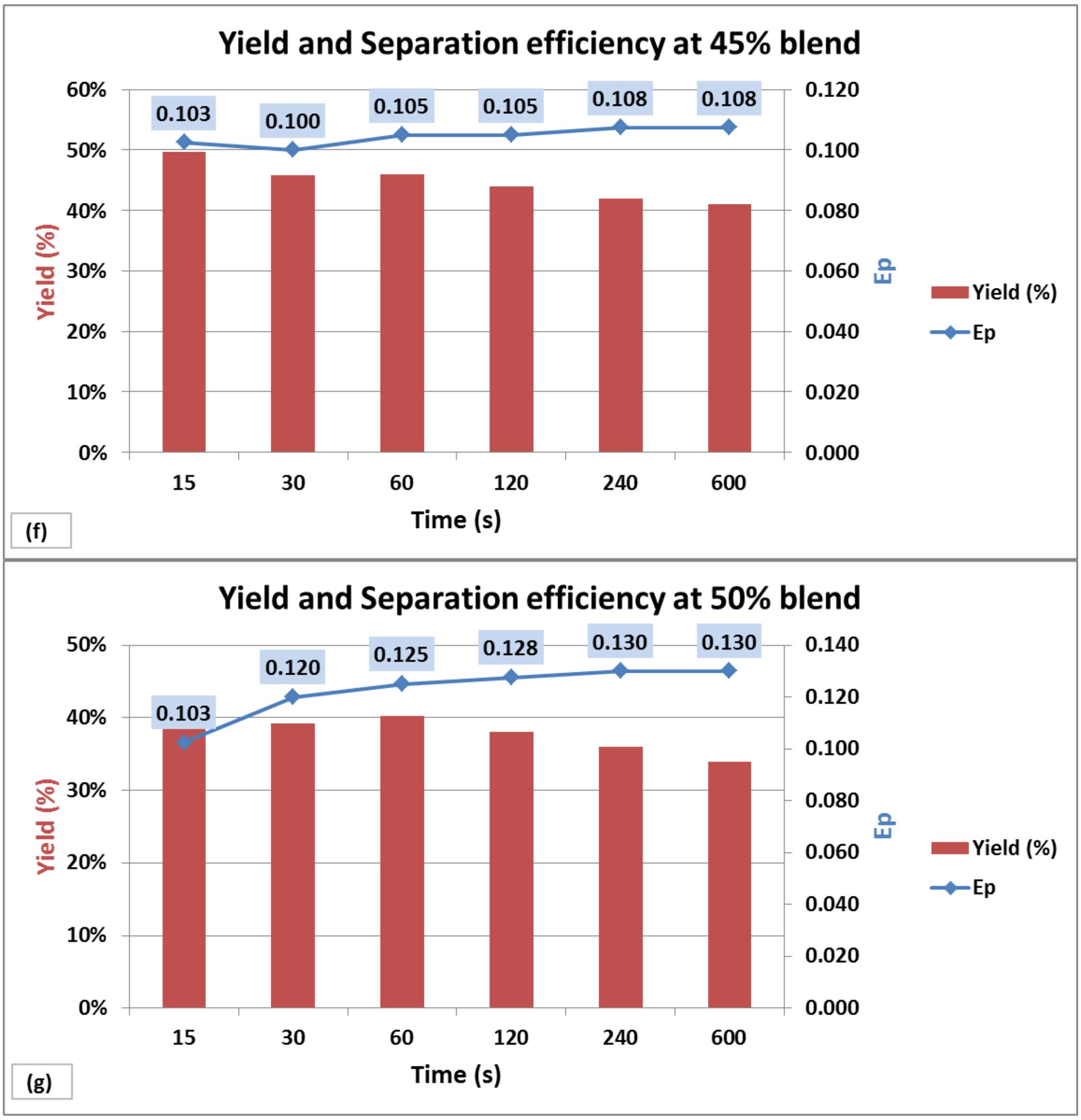

Figure B-0-36: Beneficiation results at 30 – 50% blend ratios

APPENDIX C: CONFERENCE PRESENTATIONS

Publications from this research work are attached on the next page.